

**Università degli Studi di Firenze**  
**Facoltà di S.F.M.N. – Dipartimento di Chimica**



Dottorato di Ricerca in Scienze Chimiche XXIII Ciclo  
Settore Disciplinare CHIM03

**“Synthesis and biological evaluation of new inhibitors of  
Carbonic Anhydrase”**

**Alfonso Maresca**

Relatore

Coordinatore della Scuola di Dottorato

**Prof. Andrea Scozzafava**

**Prof. Andrea Goti**

**Firenze, 2008-2011**



# Table of contents

<i>Table of contents</i> .....	I
<i>Table of short forms</i> .....	III
<i>Table of standard Amino Acids</i> .....	IV
<b>INTRODUCTION</b>	
<b>CHAPTER ONE Introduction to Carbonic Anhydrase</b> .....	2
1.1 Introduction.....	2
1.2 Catalytic and inhibition mechanisms of Carbonic Anhydrases .....	5
1.2.1 $\alpha$ -CAs .....	5
1.2.2 $\beta$ -CAs .....	11
1.2.3 $\gamma$ -CAs.....	14
1.2.4 $\delta$ -CAs.....	16
<b>CHAPTER TWO Introduction to experimental data</b> .....	18
2.1 Physiological functions of CAs, their inhibition and medicinal chemistry applications .....	18
2.2 Carbonic Anhydrase inhibitors (CAIs).....	19
2.3 Aim of the work.....	23
<b>EXPERIMENTAL SECTION</b>	
<b>CHAPTER THREE Coumarins: a novel chemotype for CA inhibition</b> .....	27
3.1 Discovery and initial screenings .....	27
3.2 Synthesis of “compound 1-related” coumarins .....	40
3.3 Assaying heterogenous coumarinic compounds.....	45
3.4 “Click Chemistry” coumarins.....	55
3.5 Conclusions.....	57
<b>CHAPTER FOUR Studies on <math>\beta</math>-Carbonic Anhydrases</b> .....	59
4.1 Kinetic characterization and inhibition studies of the most active $\beta$ -Carbonic Anhydrase from Mycobacterium tuberculosis, mtCA 2.....	59
4.1.1 Introduction .....	59
4.1.2 Structure and function of mtCA 2 .....	59
4.1.3 Kinetic investigation and inhibition studies.....	62
4.1.4 Conclusions.....	69
4.2 Substituted phenyl-1H-indole-5-sulfonamides: new $\beta$ -CAs strong inhibitors .....	70

4.2.1 Studies on mtCA 1 and mtCA 3.....	70
4.2.2 Studies on $\beta$ -CAs from <i>Cryptococcus neoformans</i> and <i>Candida albicans</i> .....	75
4.3 Conclusions.....	79
<b>CHAPTER FIVE Inhibition studies on mitochondrial CA VA and VB with sulfonamides .....</b>	<b>81</b>
5.1 CAIs as potential anti-obesity drugs.....	81
5.2 (R)-/(S)-10-Camphorsulfonyl-substituted aromatic/heterocyclic sulfonamides selectively inhibit mitochondrial over cytosolic carbonic anhydrases .....	82
<b>CHAPTER SIX Experimental section .....</b>	<b>88</b>
6.1 Chemistry.....	88
6.2 CA Inhibition Assays.....	89
6.3 Synthesis .....	90
6.3.1 General procedure for preparation of ether derivatives 6-10.....	90
6.3.2 Synthesis of compounds 32-50.....	92
6.3.2.1 General procedure for preparation of ester derivatives 30,31.....	92
6.3.2.2 General procedure for preparation of derivatives 32-35 .....	93
6.3.2.3 General procedure for preparation of derivatives 36-50 .....	95
6.3.3 Procedure for preparation of alcohol 53.....	102
6.3.4 General procedure for synthesis of derivatives 123-132.....	102
6.3.4.1 Preparation of ether compounds 116, 117 .....	102
6.3.4.2 General procedure for synthesis of phenylazides 118-122.....	103
6.3.4.3 General procedure for synthesis of triazolyl derivatives 123-132 .....	103
6.3.5 General procedure for preparation of sulfonamido derivatives 195-204 .....	109
<b>References list .....</b>	<b>116</b>
<b>Publications.....</b>	<b>123</b>

## *Table of short forms*

<b>AAZ:</b>	<i>Acetazolamide</i>
<b>ACC:</b>	<i>Acetyl-CoA Carboxylase</i>
<b>AMPA:</b>	<i><math>\alpha</math>-amino-3-hydroxy-5-methyl-4-isoxazole propionic acid</i>
<b>BRZ:</b>	<i>Brinzolamide</i>
<b>CA:</b>	<i>Carbonic Anhydrase</i>
<b>CAI:</b>	<i>Carbonic Anhydrase Inhibitor</i>
<b>CARP:</b>	<i>Carbonic Anhydrase Related Protein</i>
<b>CLX:</b>	<i>Celecoxib</i>
<b>CMT:</b>	<i>COUMATE</i>
<b>CRS:</b>	<i>Cerebrospinal Fluid</i>
<b>DCP:</b>	<i>Dichlorophenamide</i>
<b>DZA:</b>	<i>Dorzolamide</i>
<b>EMT:</b>	<i>EMATE</i>
<b>EZA:</b>	<i>Ethoxzolamide</i>
<b>GABA:</b>	<i><math>\gamma</math>-aminobutyric acid</i>
<b>IND:</b>	<i>Indisulam</i>
<b>MZA:</b>	<i>Methazolamide</i>
<b>PC:</b>	<i>Pyruvate Carboxylase</i>
<b>SAC:</b>	<i>Saccharin</i>
<b>SAR:</b>	<i>Structure-Activity Relationship</i>
<b>SLP:</b>	<i>Sulpiride</i>
<b>SLT:</b>	<i>Sulthiame</i>
<b>TPM:</b>	<i>Topiramate</i>
<b>TWCA1:</b>	<i>Thalassiosira weissflogii Carbonic Anhydrase 1</i>
<b>VLX:</b>	<i>Valdecoxib</i>
<b>ZNS:</b>	<i>Zonisamide</i>

## *Table of standard Amino Acids*

<i>Amino Acid</i>	<i>3-Letter Code</i>	<i>1-Letter Code</i>
<i>Alanine</i>	<i>Ala</i>	<i>A</i>
<i>Arginine</i>	<i>Arg</i>	<i>R</i>
<i>Asparagine</i>	<i>Asn</i>	<i>N</i>
<i>Aspartic acid</i>	<i>Asp</i>	<i>D</i>
<i>Cysteine</i>	<i>Cys</i>	<i>C</i>
<i>Glutamic acid</i>	<i>Glu</i>	<i>E</i>
<i>Glutamine</i>	<i>Gln</i>	<i>Q</i>
<i>Glycine</i>	<i>Gly</i>	<i>G</i>
<i>Histidine</i>	<i>His</i>	<i>H</i>
<i>Isoleucine</i>	<i>Ile</i>	<i>I</i>
<i>Leucine</i>	<i>Leu</i>	<i>L</i>
<i>Lysine</i>	<i>Lys</i>	<i>K</i>
<i>Methionine</i>	<i>Met</i>	<i>M</i>
<i>Phenylalanine</i>	<i>Phe</i>	<i>F</i>
<i>Proline</i>	<i>Pro</i>	<i>P</i>
<i>Serine</i>	<i>Ser</i>	<i>S</i>
<i>Threonine</i>	<i>Thr</i>	<i>T</i>
<i>Tryptophan</i>	<i>Trp</i>	<i>W</i>
<i>Tyrosine</i>	<i>Tyr</i>	<i>Y</i>
<i>Valine</i>	<i>Val</i>	<i>V</i>

# ***INTRODUCTION***

## CHAPTER ONE

### *Introduction to Carbonic Anhydrase*

#### **1.1 Introduction**

Carbonic anhydrases (CAs, also known as Carbonate Dehydratases) are metalloenzymes which catalyze CO<sub>2</sub> hydration to bicarbonate and protons. As CO<sub>2</sub>, bicarbonate and protons are essential molecules/ions in many important physiologic processes in all life kingdoms (*Bacteria*, *Archaea*, and *Eukarya*), throughout the phylogenetic tree, relatively high amounts of them are present in different tissues/cell compartments of all such organisms. CAs evolved independently at least five times, with five genetically distinct enzyme families known to date: the  $\alpha$ -CAs (present in vertebrates, *Bacteria*, algae and cytoplasm of green plants), the  $\beta$ -CAs (predominantly found in *Bacteria*, algae and chloroplasts of both mono- as well as dicotyledons), the  $\gamma$ - (mainly present in *Archaea* and some *Bacteria*), the  $\delta$ -CAs present in some marine diatoms and  $\zeta$ -CAs.<sup>1-6</sup> All of them are metalloenzymes, where  $\alpha$ -,  $\beta$ - and  $\delta$ -CAs use Zn(II) ions at the active site<sup>1-4</sup> the  $\gamma$ -CAs are probably Fe(II) enzymes (but they are active also with bound Zn(II) or Co(II) ions),<sup>5</sup> whereas the  $\zeta$ -class uses Cd(II) or Zn(II) to perform the physiologic reaction catalysis.<sup>6</sup> The active site centers of the five families of CAs are shown schematically in Figure 1.1.

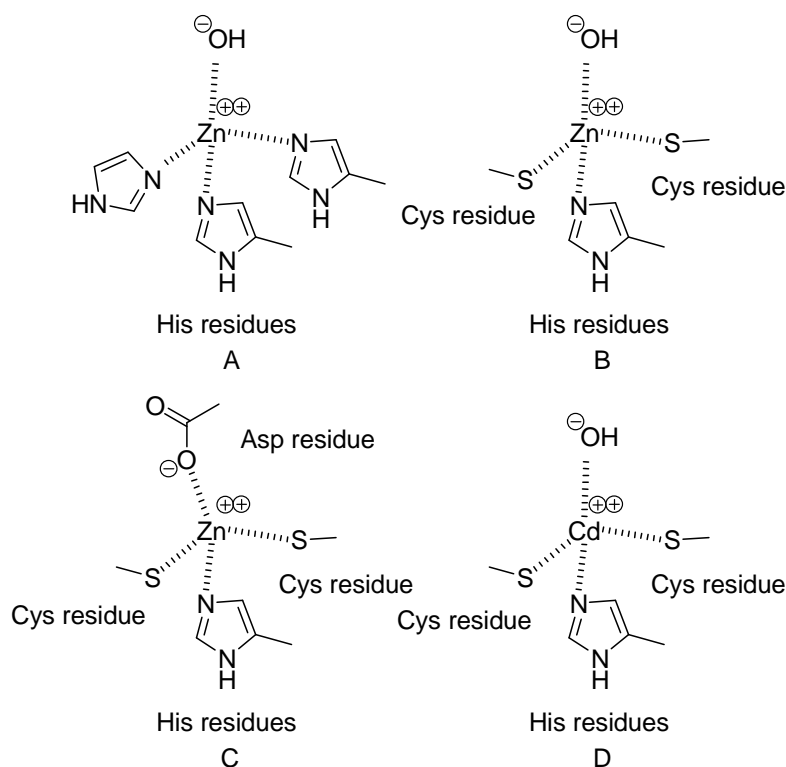


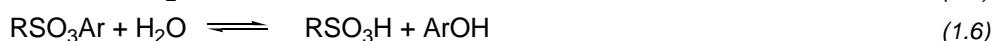
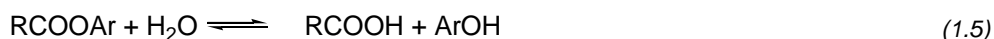
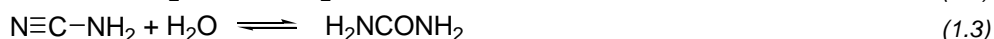
**Figure 1.1.** Metal ion coordination in CAs: A.  $\alpha$ -,  $\gamma$ - and  $\delta$ -CAs (for the  $\gamma$ -class the metal ion can also be Co(II) or Fe(II)); B.  $\beta$ -CAs, open active site; C.  $\beta$ -CAs, closed active site; D.  $\zeta$ -CAs (Cd(II) can be also substituted by Zn(II), without loss of activity).

The 3D fold of the five enzyme classes is also very different from each other, as it is their oligomerization state:  $\alpha$ -CAs are normally monomers and rarely dimers (e.g., CA IX and XII);  $\beta$ -CAs are dimers, tetramers or octamers;  $\gamma$ -CAs are trimers,<sup>1-4</sup> whereas the  $\delta$ - and  $\zeta$ -CAs are probably monomers but in the case of the last family, three slightly different active sites are present on the same protein backbone which is in fact a pseudotrimer, at least for the best studied such enzyme, from the marine diatom *Thalassiosira weissflogii*.<sup>1-6</sup> Many representatives of all these enzyme classes have been crystallized and characterized in detail, except the  $\delta$ -CAs.<sup>1-9</sup>

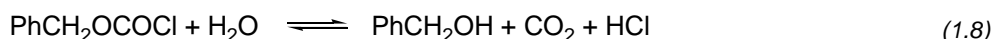
In many organisms these enzymes are involved in crucial physiological processes connected with respiration and transport of CO<sub>2</sub>/bicarbonate, pH and CO<sub>2</sub> homeostasis, electrolyte secretion in a variety of tissues/organs, biosynthetic reactions (such as gluconeogenesis, lipogenesis and ureagenesis), bone resorption, calcification, tumorigenicity, and many other physiologic or pathologic processes (thoroughly studied in vertebrates).<sup>1-3,7-10</sup> Whereas, in algae, plants and some bacteria they play an important role in photosynthesis and other biosynthetic reactions.<sup>1,4,5,11</sup> In diatoms  $\delta$ - and  $\zeta$ -CAs play a crucial role in carbon dioxide fixation.<sup>6</sup>

The 16 different  $\alpha$ -CA isoforms isolated and characterized so far in mammals (where they play important physiological roles, as briefly outlined above) are cytosolic (CA I, CA II, CA III, CA VII, CA XIII), membrane-bound (CA IV, CA IX, CA XII, CA XIV and CA XV), mitochondrial (CA VA and CA VB) or secreted (CA VI) proteins.<sup>1-3</sup> Three acatalytic forms are also known, the CA related proteins (CARP), CARP VIII, CARP X and CARP XI, which are also cytosolic proteins too.<sup>1</sup> The mammalian CAs were the first such enzymes isolated and studied in detail, and many of them are established therapeutic targets with the potential to be inhibited or activated to treat a wide range of disorders.<sup>1-3,7-10,12-15</sup> Indeed, diuretics, antiglaucoma, antiepileptic, antiobesity and anticancer drugs based on CAIs are presently known, and they target various mammalian (human)  $\alpha$ -CA isoforms.<sup>1</sup>

In addition to the physiological reaction, the reversible hydration of CO<sub>2</sub> to bicarbonate (reaction 1.1, Chart 1.1),  $\alpha$ -CAs catalyze a variety of other reactions, such as: the hydration of cyanate to carbamic acid, or of cyanamide to urea (reactions 1.2 and 1.3); the aldehyde hydration to gem-diols (reaction 1.4); the hydrolysis of carboxylic esters, or sulfonic acid esters (reactions 1.5 and 1.6), as well as other less investigated hydrolytic processes, such as those described by Eqs. 1.7–1.10 in Chart 1.1.<sup>16-18</sup>



(Ar = 2,4-dinitrophenyl)



(R = Me, Ph)



**Chart 1.1.** Reactions catalyzed by  $\alpha$ -CAs.

It is unclear at this moment whether other  $\alpha$ -CA catalyzed reactions than the CO<sub>2</sub> hydration have physiological significance. The X-ray crystal structure has been determined for nine  $\alpha$ -CAs at this moment (isozymes CA I–VA, CA IX, CA XII and XIII and CA XIV)<sup>2,8,19-26</sup> as well as for representatives of the  $\beta$ - and  $\gamma$ -CA families.<sup>27-32</sup>

## 1.2 Catalytic and inhibition mechanisms of Carbonic Anhydrases

### 1.2.1 $\alpha$ -CAs

The metal ion (which is Zn(II) in all  $\alpha$ -CAs investigated up to now) is essential for catalysis.<sup>2,19-23,33,34</sup> X-ray crystallographic data showed that the metal ion is situated at the bottom of a 15 Å deep active site cleft (Figure 1.2), being coordinated by three histidine residues (His94, His96 and His119) and a water molecule/hydroxide ion.<sup>2,19-23,33,34</sup>

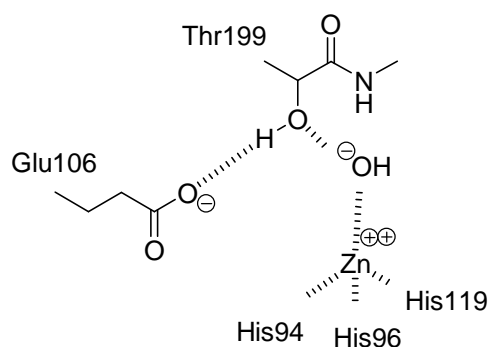


**Figure 1.2.** The Zn(II) ion coordination in the hCA II active site, with the three histidine ligands (His94, His96 and His119, isozyme I numbering) and the gate-keeping residues (Thr199 and Glu106) shown.

The zinc-bound water is also engaged in hydrogen bond interactions with the hydroxyl moiety of Thr199, which in turn is bridged to the carboxylate moiety of Glu 106; these interactions enhance the nucleophilicity of the zinc-bound water molecule, and orient the substrate ( $\text{CO}_2$ ) in a favourable location for the nucleophilic attack (Figure 1.3).<sup>2,19-23,33,34</sup> The active form of the enzyme is the basic one, with hydroxide bound to Zn(II) (Figure 1.3A). This strong nucleophile attacks the  $\text{CO}_2$  molecule bound in a hydrophobic pocket in its neighbourhood (the substrate-binding site comprises residues Val121, Val143 and Leu198 in the case of the human isozyme CA II) (Figure 1.3B), leading to the formation of bicarbonate coordinated to Zn(II) (Figure 1.3C). The bicarbonate ion is then displaced by a water molecule and liberated into solution, leading to the acid form of the enzyme, with water coordinated to Zn(II) (Figure 1.3D), which is catalytically inactive.<sup>2,19-23,33,34</sup>

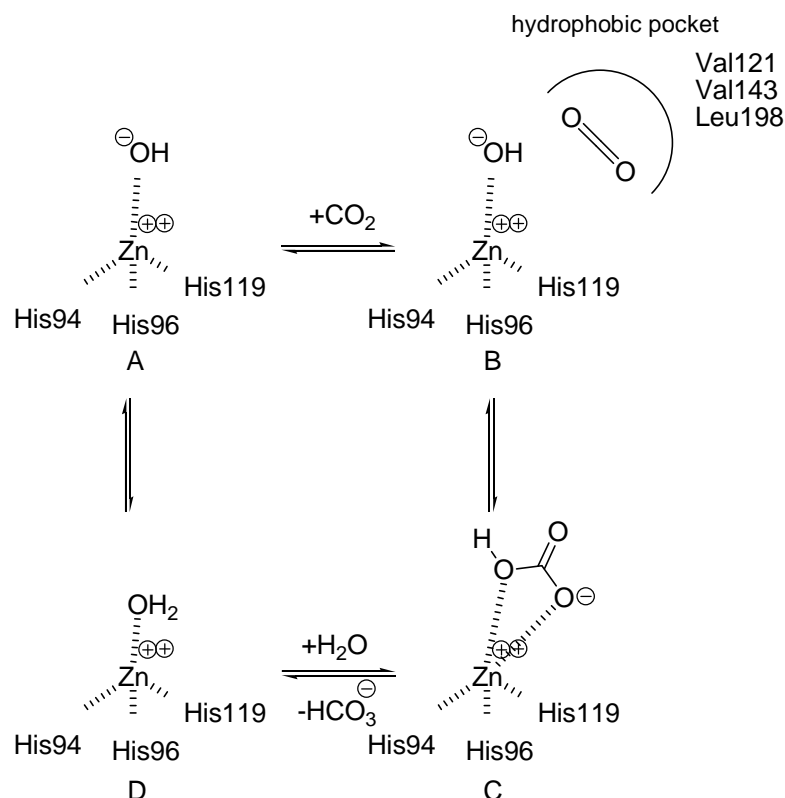
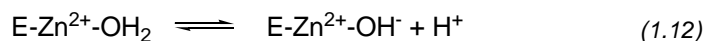
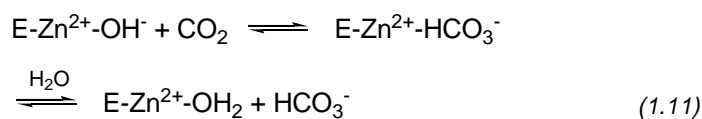


**Figure 1.3.** Schematic representation of the catalytic mechanism for the  $\alpha$ -CA catalyzed  $\text{CO}_2$  hydration. The hydrophobic pocket for the binding of substrate(s) is shown schematically at step (B).

In order to regenerate the basic form A, a proton transfer reaction from the active site to the environment takes place, which may be assisted either by active site residues (such as His64—the proton shuttle in isozymes I, II, IV, VI, VII, IX and XII–XIV among others) or by buffers present in the medium. The process may be schematically represented by Eqs. 1.11 and 1.12 below:



The rate limiting step in catalysis is the second reaction, that is, the proton transfer that regenerates the zinc-hydroxide species of the enzyme.<sup>2,19-23,33-35</sup> In the catalytically very active isozymes, such as CA II, CA IV, CA VII and CA IX, the process is assisted by a histidine residue placed at the entrance of the active site (His64), as well as by a cluster of histidines, which protrudes from the rim of the active site to the surface of the enzyme, assuring thus a very efficient proton transfer process for the most efficient CA isozyme, CA II.<sup>35</sup> This also explains why CA II is one of the most active enzymes known (with a  $K_{\text{cat}}/K_{\text{M}} = 1.5 \times 10^8 \text{ M}^{-1} \text{ s}^{-1}$ ), approaching the limit of diffusion control, and also has important consequences for the design of inhibitors with clinical applications.<sup>2,19-23,33-35</sup>

Different classes of CA inhibitors (CAIs) are known. The oldest and most studied two are: the metal complexing anions, and the unsubstituted sulfonamides, which bind to the Zn(II) ion of the enzyme either by substituting the non-protein zinc ligand (Eq. 1.13 in Figure 1.4) or add to the metal coordination sphere (Eq. 1.14 in Figure 1.4), generating trigonal–bipyramidal species.<sup>2,19-23,33,34,36</sup> Sulfonamides, which are the most important CAIs (such as the clinically used derivatives acetazolamide **AAZ**, methazolamide **MZA**, ethoxzolamide **EZA**, dichlorophenamide **DCP**, dorzolamide **DZA** and brinzolamide **BRZ**, Chart 1.2),<sup>19</sup> bind in a tetrahedral geometry of the Zn(II) ion (Figure 1.4), in deprotonated state, with the nitrogen atom of the sulfonamide moiety coordinated to Zn(II) and an extended network of hydrogen bonds, involving residues Thr199 and Glu106, also participating to the anchoring of the inhibitor molecule to the metal ion.

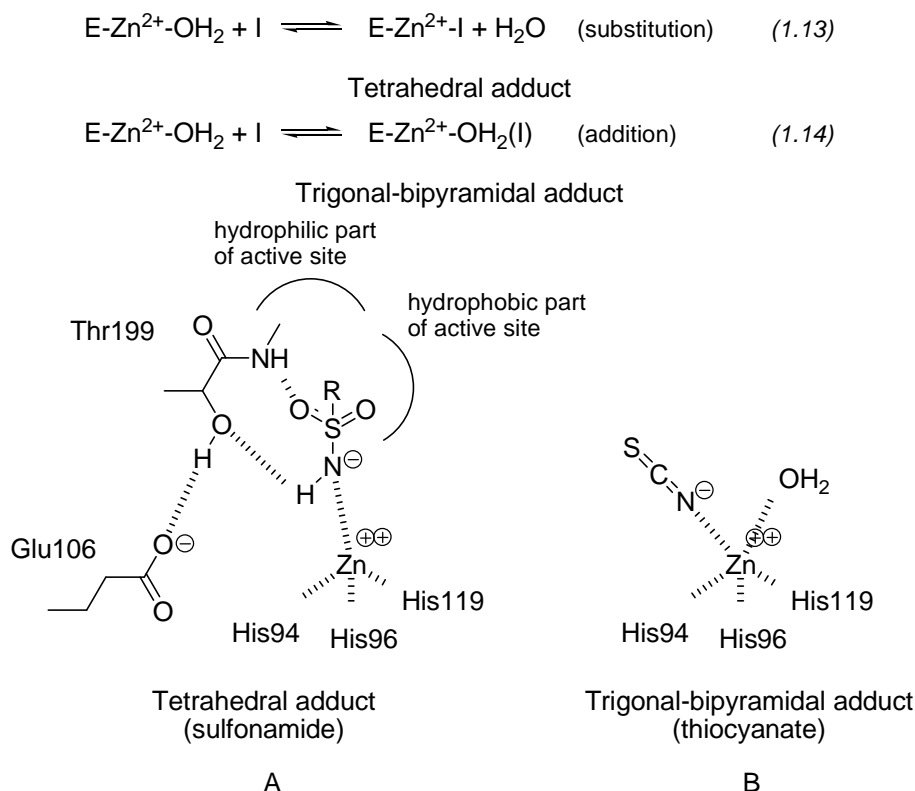


**Figure 1.4.**  $\alpha$ -CA inhibition mechanism by sulfonamide (A) and anionic (B) inhibitors. In the case of sulfonamides, in addition to the Zn(II) coordination, an extended network of hydrogen bonds ensues, involving residues Thr199 and Glu106, whereas the organic part of the inhibitor (R) interacts with hydrophilic and hydrophobic residues of the cavity. For anionic inhibitors such as thiocyanate (B) the interactions between inhibitor and enzyme are much simpler.

The aromatic/heterocyclic part of the inhibitor (R) interacts with hydrophilic and hydrophobic residues of the cavity. Anions may bind either in tetrahedral geometry of the metal ion or as trigonal–bipyramidal adducts, such as for instance the thiocyanate adduct shown in Figure 1.4B.<sup>1,36</sup>

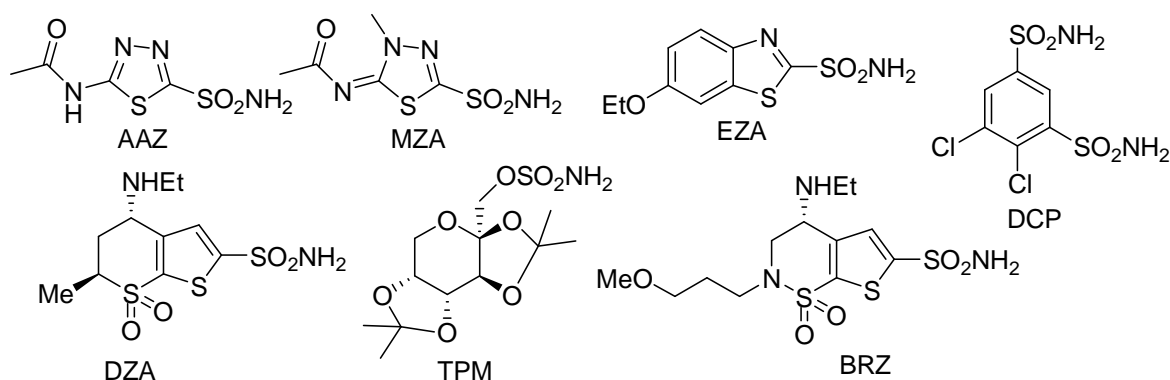


**Chart 1.2.** Sulfonamidic CAs inhibitors **AAZ-BRZ** and the sulfamate **TPM**.

X-ray crystallographic structures are available for many adducts of sulfonamide/sulfamate/sulfamide inhibitors with isozymes CA I, II and IV.<sup>36-42</sup> In all these adducts, the deprotonated sulfonamide/sulfamate/sulfamide is coordinated to the Zn(II) ion of the enzyme, and its NH moiety participates in a hydrogen bond with the O $\gamma$  of Thr199, which in turn is engaged in another hydrogen bond to the carboxylate group of Glu106.<sup>36-39,43,42,40,41</sup> One of the oxygen atoms of the sulfonamidic moiety also participates in a hydrogen bond with the backbone NH moiety of Thr199. Examples of various adducts of such inhibitors with CA II are provided in Figures 1.5 and 1.6.

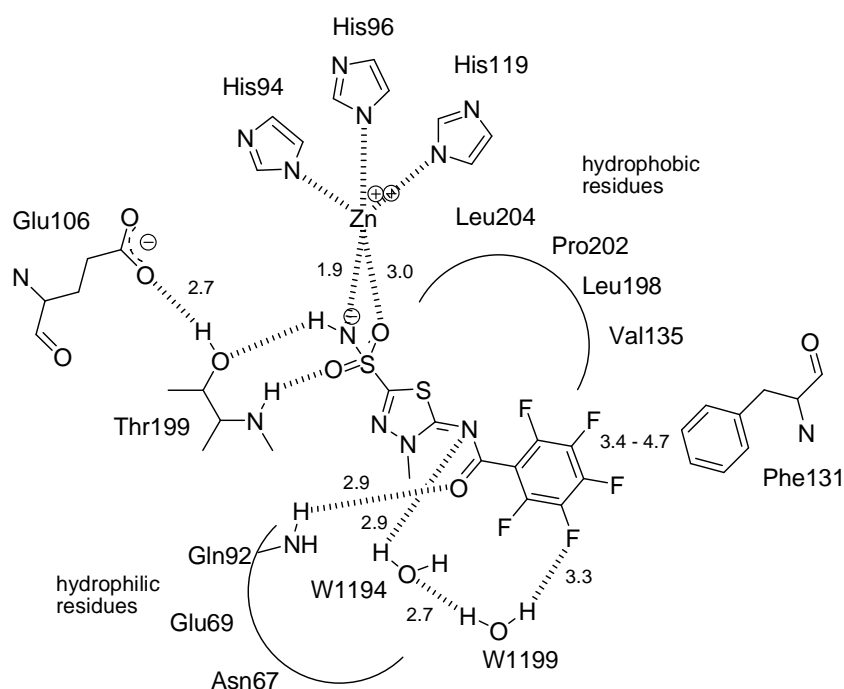


**Figure 1.5.** Schematic representation of the pentafluorobenzoyl analogue of methazolamide (**PFMZ**) bound within the hCA II active site (figures represent distances in Å).<sup>37</sup>

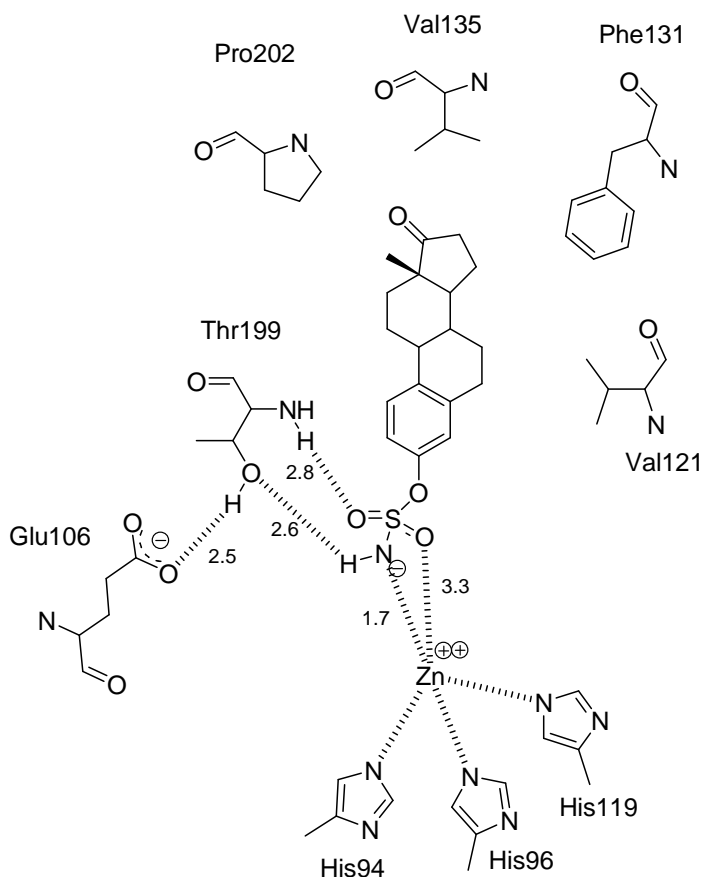


**Figure 1.6.** Binding of the sulfamate CA inhibitor **EMATE** to hCA II.<sup>38</sup>

The different types of interactions for a sulfonamidic inhibitor to have very high affinity (in the low nanomolar range) for the CA active site, are illustrated in Figures 1.5 and 1.6; in particular two examples are the fluorocontaining sulfonamide inhibitor, **PFMZ**,<sup>37</sup> (Figure 1.5) and the steroid sulfamate **EMATE**<sup>38</sup> (Figure 1.6). It can be observed that for the sulfonamide compound **PFMZ**, the ionized sulfonamide moiety has replaced the hydroxyl ion coordinated to Zn(II) in the native enzyme (Zn–N distance of 1.95 Å), with the metal ion remaining in its stable tetrahedral geometry, being coordinated in addition to the sulfonamidate nitrogen, by the imidazolic nitrogens of His94, His96 and His119. The proton of the coordinated sulfonamidate nitrogen atom also makes a hydrogen bond with the hydroxyl group of Thr 199, which in turn accepts a hydrogen bond from the carboxylate of Glu106. One of the oxygen atoms of the sulfonamide moiety makes a hydrogen bond with the backbone amide of Thr199, whereas the other one is semi-coordinated to the catalytic Zn(II) ion (O–Zn distance of 3.0 Å). The thiadiazoline ring of the inhibitor lies in the hydrophobic part of the active site cleft, where its ring atoms make van der Waals interactions with the side chains of Leu204, Pro202, Leu198 and Val135 (Figure 1.5). The amidic oxygen of **PFMZ** makes a strong hydrogen bond with the

backbone amide nitrogen of Gln92 (of 2.9 Å), an interaction also evidenced for the acetazolamide–hCA II adduct. Besides Gln92, two other residues situated in the hydrophilic half of the CA active site, that is, Glu 69 and Asn67, make van der Waals contacts with the **PFMZ** molecule complexed to hCA II. But the most notable and unprecedented interactions evidenced in this complex, regard the hydrogen bond network involving the exocyclic nitrogen atom of the inhibitor, two water molecules (Wat1194 and Wat1199) and a fluorine atom in meta belonging to the perfluorobenzoyl tail of **PFMZ** (Figure 1.5). Thus, a strong hydrogen bond (of 2.9 Å) is evidenced between the imino nitrogen of **PFMZ** and Wat1194, which in turn makes a hydrogen bond with a second water molecule of the active site, Wat1199 (with a distance of 2.7 Å). The second hydrogen of Wat1194 also participates in a weaker hydrogen bond (3.3 Å) with the carbonyl oxygen of **PFMZ**. The other hydrogen atom of Wat1199 makes a weak hydrogen bond with the fluorine atom in position 3 of the perfluorobenzoyl tail of **PFMZ** (Figure 1.5). Finally, a very interesting interaction has been observed between the perfluorophenyl ring of the inhibitor and the phenyl moiety of Phe131, a residue critical for the binding of inhibitors with long tails to hCA II.<sup>2,19,20</sup> Indeed, these two rings are almost perfectly parallel, being situated at a distance of 3.4–4.7 Å. This type of stacking interactions has never been observed in a hCA II–sulfonamide adduct. Similar interactions are also observed for the sulfamates (**EMATE**) type of CA inhibitors (Figure 1.6).<sup>38</sup>

Among the chemotypes diverse of sulfonamides and their bioisosteres investigated in great detail ultimately, are the phenols and polyphenols.<sup>44-49</sup> Initially, simple mono- or polysubstituted phenols/naphthols have been investigated for their interaction with all 13 catalytically active mammalian isozymes, with many low micromolar inhibitors being detected.<sup>44,45</sup> Further studies evidenced better inhibitors, among various salicylic acid derivatives, antioxidant phenols/biphenyl phenols, phenolic acids and other natural products, some of which were nanomolar inhibitors of several isoforms, such as the mitochondrial ones CA VA and VB.<sup>46-49</sup> Phenols and their derivatives, constitute thus a class of scarcely investigated CAIs with great promise. Unfortunately, there are very few structural information regarding how this class of CAIs bind to the enzyme active site, since only the X-ray structure of the adduct of simple phenol (PhOH) with CA II has been reported by Christianson's group.<sup>50</sup> The schematic representation of phenol inhibition mechanism is reported in Figure 1.7.

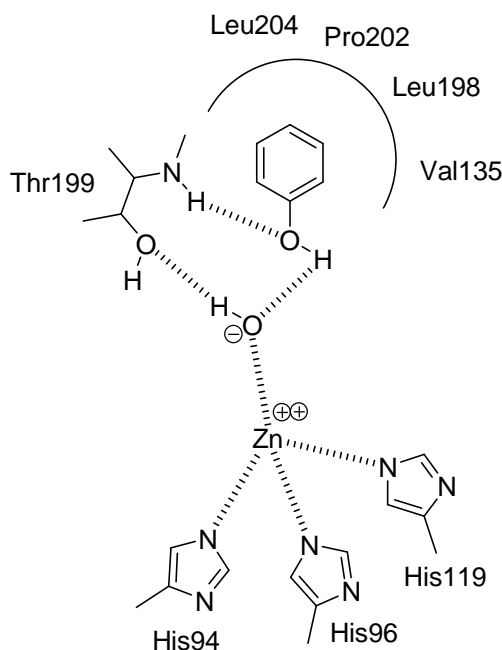


**Figure 1.7.** Binding of Phenol to hCA II.<sup>50</sup>

Another class of CAIs, only recently emerged, is represented by the Coumarins.<sup>51</sup> This chemotype shows a totally different inhibition approach towards CAs, I'll talk about later, as it's one of the main themes of this thesis.

### 1.2.2 $\beta$ -CAs

Many species belonging to *Bacteria*, some *Archaea* (such as *Methanobacterium thermoautotrophicum*), algae and the chloroplasts of superior plants contain CAs belonging to the  $\beta$ -class.<sup>21,27,28,30</sup> The principal difference between these enzymes and the  $\alpha$ -CAs discussed above consists in the fact that usually the  $\beta$ -CAs are oligomers, generally formed of 2–6 monomers of molecular weight of 25–30 kDa. The first reported  $\beta$ -CA X-ray structure was that of *P. purpureum*, a red alga, in 2000.<sup>32</sup> This was quickly followed by structures for a plant (*P. sativum*)<sup>30</sup> and a bacterial (*E. coli*)  $\beta$ -CA.<sup>27</sup> to date, 6 additional  $\beta$ -CA X-ray crystal structures are known, including in order of appearance, an archaeal  $\beta$ -CA (*M. thermoautotrophicum*),<sup>52</sup> two enzymes (mtCA 1 and mtCA 2) from *M. tuberculosis*,<sup>29</sup> the second crystallizing in two different active site and oligomerization structures,<sup>13</sup> a carboxysomal  $\beta$ -CA (*H. neapolitanus*),<sup>53</sup> and *Haemophilus influenzae*  $\beta$ -CA.<sup>54</sup>

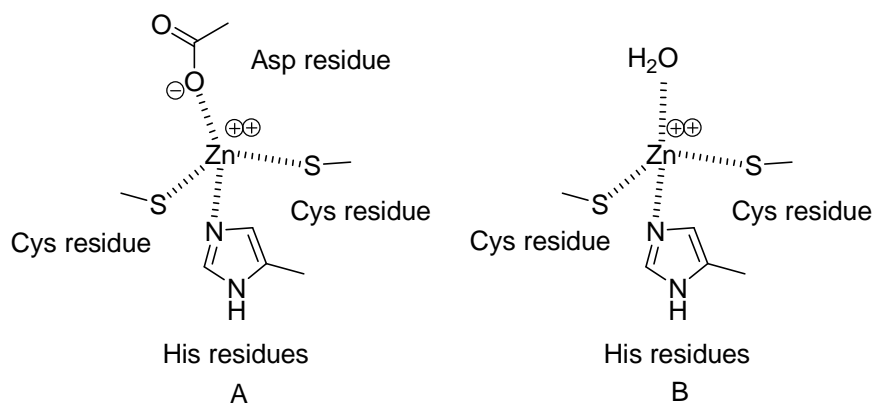


**Figure 1.8.** Schematic representation of the Zn(II) coordination sphere in  $\beta$ -CAs: (A) *Porphyridium purpureum*<sup>32</sup> and *Escherichia coli*<sup>27</sup> enzymes; (B) *Pisum sativum* chloroplast and *Methanobacterium thermoautotrophicum* enzyme,<sup>28</sup> as determined by X-ray crystallography.

The *Po. purpureum* CA monomer is composed of two internally repeating structures, being folded as a pair of fundamentally equivalent motifs of an  $\alpha/\beta$  domain and three projecting  $\alpha$ -helices. The motif is very distinct from that of either  $\alpha$ - or  $\gamma$ -CAs. This homodimeric CA appeared like a tetramer with a pseudo 2-2-2 symmetry.<sup>32</sup>  $\beta$ -CAs are thus very different from the  $\alpha$ -class enzymes. The Zn(II) ion is essential for catalysis in both families of enzymes, but its coordination is different and rather variable for the  $\beta$ -CAs: thus, in the prokaryotic  $\beta$ -CAs the Zn(II) ion is coordinated by two cysteinate residues, an imidazole from a His residue and a carboxylate belonging to an Asp residue (Figure 1.8A), whereas the chloroplast enzyme has the Zn(II) ion coordinated by the two cysteinates, the imidazole belonging to a His residue and a water molecule (Figure 1.8B).<sup>30-32</sup> The polypeptide chain folding and active site architecture are obviously very different from those of the CAs belonging to the  $\alpha$ -class. Since no water is directly coordinated to Zn(II) for some members of the  $\beta$ -CAs (Figure 1.8A), the main problem is whether the zinc-hydroxide mechanism presented in this chapter for the  $\alpha$ -CAs is valid also for enzymes belonging to the  $\beta$ -family. A response to this question has been given by Mitsuhashi *et al.*<sup>32</sup> who have proposed the catalytic mechanism shown below in Figure 1.9.

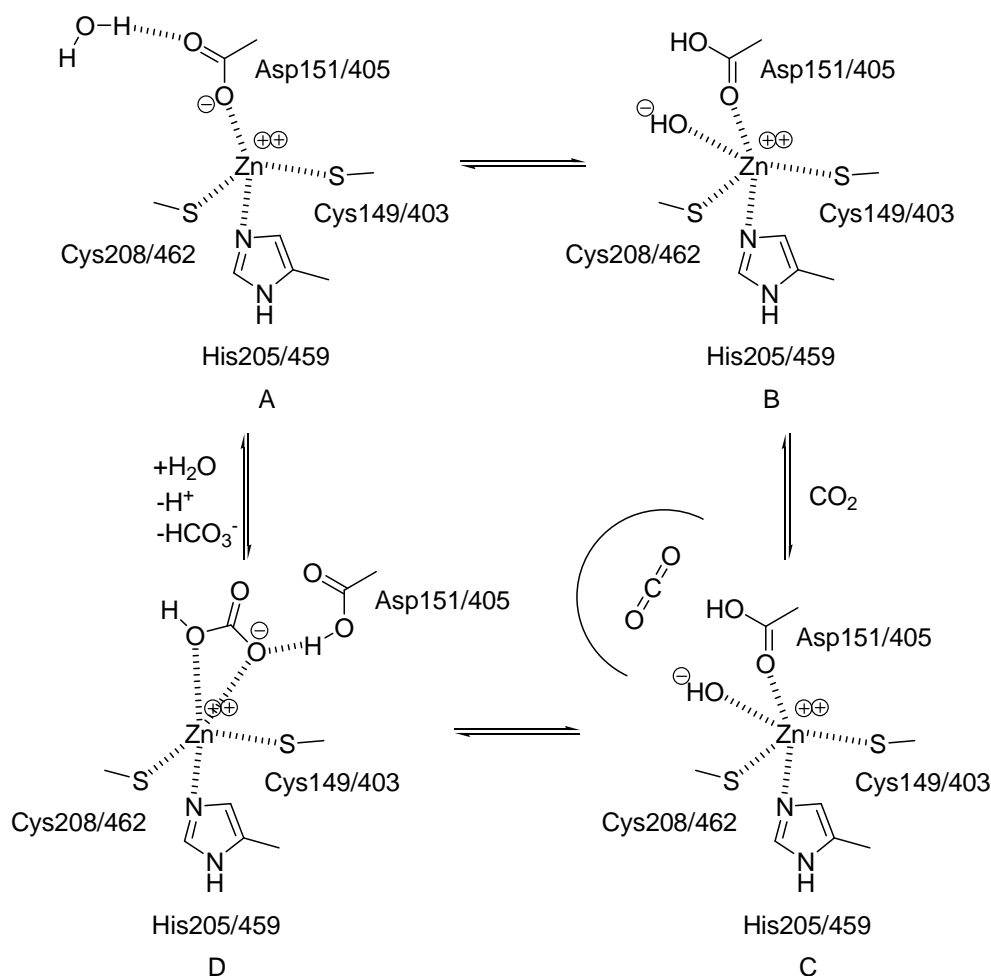


**Figure 1.9.** Proposed catalytic mechanism for prokaryotic  $\beta$ -CAs (*Porphyridium purpureum* enzyme numbering).

As there are two symmetrical structural motifs in one monomer of the *Po. purpureum* enzyme, resulting from two homologous repeats which are related to each other by a pseudo twofold axis, there are two Zn(II) ions coordinated by the four amino acids mentioned above. In this case these pairs are: Cys149/Cys403, His205/His459, Cys208/Cys462 and Asp151/Asp405.<sup>32</sup> A water molecule is also present in the neighbourhood of each metal ion, but it is not directly coordinated to it, forming a hydrogen bond with an oxygen belonging to the zinc ligand Asp151/Asp405 (Figure 1.9A). It is hypothesized that a proton transfer reaction may occur from this water molecule to the coordinated carboxylate moiety of the aspartate residue, with generation of a hydroxide ion which may be then coordinated to Zn(II), which acquires a trigonal-bipyramidal geometry (Figure 1.9B). Thus, the strong nucleophile which may attack CO<sub>2</sub> bound within a hydrophobic pocket of the enzyme is formed (Figure 1.9C), with generation of bicarbonate bound to Zn(II) (Figure 1.9D). This intermediate is rather similar to the reaction intermediate proposed for the  $\alpha$ -CA catalytic cycle (Figure 1.3C), except that for the  $\beta$ -

class enzyme, the aspartic acid residue, originally coordinated to zinc, is proposed here to participate in a hydrogen bond with the coordinated bicarbonate (Figure 1.9D). In the last step, the coordinated bicarbonate is released in solution, together with a proton (no details regarding this proton transfer process are available), the generated aspartate re-coordinates the Zn(II) ion, and the accompanying water molecule forms a hydrogen bond with it. The enzyme is thus ready for another cycle of catalysis.

The structure of the  $\beta$ -CA from the dicotyledonous plant *Pi. sativum* at 1.93 Å resolution has also been reported.<sup>30</sup> The molecule assembles as an octamer with a novel dimer of dimers arrangement. The active site is located at the interface between two monomers, with Cys160, His220 and Cys223 binding the catalytic zinc ion and residues Asp162 (oriented by Arg164), Gly224, Gln151, Val184, Phe179 and Tyr205 interacting with acetic acid. The substrate-binding groups have a one to one correspondence with the functional groups in the  $\alpha$ -CA active site, with the corresponding residues being closely superimposable by a mirror plane. Therefore, despite differing folds,  $\alpha$ - and  $\beta$ -CAs have converged upon a very similar active site design and are likely to share a common mechanism of action.<sup>30</sup> Cab exists as a dimer with a subunit fold similar to that observed in plant-type  $\beta$ -CAs. The active site zinc ion was shown to be coordinated by the amino acid residues Cys32, His87, and Cys90, with the tetrahedral coordination completed by a water molecule.<sup>55</sup> The major difference between plant- and cab-type  $\beta$ -CAs is in the organization of the hydrophobic pocket (except for the zinc coordination mentioned above). The structure also revealed a HEPES buffer molecule bound 8 Å away from the active site zinc, which suggests a possible proton transfer pathway from the active site to the solvent.<sup>55</sup> No structural data are available at this moment regarding the binding of inhibitors to this type of CAs, except for the fact that acetate coordinates to the Zn(II) ion of the *Pi. sativum* enzyme.<sup>52</sup>

$\beta$ -CAs from *Mycobacterium tuberculosis* have recently been cloned by Covarrubias *et al.*,<sup>29</sup> among them I'll talk about the kinetic and inhibition profile of the most active mtCA 2, encoded by gene Rv-3588c.

### 1.2.3 $\gamma$ -CAs

The prototype of the  $\gamma$ -class CAs, 'Cam', has been isolated from the methanogenic archaeon *Methanosarcina thermophila*.<sup>56</sup> The crystal structures of zinc-containing and cobalt-substituted Cam were reported in the unbound form and co-crystallized with sulfate or bicarbonate. Cam has several features that differentiate it from the  $\alpha$ - and  $\beta$ -CAs. Thus,

the protein fold is composed of a left-handed  $\beta$ -helix motif interrupted by three protruding loops and followed by short and long  $\alpha$ -helices. The Cam monomer self-associates in a homotrimer with the approximate molecular weight of 70 kDa.<sup>56</sup> The Zn(II) ion within the active site is coordinated by three histidine residues, as in  $\alpha$ -CAs, but relative to the tetrahedral coordination geometry seen at the active site of  $\alpha$ -CAs, the active site of this  $\gamma$ -CA contains additional metal-bound water ligands, so that the overall coordination geometry is trigonal-bipyramidal for the zinc-containing Cam and octahedral for the cobaltsubstituted enzyme. Two of the His residues coordinating the metal ion belong to one monomer (monomer A), whereas the third one is from the adjacent monomer (monomer B). Thus, the three active sites are located at the interface between pairs of monomers.<sup>56</sup> The catalytic mechanism of  $\gamma$ -CAs was proposed to be similar to the one presented for the  $\alpha$ -class enzymes (Figure 1.10).

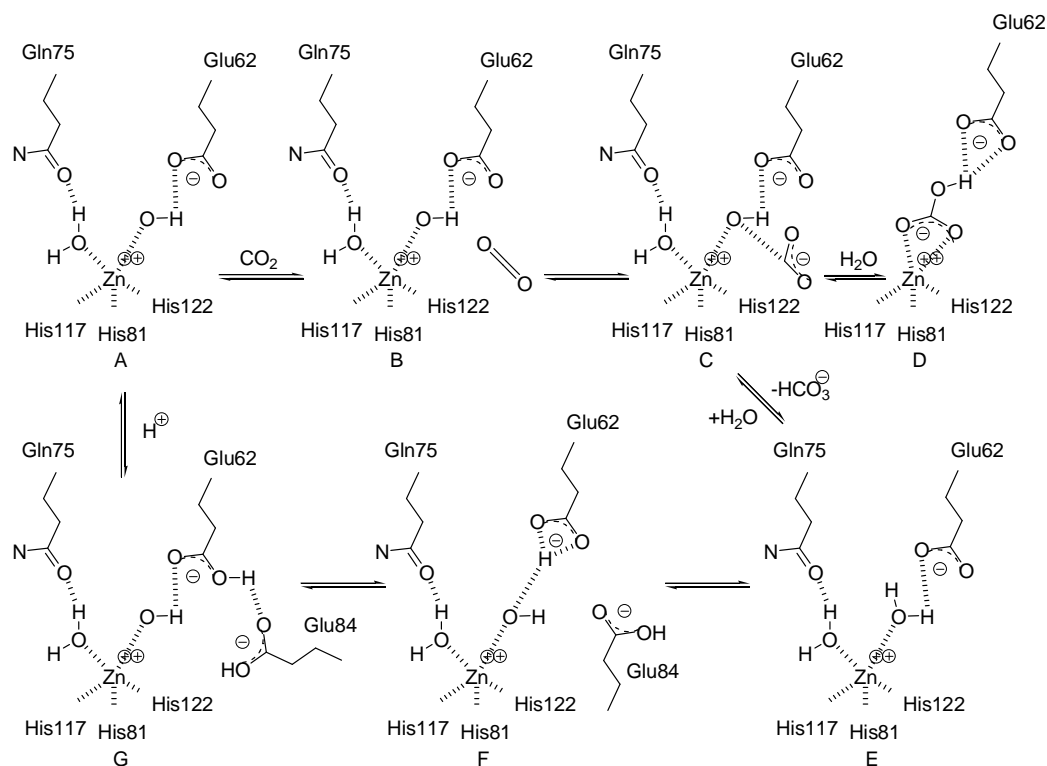


**Figure 1.10.** Proposed reaction mechanism for Cam. The reaction mechanism is drawn using Zn-Cam as the template. Co-Cam should have a similar reaction mechanism with an additional water molecule as an active site ligand. (A) Zn<sup>2+</sup> is coordinated to one water molecule and one hydroxide ion at the beginning of the first half-reaction. (B) Carbon dioxide enters the active site along the hydrophobic pocket. (C) Carbon dioxide is attacked by the hydroxide bound to the zinc. (D) The bicarbonate may have several stable binding modes. This bidentate binding mode, which requires loss of a metal ligand water molecule, is similar to that seen in the structure of Zn-Cam in complex with HCO<sub>3</sub><sup>-</sup>. (E) The first half-reaction ends with exchange of bicarbonate and a water molecule from the solvent. This state is crystallographically indistinguishable from that shown in state A, and may be represented by the structures of Zn-Cam or Co-Cam. (F) The second half-reaction begins with the deprotonation of one zinc-bound water molecule, with the proton transferred to Glu62. During this process, the side chain of Glu84 swings in so that it may accept the proton. This step is represented by the structure of water-liganded Zn-Cam with the Glu84 side chain. (G) The proton is passed from Glu62 to Glu84. With the transfer of proton to the solvent, the second half-reaction is complete and state A is regenerated.

Still, the finding that Zn(II) is not tetraordinated as originally reported but pentacoordinated, with two water molecules bound to the metal ion, demonstrates that much is still to be understood regarding these enzymes. At this moment, the zinc hydroxide mechanism is accepted as being valid for  $\gamma$ -CAs, as it is probable that an equilibrium exists between the trigonal–bipyramidal and the tetrahedral species of the metal ion from the active site of the enzyme.<sup>56</sup> Ligands bound to the active site were shown to make contacts with the side chain of Glu62 in a manner that suggests this side chain to be probably protonated. In the uncomplexed zinc-containing Cam, the side chains of Glu62 and Glu84 appear to share a proton; additionally, Glu84 exhibits multiple conformations. This suggests that Glu84 may act as a proton shuttle, which is an important aspect of the reaction mechanism of  $\alpha$ -CAs, for which a histidine active site residue generally plays this function, usually His64. Anions and sulfonamides were shown to bind to Cam.<sup>57,58</sup>

#### 1.2.4 $\delta$ -CAs

X-ray absorption spectroscopy at the Zn K-edge indicates that the active site of the marine diatom *Thalassiosira weissflogii* CA (TWCA1) is strikingly similar to that of mammalian  $\alpha$ -CAs. The zinc has three histidine ligands and a single water molecule, being quite different from the  $\beta$ -CAs of higher plants in which zinc is coordinated by two cysteine thiolates, one histidine and a water molecule.<sup>28</sup> The diatom carbonic anhydrase shows no significant sequence similarity with other carbonic anhydrases and may represent an example of convergent evolution at the molecular level. In the same diatom a rather perplexing discovery has been then made: the first cadmium-containing enzyme, which is a CA-type protein.<sup>34</sup> The marine diatom *T. weissflogii* growing under conditions of low zinc, typical of the marine environment, and in the presence of cadmium salts, led to increased levels of cellular CA activity, although the levels of TWCA1, the major intracellular Zn-requiring isoform of CA in *T. weissflogii*, remained low.<sup>34</sup> <sup>109</sup>Cd labelling comigrates with a protein band that showed this CA activity to be distinct from TWCA1 on native PAGE of radiolabelled *T. weissflogii* cell lysates. The levels of the Cd protein were modulated by CO<sub>2</sub> in a manner that was shown to be consistent with a role for this enzyme in carbon acquisition. Purification of the CA-active fraction leads to the isolation of a Cd-containing protein of 43 kDa being clear that *T. weissflogii* expresses a Cd-specific CA, which, particularly under conditions of Zn limitation, can replace the Zn enzyme TWCA1 in its carbon-concentrating mechanism.<sup>34</sup>



## CHAPTER TWO

### *Introduction to experimental data*

#### **2.1 Physiological functions of CAs, their inhibition and medicinal chemistry applications**

It is not clear whether other reactions catalyzed by CAs (Figure 1.2), except for CO<sub>2</sub> hydration/bicarbonate dehydration, have physiological relevance.<sup>2,20</sup> Thus, presently, only reaction 1.1 is considered to be the physiological one in which these enzymes are involved.

In prokaryotes, as shown also in the preceding sections, CAs possess two general functions: (i) transport of CO<sub>2</sub>/ bicarbonate between different tissues of the organism; (ii) provision of CO<sub>2</sub>/bicarbonate for enzymatic reactions.<sup>21</sup> In aquatic photosynthetic organisms, an additional role is that of a CO<sub>2</sub>-concentrating mechanism, which helps overcome CO<sub>2</sub> limitation in the environment.<sup>22,59</sup> For example, in *Chlamydomonas reinhardtii* this CO<sub>2</sub>-concentrating mechanism is maintained by the pH gradient created across the chloroplast thylakoid membranes by photosystem II-mediated electron transport processes.<sup>59</sup> A large number of non-photosynthetic prokaryotes catalyze reactions for which CA could be expected to provide CO<sub>2</sub>/bicarbonate in the nearby of the active site, or to remove such compounds in order to improve the energetics of the reaction.<sup>21</sup>

In vertebrates, including *Homo sapiens*, the physiological functions of CAs have widely been investigated over the last 70 years, but much is still to be learnt about this large family of metalloenzymes.<sup>19,23,28,60</sup> Thus, isozymes I, II and IV are involved in respiration and regulation of the acid/base homeostasis.<sup>19</sup> These complex processes involve both the transport of CO<sub>2</sub>/bicarbonate between metabolizing tissues and excretion sites (lungs, kidneys), facilitated CO<sub>2</sub> elimination in capillaries and pulmonary microvasculature, elimination of protons in the renal tubules and collecting ducts, as well as reabsorption of bicarbonate in the brush border and thick ascending Henle loop in kidneys.<sup>19</sup> Usually, isozymes I, II and IV are involved in these processes. By producing the bicarbonate-rich aqueous humor secretion (mediated by ciliary processes isozymes CA II, CA IV and CA XII) within the eye, CAs are involved in vision, and their malfunctioning leads to high intraocular pressure, and glaucoma.<sup>19</sup> CA II is also involved in the bone development and function, such as the differentiation of osteoclasts, or the provision of acid for bone

resorption in osteoclasts. CAs are involved in the secretion of electrolytes in many other tissues/organs, such as: CSF formation, by providing bicarbonate and regulating the pH in the choroid plexus; saliva production in acinar and ductal cells; gastric acid production in the stomach parietal cells; bile production, pancreatic juice production, intestinal ion transport.<sup>19,61</sup> CAs are also involved in gestation and olfaction, protection of gastrointestinal tract from extreme pH conditions (too acidic or too basic), regulation of pH and bicarbonate concentration in the seminal fluid, muscle functions and adaptation to cellular stress. Some isozymes, such as CA V, are involved in molecular signalling processes, such as insulin secretion signalling in pancreas  $\beta$  cells.<sup>19,61</sup> Isozymes II and VA are involved in important metabolic processes, as they provide bicarbonate for gluconeogenesis, fatty acids *ex novo* biosynthesis or pyrimidine base synthesis.<sup>19</sup> Finally, some isozymes (such as CA IX, CA XII, CARP VIII) are highly abundant in tumours, being involved in oncogenesis and tumour progression.<sup>60,62,63</sup>

## 2.2 Carbonic Anhydrase inhibitors (CAIs)

CAIs include the classical inhibitors acetazolamide (**AAZ**), methazolamide (**MZA**), ethoxzolamide (**EZA**), sulthiame (**SLT**) and dichlorophenamide (**DCP**). Further, they also include more recent drugs/investigational agents such as dorzolamide (**DZA**), brinzolamide (**BRZ**), indisulam (**IND**), topiramate (**TPM**), zonisamide (**ZNS**), sulpiride (**SLP**), **COUMATE** (**CMT**), **EMATE** (**EMT**), celecoxib (**CLX**), valdecoxib (**VLX**) and saccharin (**SAC**) (Chart 2.1; Table 2.1). Derivatives **A** and **B** are investigational agents for targeting the tumour-associated isoform CA IX. Many of these compounds were initially developed years ago in the search for diuretics; among them the thiazides, compounds **C1-5**, as well as derivatives **D-I** are still widely clinically used (Chart 2.1).<sup>2,19</sup> However, some of these enzyme inhibitors could also be used for the systemic treatment of glaucoma, and more recently, newer derivatives have been discovered showing the potential as topical antiglaucoma agents, as well as antitumour, anti-obesity or anti-infective drugs.<sup>2,19,62-72,39,73-76,43,77-79</sup>

The inhibitory effects of some of these clinically used drugs against the mammalian isoforms CA I – XIV, of human or mouse origin, are shown in Table 2.1.

**Table 2.1.** Inhibition data with selected sulfonamides/sulfamates against isozymes I–XIV\*

<b>K<sub>I</sub></b> (nM)	<b>Isozyme (h = human, m = mouse)</b>											
	<b>hCAI<sup>‡</sup></b>	<b>hCAII<sup>‡</sup></b>	<b>hCAIII<sup>‡</sup></b>	<b>hCAIV<sup>‡</sup></b>	<b>hCAVA<sup>‡</sup></b>	<b>hCAVB<sup>‡</sup></b>	<b>hCAVI<sup>‡</sup></b>	<b>hCAVII<sup>‡</sup></b>	<b>hCAIX<sup>§</sup></b>	<b>hCAXII<sup>§</sup></b>	<b>mCAXIII<sup>‡</sup></b>	<b>hCAXIV<sup>‡</sup></b>
<b>AAZ</b>	250	12	2x10 <sup>5</sup>	74	63	54	11	2.5	25	5.7	17	41
<b>MZA</b>	50	14	7x10 <sup>5</sup>	6.20	65	62	10	2.1	27	3.4	19	43
<b>EZA</b>	25	8	1x10 <sup>6</sup>	93	25	19	43	0.8	34	22	50	2.5
<b>SLT</b>	374	9	6.3x10 <sup>5</sup>	95	81	91	134	6	43	56	1450	1540
<b>DCP</b>	1200	38	6.8x10 <sup>5</sup>	15000	630	21	79	26	50	50	23	345
<b>DZA</b>	50000	9	7.7x10 <sup>5</sup>	8500	42	33	10	3.5	52	3.5	18	27
<b>BRZ</b>	45000	3	1.1x10 <sup>5</sup>	3950	50	30	0.9	2.8	37	3.0	10	24
<b>IND</b>	31	15	10400	65	79	23	14	122	24	3.4	11	106
<b>TPM</b>	250	10	7.8x10 <sup>5</sup>	4900	63	30	45	0.9	58 <sup>  </sup>	3.8	47	1460
<b>ZNS</b>	56	35	2.2x10 <sup>6</sup>	8590	20	6033	89	117	5.1	11000	430	5250
<b>SLP</b>	12000	40	10600	6.5x10 <sup>5</sup>	174	18	0.8	3.630	46	3.9	295	110
<b>CMT</b>	3450	21	7.0x10 <sup>5</sup>	24	765	720	653	23	34	12	1050	755
<b>EMT</b>	37	10	6.5x10 <sup>5</sup>	NT	NT	NT	NT	NT	30	7.5	NT	NT
<b>CLX</b>	50000	21	7.4x10 <sup>4</sup>	880	794	93	94	2170	16	18	98	689
<b>VLX</b>	54000	43	7.8x10 <sup>4</sup>	1340	912	88	572	3900	27	13	425	107
<b>SAC</b>	18540	5950	1.0x10 <sup>6</sup>	7920	10060	7210	935	10	103	633	12100	773
<b>A</b>	1300	45	1.3x10 <sup>6</sup>	650	134	76	145	18	24	5	76	33
<b>B</b>	4000	21	3.1x10 <sup>5</sup>	60	88	70	65	15	14	7	21	13
<b>C</b>	328	290	7.9x10 <sup>5</sup>	427	4225	603	3655	5010	367	355	3885	4105
<b>D</b>	35000	1260	NT	NT	NT	NT	NT	NT	NT	NT	NT	NT
<b>E</b>	54000	2000	6.1x10 <sup>5</sup>	216	750	312	1714	2.1	320	5.4	15	5432
<b>F</b>	348	138	1.1x10 <sup>4</sup>	196	917	9	1347	2.8	23	4.5	15	4130
<b>G</b>	51900	2520	2.3x10 <sup>5</sup>	213	890	274	1606	0.23	36	10	13	4950
<b>H</b>	62	65	3.2x10 <sup>6</sup>	564	499	322	245	513	420	261	550	52
<b>I</b>	4930	6980	3.4x10 <sup>6</sup>	303	700	NT	NT	NT	25.8	21.2	2570	250

\*The isoforms CA VIII, X and XI are devoid of catalytic activity and probably do not bind sulfonamides as they do not contain Zn<sup>2+</sup> ions. ‡Full-length enzyme. §Catalytic domain. ||The data against the full-length enzyme is of 1,590 nM. NT, not tested, data not available.

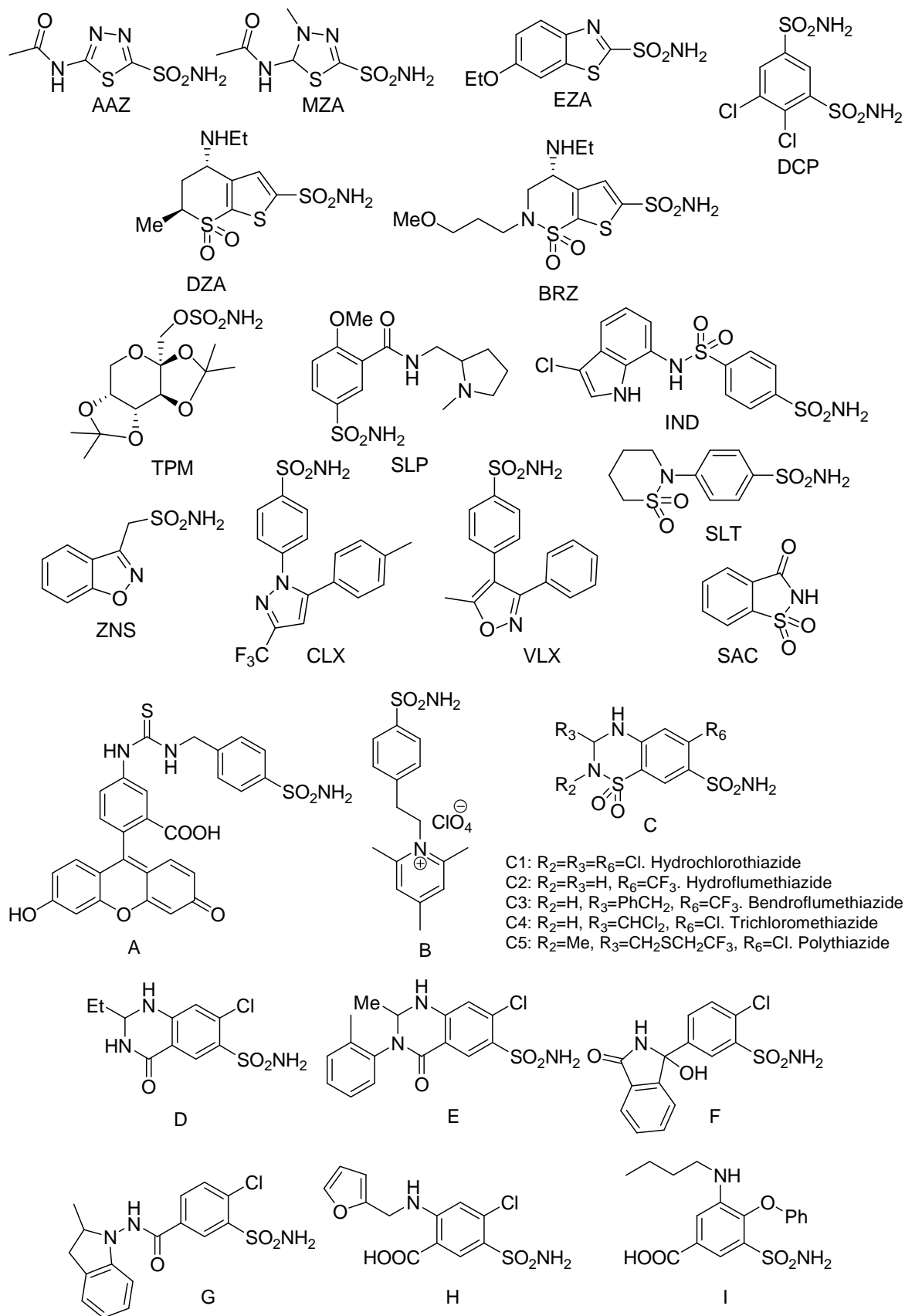


Chart 2.1. Structures of Carbonic Anhydrase inhibitors.

As specific isozymes are responsible for different biological responses, the diverse inhibition profiles of the various isozymes may explain the various actual and potential clinical applications of the CAIs, which range from diuretics and antiglaucoma agents, to anticancer, anti-obesity and anti-epileptic drugs. However, a crucial problem in CAI design is related to the high number of isoforms, their diffuse localization in many tissues and organs, and the lack of isozyme selectivity of the presently available inhibitors. It can be observed that there are sulfonamide- and sulfamate-avid isoforms, such as CA II, VI, VII, IX, XII and XIII, which generally show low nanomolar affinity for most of these inhibitors. Other isozymes, however, such as CA I, IV, VA, VB and XIV show less propensity to be inhibited by these compounds, with inhibition constants in the nanomolar to micromolar range. This leaves CA III as the only isoform that is not susceptible to inhibition by sulfonamides or sulfamates.

Few of the derivatives **AAZ-SAC** (Chart 2.1; Table 2.1) show selectivity for a specific isoform: the classical inhibitors, such as compounds **AAZ-DCP**, and the topically acting antiglaucoma sulfonamides **DZA** and **BRZ** together with indisulam, are promiscuous CAIs, with strong affinities for isoforms II, VA, VB, VI, VII, IX, XII, XIII and XIV.<sup>62,65-72,39,80</sup> Topiramate (**TPM**) is a subnanomolar CA VII inhibitor but it also effectively inhibits isoforms II, VB and XII.<sup>62,65-72,39,80</sup> Zonisamide (**ZNS**) shows a good affinity for CA IX but appreciably inhibits also CA II and VA, while having lower affinities for the other isoforms. Sulpiride (**SLP**) is a potent CA VI and CA XII inhibitor and shows lower affinity for other isoforms. Valdecoxib (**VLX**) is a strong CA XII inhibitor,<sup>62,65-72,39,80</sup> whereas Saccharin (**SAC**) is a CA VII-specific inhibitor ( $K_I$  of 10 nM against this isoform and much higher for the other CAs).<sup>73</sup>

Progress in the design of CA-selective and isozyme-specific CAIs has recently been made. Owing to the extracellular location of some CA isozymes, such as CA IV, IX, XII and XIV (Table 2.1), it is possible to design membrane-impermeant CAIs, which would therefore specifically inhibit membrane-associated CAs without interacting with the cytosolic or mitochondrial isoforms. This possibility has been explored through the design of positively charged sulphonamides that generally incorporate pyridinium moieties, compound **B** is a representative.<sup>74-76</sup> The inhibitors obtained in this way showed nanomolar affinities for CA II as well as CA IV and CA IX, and, more importantly, they were unable to cross the plasma membranes *in vivo*.<sup>74-76</sup> This new class of potent, positively charged CAIs, was able to discriminate between the membrane-bound and the cytosolic isozymes, selectively inhibiting only CA IV, in two model systems.<sup>74-76</sup> Another approach for the design of

isoform-selective CAIs exploited the presence of an Ala65 amino-acid residue, which is present only in the ubiquitous CA II mammalian isoform.<sup>43</sup> Compared with Topiramate, its sulfamide analogue is a 210-times less potent inhibitor of isozyme CA II, but effectively inhibits isozymes CA VA, VB, VII, XIII and XIV ( $K_{1s}$  in the range of 21 – 35 nM). The weak binding of the sulfamide analogue to CA II was shown to be due to a clash between one methyl group of the inhibitor with the Ala65 amino-acid residue, which might therefore be exploited for the design of compounds with lower affinity for this isoform.<sup>43</sup> A further approach for selectively inhibiting the tumour-associated isoforms CA IX (and XII) present in hypoxic tumour tissues envisaged bioreductive prodrugs that are activated by hypoxia.<sup>77,78</sup> The chosen strategy was to use the disulfide bond as a bioreducible function. The reducing conditions present in hypoxic tumours, in combination with the presence of the redox protein thioredoxin 1, mediates the reduction of the disulfide bond with the formation of thiols.<sup>77,78</sup> The reduced compounds (thiols) are less bulky and show excellent CA inhibitory activity (in the low nanomolar range) compared with the corresponding sterically hindered disulfides, which have difficulty entering the limited space of the enzyme active site.<sup>77,78</sup> Later in the text I'll talk about the coumarins, a chemotype with inhibitory activity towards CAs, able to develop selectivity for precise isoforms, exploiting their excellent ability to arrange in the active site.

### 2.3 Aim of the work

The body of my work is composed by manifold, heterogenous projects regarding various fields of Carbonic Anhydrase application. The main theme of this thesis concerns the study of coumarins as novel class of CAs inhibitors. This old and well-known chemical class recently emerged as potential inhibitor for CAs, showing the ability to exert, in some cases, interesting features of selectivity towards specific isoforms. As there is a desperate need to find out selective scaffolds, able to interact with desired enzymes, avoiding the rising of complications and side effects, the behaviour showed by the first coumarin studied as CA inhibitor (6-(1*S*-hydroxy-3-methylbutyl)-7-methoxy-2H-chromen-2-one, compound **1**, see below), prompted me to develop studies in this regard. In particular, I proceeded in three parallel ways: testing, with a stopped flow analyser, a library of variously substituted coumarins in order to increase SAR informations; synthesizing a series of coumarin derivatives, designed from considerations about compound **1**; synthesizing a series of coumarins, obtained with a “click chemistry” strategic approach. From this work emerged a series of 8-acethoxy-7-ether-coumarins (compounds **34**, **42-47**),



Finally, I considered one of the most interesting applications for CA inhibitors: the design of sulfonamidic derivatives as selective CA VA and VB (located in mitochondria) inhibitors, as antiobesity agents. The considered strategy for this synthesis was the so called “tail approach” which consists in coupling an aromatic/heterocyclic sulfonamidic scaffold with a particularly substituted portion. In this case I used, the two enantiomers of ( $\pm$ )-10-camphorsulfonyl chloride, in order: to increase the intrinsic lipophilicity of such derivatives (allowing them to pass through the cellular membrane); to equip such scaffolds with a mobile carbonic frame, able to rearrange itself inside the cavity of the active site to interact eventually with allosteric side portions; to study how the different geometries of the stereogenic centers could modulate the affinity and the activity of such molecules towards the different CAs isoforms. The new sulfonamides selectively inhibited the mitochondrial isoenzymes, over the two offtarget hCA I and II, with inhibition constants in the low nanomolar range. The nature, the chirality and position of the substituting groups greatly influenced CA inhibitory properties.

# ***EXPERIMENTAL SECTION***

## CHAPTER THREE

### *Coumarins: a novel chemotype for CA inhibition*

#### 3.1 Discovery and initial screenings

In 2008, through a screening of natural product extracts using electrospray ionization Fourier transform ion cyclotron resonance mass spectrometry (ESI-FTICR-MS), Vu *et al.* discovered<sup>81</sup> that compound **1** was able to bind in a non-covalent mode bovine CA II. Derivative **1**, named 6-(1*S*-hydroxy-3-methylbutyl)-7-methoxy-2H-chromen-2-one (Chart 3.1), was a natural product isolated from the plant *Leionema ellipticum*, typical of the eastern Australia. The relevance of this study and the possibility to find new CAs-affine substrates, other than sulfonamides or their bioisosteres, prompted me to confirm the effective inhibitory activity of **1**, assaying it on the 13 catalytically active mammalian isoforms of CA, in comparison with other two commercially available coumarins: the unsubstituted coumarin **2** and its 7-methoxy derivative **3** (Chart 3.1).

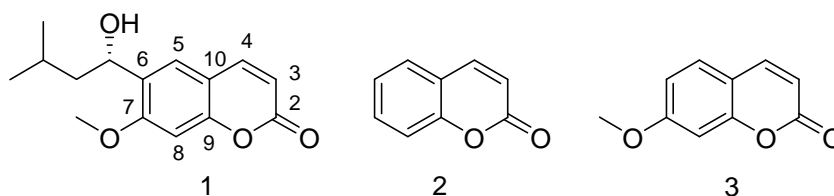


**Chart 3.1.** Structures of compounds **1-3**.

Working with all other types of CAIs (sulfonamides, phenols, complexing inorganic anions), a period of 15 minutes is enough to form the enzyme-inhibitor complex and test the effective inhibitory activity.<sup>82-84,50,85</sup> In the same conditions, working with coumarins, I was not able to detect any significant decrease in enzyme activity, but only a weak micromolar to millimolar inhibition profile (data not shown). However I hypothesized that the incubation time was able to modulate the inhibition profile of such derivatives and I decided to extend it, measuring the inhibition constants ( $K_I$ ), after 30 min, 1 h, 4 h, 6 h and 24 h of incubation. For all investigated CA isoforms a progressive decrease, in terms of inhibition constants, was observed as the incubation time increased up to 6 h; while from 6 to 24 h of incubation no further changes of  $K_I$  were evidenced. Table 3.1 shows the  $K_I$  values ( $\mu\text{M}$ ) for compounds **1-3** following 6 h of incubation with the  $\alpha$ -CA I-XV.

**Table 3.1.** Inhibition of Mammalian Isozymes CA I-XV with Coumarins 1-3 by a Stopped-Flow, CO<sub>2</sub> Hydration Assay Method<sup>82</sup>

<i>isozyme</i> <sup>a</sup>	$K_I$ ( $\mu$ M) <sup>c</sup>		
	<i>1</i> <sup>d</sup>	<i>2</i> <sup>d</sup>	<i>3</i> <sup>d</sup>
<i>hCA I</i>	0.08	3.1	5.9
<i>hCA II</i>	0.06	9.2	0.07
<i>hCA III</i>	>1000	>1000	161
<i>hCA IV</i>	3.8	62.3	7.8
<i>hCA VA</i>	96.0	>1000	645
<i>hCA VB</i>	17.7	578	48.6
<i>hCA VI</i>	35.7	>1000	61.2
<i>hCA VII</i>	27.9	>1000	9.1
<i>hCA IX</i> <sup>b</sup>	54.5	>1000	767
<i>hCA XII</i> <sup>b</sup>	48.6	>1000	167.4
<i>mCA XIII</i>	7.9	>1000	6.0
<i>hCA XIV</i>	7.8	>1000	9.7
<i>mCA XV</i>	93.1	>1000	>1000

<sup>a</sup> h ) human; m ) murine isozyme; nt ) not tested. <sup>b</sup> Catalytic domain. <sup>c</sup> Errors in the range of  $\pm 5\%$  of the reported data from three different assays. <sup>d</sup> Preincubation of 6 h between enzyme and inhibitor.

Against isoforms I and II (ubiquitous, cytosolic CAs)<sup>1</sup> **1-3** show effective inhibition, with  $K_{IS}$  in the range 80 nM-5.9  $\mu$ M (hCA I) and 60 nM-9.2  $\mu$ M (hCA II), respectively. The best hCA I and II inhibitor was always the natural product **1**. The remaining CA isoforms were typically inhibited only weakly by the simple coumarin derivatives **2** and **3** (many of them showed  $K_{IS} > 1000 \mu$ M) with few exceptions: notably compound **3** against CA IV, VII, XIII, and XIV ( $K_{IS}$  in the range 6.0-9.1  $\mu$ M). The natural product **1** was an effective inhibitor of all CAs investigated here (except CA III,  $K_I > 1000 \mu$ M), with inhibition constants in the range 3.8-93.1  $\mu$ M against isoforms CA IV-XV (Table 3.1). The results observed with this panel of coumarin derivatives showed that there was a wide distribution of inhibition constants for the same compound against the various CA isoforms (e.g., **1** showed inhibition constants in the range 59 nM-1000  $\mu$ M). The inhibitory properties of **1-3** were also dependent on the substitution pattern of the coumarin ring, with the number of these groups influencing inhibitory activity. The least active coumarin **2** lacked substitution on the aromatic coumarin scaffold and coumarin **1** had two substituents (in the 6 and 7 positions), while coumarin **3** had a single substituent (7 position). For all these considerations, this chemotype immediately emerged as a promising opportunity to obtain potent and potentially isozyme-selective inhibitors for CAs. To understand the inhibitory mechanism with this new class of CAI, one of our collaborators resolved the X-ray crystal structure (at a resolution of 2.0 Å) of the most novel and potent of these inhibitors, coumarin **1**, in adduct with the physiologically dominant CA isoform, hCA II.<sup>1,51</sup>

Inspection of the electron density maps (Figure 3.1) at various stages of the refinement showed features compatible with the presence of one molecule of inhibitor bound within the active site, but compound **1** could not be fitted in the observed electron density. Instead, its hydrolysis product, the *cis*-2-hydroxy-4-(1*S*-3-methylbutyl)-3-methoxy-cinnamic acid **4Z** (Scheme 1), perfectly fitted within this electron density (Figure 3.1).

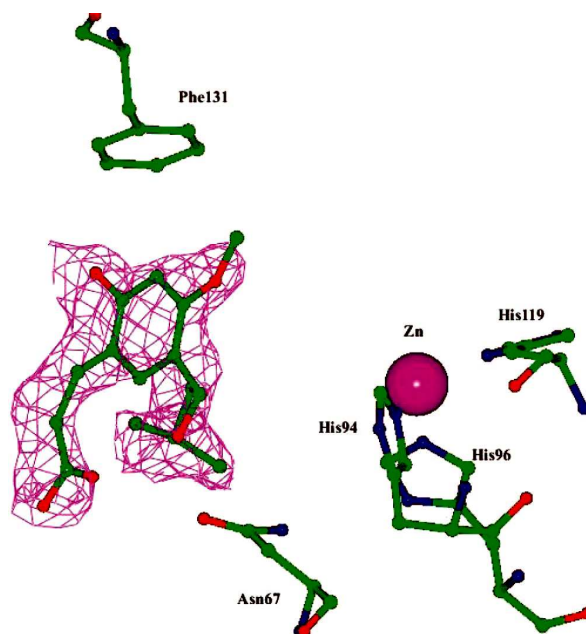
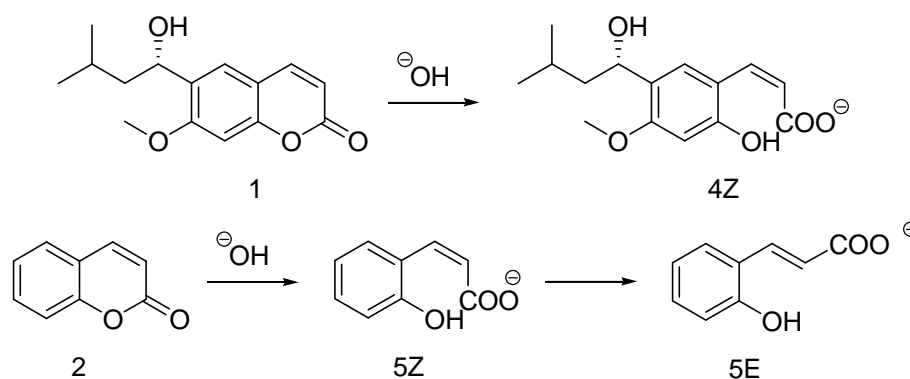


**Figure 3.1.** Omit map corresponding to the hydrolyzed coumarin **1** (i.e., the *cis*-2-hydroxy-cinnamic acid derivative **4Z**), of some relevant CA II active site residues and the Zn(II) ion (violet sphere).



**Scheme 3.1.** Hydrolysis of Coumarins **1** and **2** to the corresponding hydroxy-cinnamic acid derivatives **4Z** and **5Z/5E**.

The zinc bound hydroxide anion of the CA enzyme, responsible for the various catalytic activities of CAs,<sup>1,86</sup> including the esterase activity,<sup>87</sup> appeared likely to have hydrolyzed the lactone ring of **1** leading to the formation of **4Z**. The inhibitor **4Z** was found bound at the entrance of the active site cavity (Figure 3.2) with the two bulky arms in an extended

conformation effectively plugging this entrance. The hydroxypentyl arm oriented toward the hydrophilic half of the active site, while the *cis*-carboxyethylene arm pointed toward the hydrophobic half. In particular, the 1*S*-OH moiety of the hydroxypentyl arm exerted a strong dipole-dipole interaction with the carbonyl oxygen of the side chain of Asn67; an edge-to-face (CH- $\pi$ )<sup>88,89</sup> stacking between the aromatic ring of **4Z** and the phenyl group of Phe131 was also evidenced (with a distance of  $\sim 3.5$  Å between them), while three active site water molecules further stabilized the interaction of **4Z** with the enzyme (Figure 3.2). This binding mode was totally different, compared to the other CAIs classes mechanism, characterized by the total absence of any direct interaction with the catalytic metal ion.

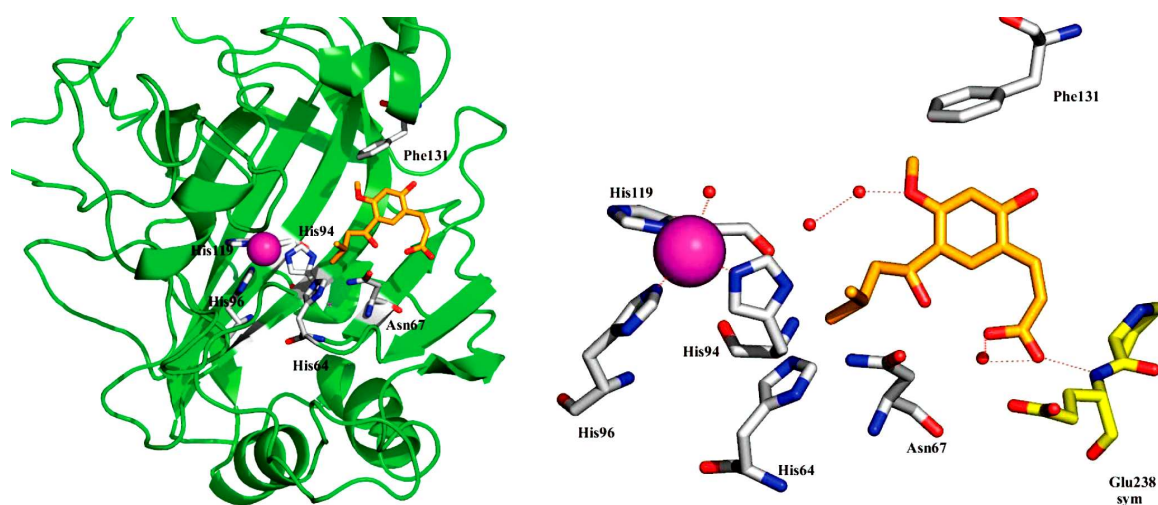


**Figure 3.2.** A) The hCA II-**4Z** adduct. B) Detailed interactions between CA II and inhibitor **4Z** when bound to the enzyme. The catalytic Zn(II) ion is shown as violet sphere, with its three His ligands (His94, 96, and 119) and coordinated water molecule (red smaller sphere) also evidenced. The inhibitor molecule (gold) interacts with three active site ordered water molecules (red spheres), with Phe131 and Asn67 (CPK colors) from the active site as well as with Glu238sym (yellow) from a symmetry related enzyme molecule. The proton shuttle residue His64 is also shown (CPK colors).

Another important consideration emerged from the crystallographic studies: looking at the superposition<sup>90</sup> of compounds **1** and **2** (Figure 3.3), complexed with hCAII, was evident that the first one, in its hydrolyzed form **4Z**, was bound within the cavity of the active site, as the *cis* isomer, while the second one, always in its 2-hydroxy-cinnamic acid derivative **5E**, was bound in its *trans* isomer, more stable in thermodynamic terms. We tried to explain this unusual bound geometry in terms of steric hindrance: the cinnamic derivative of **1**, in its *trans* isomer derivative, would be too bulky in the restricted space of the active site, that was able to promote even the less stable *cis* form.

This evidence prompted me to consider the substitution pattern on the benzopyrone ring as the key element to modulate the orientation of the molecule within the active site, in a zone

that, all over the  $\alpha$ -CAs, is very diversified; with the possibility to develop selectivity towards particular CA isoforms.

To resume, the unusual binding mode, the time dependent inhibitory activity and the variation on the inhibition profile related to little modifications on the substitution pattern, introduced the coumarin chemotype as a very interesting research field in the Carbonic Anhydrase inhibition. The next step in my study, was to gain other structure-activity relationship data; so I tested some variously substituted coumarin and thiocoumarin derivatives, to bring novel insights regarding the inhibition mechanism as well as the structural requirements for such heterocyclic compounds to show pronounced affinity towards the various CA isoforms.

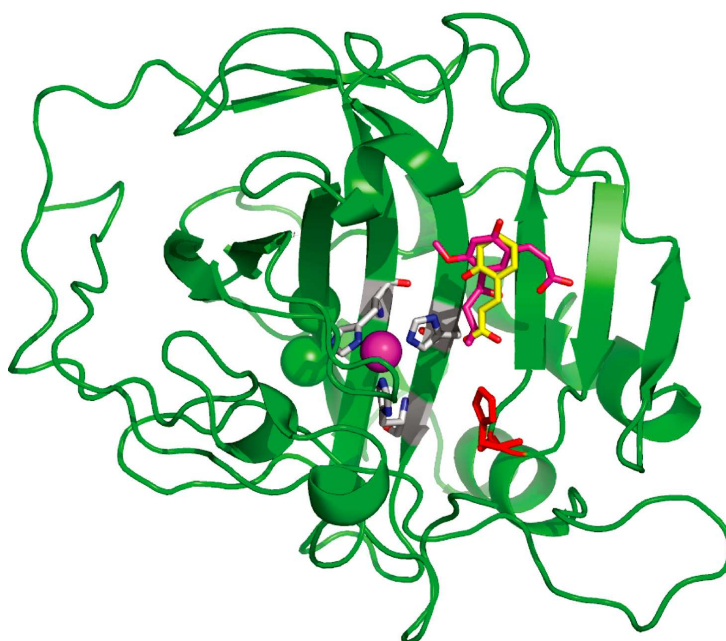


**Figure 3.3.** Binding of the coumarin **2** hydrolysis product (*trans*-2-hydroxy-cinnamic acid **5E** in yellow) and coumarin **1** hydrolysis product (*cis*-2-hydroxycinnamic acid **4Z**, magenta) to the hCA II active site.<sup>90</sup>

With the one of our collaborating groups, I included in this new study a series of diversely substituted coumarins and thiocoumarins, of type **6-23** (Chart 3.2). Such derivatives incorporated different moieties, in the 3-, 6-, 7-, 3,6-, 4,7-, and 3,8- positions of the (thio)coumarin ring; they were considered in order to delineate the initial SAR features for this class of CAI, considering that the side chains present in the natural product coumarin **1**, were shown to interact extensively with the enzyme active site when bound (in hydrolyzed form) within it.<sup>51</sup> The 7-monosubstituted coumarins, **6-10** possessed various 7-alkoxy moieties, such as the aliphatic C2-C4 groups, together with the benzyl- and phenethyl- moieties. They were chosen to be investigated as the 7-methoxy group was present in the lead **1**, and X-ray crystal data for the hCA II-**1** adduct, showed the methoxy

group to participate in hydrogen bonds with ordered water molecules present within the CA active site, stabilizing thus the enzyme-inhibitor complex.<sup>51</sup> Thus, observing the way the length and nature of this moiety could influence inhibitory activity, seemed to constitute an important aspect of the SAR.

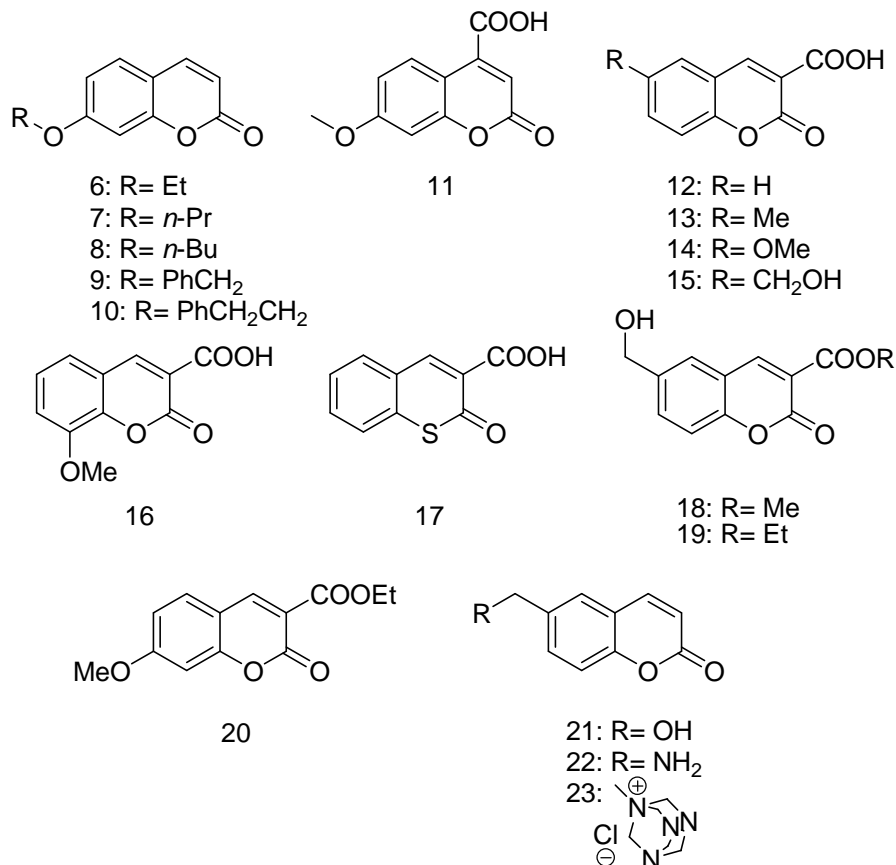


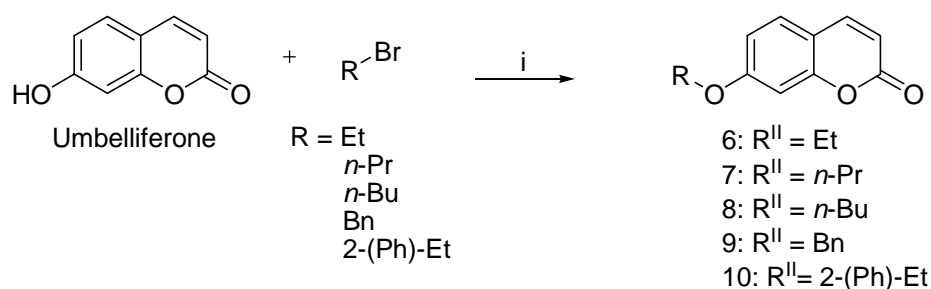
**Chart 3.2.** (Thio)coumarin derivatives **6-23** for SAR study.

Disubstituted coumarins **11-16**,<sup>91-93</sup> possessing a carboxylic acid as well as methyl-, methoxy-, and hydroxymethyl moieties in various positions of the ring, were also included in the study. Thiocoumarin **17**<sup>94</sup> was the only compound incorporating this ring system in our study and was chosen to understand whether substitution of oxygen by sulphur in the coumarin ring led to CA inhibitory properties for this class of compounds never investigated before, but also because the corresponding carboxy-substituted coumarin **12** was present among the investigated derivatives. Disubstituted coumarins **18-20**<sup>91-93</sup> incorporated ester moieties instead of the corresponding carboxylic acid present in the parent compound **15**, whereas **20** was an ester analogue of the simple lead **3**, investigated earlier.<sup>51</sup> Because the lead **1** possessed a bulky moiety in position 6 of the coumarin ring, derivatives **21-23**<sup>91-93</sup> were included in the study due to the presence of both smaller, simpler such moieties (hydroxymethyl and aminomethyl), which can be easily derivatized,

and also of the much bulkier hexamethylene-tetramine one, present in **23**. Compounds **6-10** were prepared from the commercially available 7-hydroxy-coumarin (umbelliferone), by alkylation in Williamson conditions, with alkyl/arylalkyl halides, in presence of sodium hydride, as described in the literature (Scheme 3.2).<sup>95</sup>

Compounds **11-23** were reported earlier in the search of serine protease inhibitors by Delarge's and Masereel's groups.<sup>91-94</sup>

Scheme 3.2. Synthesis of derivatives **6-10**.<sup>95</sup>



i: dry DMF, NaH 60%, r.t, 16h

Inhibition data for compounds **6-23** against all 13 catalytically active mammalian (h = human, m = murine) CA isoforms, CA I-IV, VA, VB, VI, VII, IX, and XII-XV, are presented in Table 3.2.

**Table 3.2.** Inhibition of Mammalian Isozymes CAI-XV(h=Human,m=Murine Isoform) with Coumarins/Thiocoumarins **6-23**, by a Stopped-Flow, CO<sub>2</sub> Hydration Assay Method (6 h Incubation Time between Enzyme and (Thio)coumarin).<sup>82</sup>

<b>K<sub>I</sub> (μM)<sup>c</sup></b>									
<i>isozyme<sup>a</sup></i>	<b>6</b>	<b>7</b>	<b>8</b>	<b>9</b>	<b>10</b>	<b>11</b>	<b>12</b>	<b>13</b>	<b>14</b>
<b><i>hCA I</i></b>	31.4	23.1	37.0	26.9	31.4	3.72	9.3	6.8	6.6
<b><i>hCA II</i></b>	12.4	145	213	224	243	0.099	44.7	42.5	15.3
<b><i>hCA III</i></b>	29.0	38.6	50.3	40.2	49.5	>500	9.1	13.4	14.5
<b><i>hCA IV</i></b>	22.7	24.6	24.9	19.2	18.5	72.3	3.8	5.6	4.9
<b><i>hCA VA</i></b>	7.3	8.1	9.0	7.6	6.6	>500	9.0	8.6	8.7
<b><i>hCA VB</i></b>	6.09	71.7	76.4	65.1	69.4	>500	6.8	8.3	7.6
<b><i>hCA VI</i></b>	5.8	37.4	26.8	9.7	8.5	>500	31.3	31.7	10.5
<b><i>hCA VII</i></b>	7.2	7.7	15.0	11.8	15.9	9.4	5.1	29.6	4.9
<b><i>hCA IX<sup>b</sup></i></b>	1.6	3.3	4.5	1.7	3.9	>500	4.7	7.7	6.6
<b><i>hCA XII<sup>b</sup></i></b>	4.7	8.6	8.5	8.3	5.2	>500	9.0	8.6	9.0
<b><i>mCA XIII</i></b>	27.4	34.3	8.2	9.6	9.8	31.7	7.3	7.4	3.8
<b><i>hCA XIV</i></b>	4.7	5.0	4.3	2.0	5.5	82.3	7.4	13.0	39.6
<b><i>mCA XV</i></b>	76.3	54.7	65.2	43.1	44.5	>500	5.6	6.7	7.2

$K_I$ ( $\mu\text{M}$ ) <sup>c</sup>									
isozyme <sup>a</sup>	<b>15</b>	<b>16</b>	<b>17</b>	<b>18</b>	<b>19</b>	<b>20</b>	<b>21</b>	<b>22</b>	<b>23</b>
<b>hCA I</b>	9.3	1.3	0.100	0.098	3.3	2.4	7.8	7.1	4.1
<b>hCA II</b>	44.5	30.1	6.2	0.032	50.5	31.4	32.4	3.7	3.2
<b>hCA III</b>	9.7	17.1	9.0	8.9	9.6	9.1	9.8	9.6	8.1
<b>hCA IV</b>	4.3	5.8	4.1	6.5	0.048	5.7	5.1	5.4	6.2
<b>hCA VA</b>	6.2	9.4	8.4	8.4	3.0	9.5	8.9	9.7	8.2
<b>hCA VB</b>	8.6	6.5	7.5	7.1	2.9	8.0	6.8	6.2	5.6
<b>hCA VI</b>	15.6	25.6	8.8	9.5	1.5	42.0	9.9	9.2	8.9
<b>hCA VII</b>	6.6	6.1	7.3	7.3	0.045	20.3	6.9	8.1	3.1
<b>hCA IX<sup>b</sup></b>	5.6	7.4	0.047	0.045	0.047	6.5	0.093	6.7	0.048
<b>hCA XII<sup>b</sup></b>	8.9	8.6	8.7	5.6	8.4	8.8	8.2	8.6	3.2
<b>mCA XIII</b>	0.048	7.8	0.042	0.041	6.1	6.2	0.046	0.040	3.8
<b>hCA XIV</b>	8.4	1.0	7.4	7.3	4.6	9.6	9.5	8.8	7.7
<b>mCA XV</b>	8.6	6.4	4.8	7.4	0.046	6.6	7.4	7.1	8.2

<sup>a</sup> h ) human; m ) murine isozyme. <sup>b</sup> Catalytic domain. <sup>c</sup> Errors in the range of  $\pm 5\%$  of the reported data from three different assays.

From Table 3.2 the following considerations emerged as interesting:

1. Isoform hCA I was inhibited by all coumarins/thiocoumarin **6-23**, with inhibition constants in the range of 78 nM-37.0  $\mu\text{M}$ . The best inhibitors were the thiocoumarin **17**, as well as the hydroxy-methyl-substituted ester **18** ( $K_I$ s of 78-100 nM). Substitution patterns leading to reduced hCA I inhibitory activity were those present in **6-10** (longer aliphatic/arylalkyl chains in position 7 are thus detrimental to the inhibitory activity of these compounds compared to the unsubstituted **2** or methoxysubstituted compound **5**) and **11** (possessing a 4-carboxy moiety) because these derivatives showed  $K_I$ s  $> 9.3 \mu\text{M}$ . The remaining coumarins investigated here were medium potency hCA I inhibitors, with inhibition constants in the range of 1.3-9.3  $\mu\text{M}$
2. The physiologically dominant cytosolic isozyme hCA II was also inhibited by all these derivatives, with inhibition constants in the range of 32 nM-243  $\mu\text{M}$ . The best inhibitor was again the methyl ester **18** ( $K_I$  of 32 nM) the carboxylic acid **11** ( $K_I$  of 99 nM). Again, the monosubstituted derivatives **6-10** incorporating bulky chains in position 7 of the coumarin ring showed reduced inhibitory activity compared to the lead **3** ( $K_I$ s of 12.4-243  $\mu\text{M}$ ), proving that substituents other than methoxy are not tolerated in that position for effective binding to hCA II. Not very effective hCA II inhibitors were also derivatives **12-16**, possessing the free COOH moiety in position 3. The thiocoumarin **17** was on the other hand a more effective inhibitor

( $K_I$  of 6.2  $\mu\text{M}$ ). It is, however, worth noting that there is a very large difference of activity between the carboxylic acid **15** and the corresponding esters **18** and **19**, with the methyl ester **18** being a very potent, nanomolar inhibitor ( $K_I$  of 32 nM), whereas the free acid **15** and the ethyl ester **19** were 1390-1578 times less effective hCA II inhibitors. Such a sharp SAR for minimal structural changes (i.e., a  $\text{CH}_2$  group) was never before evidenced for other classes of CAIs, such as the sulfonamides or the sulfamates,<sup>19</sup> and constitutes a valuable feature for this type of inhibitor.

3. The muscle isoform hCA III, which is not easily inhibited by sulfonamides,<sup>80</sup> was weakly or not at all inhibited by coumarins **11** ( $K_{IS}$  of 161 f 500  $\mu\text{M}$ ), whereas coumarins **6-10** and **13, 14** showed more efficient inhibitory activity, with  $K_{IS}$  in the range of 13.4-50.3  $\mu\text{M}$ . Even better activity was observed for the thiocoumarin **17** and coumarins **12, 15, 18-23**, with  $K_{IS}$  in the range of 8.1-9.8  $\mu\text{M}$ .
4. The coumarin ester **19** was a nanomolar inhibitor of the extracellular isoform hCA IV ( $K_I$  of 48 nM), whereas most other such derivatives (e.g., **12-18** and **20-23**) showed effective inhibition, in the low micromolar range, with  $K_{IS}$  of 3.8-7.8  $\mu\text{M}$ . Compounds with bulky groups in position 7 of the coumarin ring such as **6-10** showed also weak inhibition ( $K_{IS}$  of 18.5- 24.9  $\mu\text{M}$ ) compared to the methoxy-substituted coumarin **3**.
5. The mitochondrial isoform hCA VA was not inhibited by **11** ( $K_I > 500 \mu\text{M}$ ) but all other coumarins investigated here and the thiocoumarin **17** were, on the other hand, effective low micromolar hCA VA inhibitors ( $K_{IS} < 10 \mu\text{M}$ ), with the best inhibitor being the ester **19** ( $K_I$  of 3.0  $\mu\text{M}$ ). Thus, in the case of this isozyme, even the bulky derivatives **6-10** act as efficient CAIs.
6. The second mitochondrial isoform, hCA VB, showed a very different inhibition profile with compounds **6-23** compared to hCA VA. Thus, **11** showed no inhibitory activity ( $K_I > 500 \mu\text{M}$ ), the monosubstituted derivatives **6-10** were weak inhibitors ( $K_{IS}$  in the range of 60.9-76.4  $\mu\text{M}$ ), whereas the remaining coumarins **12-16** and **18-23**, as well as the thiocoumarin **17**, were effective hCA VB inhibitors, with inhibition constants in the range of 2.9-8.6  $\mu\text{M}$ . Even in this case, minimal structural changes in the coumarin scaffold influenced very much the inhibitory activity.
7. The secreted (saliva, milk) isoform hCA VI was not inhibited by **11** ( $K_I > 500 \mu\text{M}$ ), and was weakly inhibited by the following coumarins: **7, 8, 12, 13, 15, 16**, and **20**

( $K_{iS}$  in the range of 15.6-61.2  $\mu\text{M}$ ). Thus, SAR is less defined here compared to other CA isoforms discussed above (e.g., for the bulky-substituted compounds **6-10**, there is no linear correlation between the length of the substituent present in the 7 position and the hCA VI inhibitory activity). Effective hCA VI inhibitory activity ( $K_{iS}$  in the range of 1.5-10.5  $\mu\text{M}$ ) was observed for derivatives **6, 9, 10, 14, 17** (thiocoumarin), **18, 19**, and **21-23**. The best inhibitor was the ester **19** ( $K_I$  of 1.5  $\mu\text{M}$ ).

8. The cytosolic isoform hCA VII was inhibited by all compounds **6-23** investigated here, with  $K_{iS}$  in the range of 45 nM-29.6  $\mu\text{M}$ . The only nanomolar inhibitor was the ester **19** ( $K_I$  of 45 nM), whereas most of these derivatives were low micromolar inhibitors. The least effective inhibitors were **1, 13**, and **20** ( $K_{iS}$  in the range 20.3-29.6  $\mu\text{M}$ ). Again, small structural variations in the coumarin scaffold led to important differences of activity (e.g., the comparison between **12** and **13**, differing by a methylene unit but by a factor of almost 6 in their CA VII inhibitory activity).
9. A large number of derivatives showed effective or very effective inhibitory activity against hCA IX, which represents a new drug target for developing antitumor therapies or diagnostic agents.<sup>7,9,63</sup> Thus, thiocoumarin **17** and several coumarins (**18, 19, 21**, and **23**) showed low nanomolar affinity for this enzyme, with inhibition constants in the range of 45-98 nM. These coumarins incorporated the 6-hydroxymethyl- and 3-ester moieties (**18** and **19**), with no important differences of activity between the methyl and ethyl esters in this case. The monosubstituted derivatives **21** and **23** on the other hand contained either a compact ( $\text{CH}_2\text{OH}$ ) or a rather bulky (hexamethylenetetramine) group in position 6 of the coumarin ring, which render these findings quite important, as it was clear that for effective CA IX inhibition, a large variations of structural motifs were allowed in the 3- and 6-positions of the (thio)coumarin ring. It was interesting to note that the isostructural (to **21**) amine **22**, was 72 times less potent than the alcohol **21**. It was not improbable that the enhanced basicity of the amine **22**, compared to the alcohol **21**, resulted detrimental to binding within the enzyme active site, due to a different pattern hydrogen bonds between the two moieties and amino acid residues at the entrance of the cavity, where presumably these moieties are found. However this hypothesis has to be checked by X-ray crystallography, which will raise new understandings regarding the way of various substituents on the coumarin ring to interact with amino acid residues within the enzyme active site. The remaining

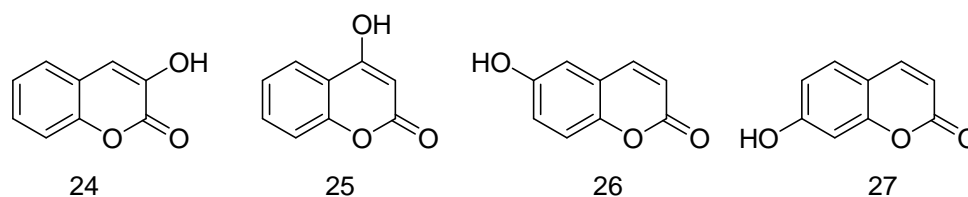
coumarins, e.g., **6-10**, **12-16**, **20**, and **21**, showed efficient, low micromolar inhibition of CA IX, with inhibition constants in the range of 1.6-7.7  $\mu\text{M}$ . It may be seen that many substitution patterns on the (thio)coumarin ring led to effective nanomolar-low micromolar CA IX inhibitors, affording for drug design campaigns for this important drug target.<sup>1</sup>

10. Most of the investigated (thio)coumarins were effective, low micromolar inhibitors on hCA XII, another transmembrane isoform present in tumors, with  $K_{\text{IS}}$  in the range of 3.2-9.0  $\mu\text{M}$ . Thus, a lot of substitution patterns present in compounds **6-23** investigated here showed effective inhibition, although compounds with nanomolar affinity for this isozyme were not evidenced so far.
11. Several low nanomolar mCA XIII inhibitors were observed among the investigated compounds, such as the thiocoumarin **17** and the coumarins **15**, **18**, **21**, and **22**, possessing inhibition constants of 40-48 nM. Together with CA IX, CA XIII is thus the isoform leading to the highest number of nanomolar inhibitors in this class of derivatives. Unlike other isoforms, CA XIII was equally inhibited by the free carboxylic acid **15** and its methyl ester **18** ( $K_{\text{IS}}$  of 41-48 nM), whereas the longer ethyl ester **19** was 127-148 times less inhibitory than **15-18**. Moderate inhibitory activity against CA XIII was observed with the coumarins **6**, **7**, and **11**, whereas compounds **8-10**, **12-14**, **16**, **19**, **20**, and **23** were medium potency, low micromolar inhibitors ( $K_{\text{IS}}$  of 3.8-9.6  $\mu\text{M}$ ).
12. The transmembrane isoforms hCA XIV showed an inhibition profile with the investigated derivatives rather similar to that of hCA XII, with which it shares some relevant sequence homology.<sup>8</sup> Thus **11** and **14** were ineffective inhibitors ( $K_{\text{IS}}$  of 39.6 and 82.3  $\mu\text{M}$ ), whereas all other coumarins and the thiocoumarin investigated here showed effective, low micromolar inhibitory activity ( $K_{\text{IS}}$  of 1.0-13.0  $\mu\text{M}$ ). The best hCA XIV inhibitor was the 3,8-disubstituted coumarin **16** ( $K_{\text{I}}$  of 1.0  $\mu\text{M}$ ), which urges to investigate also this substitution pattern represented here only by this unique compound.
13. mCA XV, the latest mammalian CA isoform described so far,<sup>96</sup> was not inhibited by **2**, **5** and **11** and was weakly inhibited by derivatives **1** and **6-11**, ( $K_{\text{IS}}$  of 43.1- $>500\mu\text{M}$ ). The ester **19** was, on the other hand, a low nanomolar mCA XV inhibitor ( $K_{\text{I}}$  of 46 nM), whereas the remaining coumarins and the thiocoumarin **17** showed effective, low micromolar inhibitory activity ( $K_{\text{IS}}$  of 4.8-8.6  $\mu\text{M}$ ).

All these data showed the potential of the coumarin/ thiocoumarin motif to selectively and potently inhibit some CA isoforms among the 13 catalytically active ones described in mammals. For example, **23** was a low nanomolar inhibitor of only CA IX ( $K_I$  of 48 nM), whereas it inhibited in the micromolar range all other 12 CAs, a feature never evidenced before for a sulfonamide CAI.<sup>1,19</sup> The same for **15** and **22**, which acted as nanomolar inhibitors against mCA XIII ( $K_I$ s of 40-48 nM), whereas the remaining 12 isoforms were inhibited in the micromolar range by these compounds.

This studies confirmed our original consideration, it was possible for this kind of structures to develop selectivity towards one or few isoforms. Working with a mini-library of hydroxyl-substituted coumarins type **24-27** (comprehending 6-hydroxy and 7-hydroxycoumarins), I observed that this kind of derivatives had a greater affinity for the two tumor-associated isoenzymes hCA IX and XII, emerging as therapeutic target and diagnostic tools, over the two dominant hCA I and II.<sup>97,98</sup> Results of these assaya are represented in Table 3.3.

**Table 3.3.** Inhibition of Mammalian Isozymes CA I, II, IX and XII with Coumarins **24-27** by a Stopped-Flow, CO<sub>2</sub> Hydration Assay Method.<sup>82</sup>



$K_I$ ( $\mu\text{M}$ ) <sup>c</sup>				
<i>Compound</i>	<i>hCA I</i> <sup>a</sup>	<i>hCA II</i> <sup>a</sup>	<i>hCA IX</i> <sup>a,b</sup>	<i>hCA XII</i> <sup>a,b</sup>
<b>24</b> <sup>d</sup>	79.4	>100	0.508	9.60
<b>25</b> <sup>d</sup>	95.0	>100	0.418	6.30
<b>26</b> <sup>d</sup>	>100	>100	0.198	0.683
<b>27</b> <sup>d</sup>	58.4	>100	0.482	0.754

<sup>a</sup> h ) human. <sup>b</sup> Catalytic domain. <sup>c</sup> Errors in the range of  $\pm 5\%$  of the reported data from three different assays. <sup>d</sup> Preincubation of 6 h between enzyme and inhibitor.

The following structure–activity relationship (SAR) observations can be drawn from data of Table 3.3:

1. The slow cytosolic isoform hCA I was weakly inhibited by coumarins **24-27**, with inhibition constants in the range of 58.4 to >100  $\mu\text{M}$ , unlike the natural product **1** which was a very effective inhibitor ( $K_I$  of 0.078  $\mu\text{M}$ ). The ‘best’ hCA I inhibitor

among the newly investigated derivatives was 7-hydroxy-coumarin **27** ( $K_I$  of 58.4  $\mu\text{M}$ ) which was anyhow 748 times weaker than **1**. Thus, irrespective of the position of the hydroxy moiety in the coumarin ring, in the 3-, 4-, or 6-position, these compounds were very weak or totally ineffective hCA I inhibitors.

2. The second offtarget isoform, hCA II, was not inhibited at all by coumarins **24-27** investigated here ( $K_{IS} > 100 \text{ nM}$ ). This is a very significant result, especially considering the fact that **1** was an effective hCA II inhibitor ( $K_I$  of 0.059  $\mu\text{M}$ ).
3. Although the tumor-associated hCA IX is not significantly inhibited by coumarins **1** (Table 3.1), derivatives **24-27** investigated here showed effective inhibition, with  $K_{IS}$  in the range of 0.198–0.508  $\mu\text{M}$ . The most effective hCA IX inhibitors were 6-hydroxycoumarin, with  $K_I$  of 0.198  $\mu\text{M}$ .
4. The same behavior as that observed for hCA IX was also detected for the inhibition of the second tumor-associated isoform, hCA XII; with the coumarins investigated here. Thus, the leads **1** was ineffective as hCA XII inhibitors ( $K_{IS} > 48.6 \text{ nM}$ ) (Table 3.1), whereas **24-27** behaved as much more effective inhibitors, with  $K_{IS}$  in the range of 0.683–9.60  $\mu\text{M}$ . Coumarins **26** and **27** showed submicromolar hCA XII inhibition ( $K_{IS}$  of 0.683–0.754  $\mu\text{M}$ ) whereas the remaining ones were low micromolar inhibitors ( $K_{IS}$  of 6.30–9.60  $\mu\text{M}$ ).

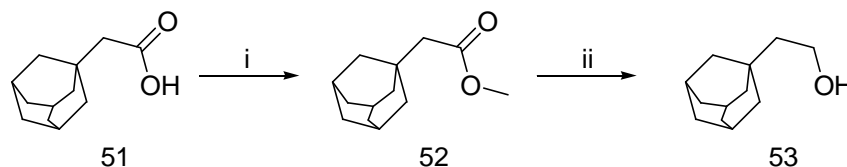
In conclusion such derivatives showed to be interesting leads for the design of novel CAIs and I further proceeded developing a new series of compounds starting from these consideration (see further).





ethanol **53** was synthesized starting from 1-adamantane acetic acid **51** converted in its methyl ester derivative **52**, with anhydrous methanol in presence of thionyl chloride. Such intermediate was reduced to primary alcohol **53** using  $\text{LiAlH}_4$  in THF (Scheme 3.4).<sup>101</sup>

**Scheme 3.4.** Synthesis of derivative **53**.



My initial aim was to isolate only 6,7 disubstituted derivatives, but I decided to go on even with their regioisomers to implement the SAR data. Inhibition data with umbelliferone and **32-50** against four CA isozymes, i.e., hCA I, II, IX and XII,<sup>82</sup> are shown in Table 3.4.

**Table 3.4.** Inhibition of Mammalian Isozymes CA I, II, IX and XII with Coumarins **32-50** by a Stopped-Flow,  $\text{CO}_2$  Hydration Assay Method.<sup>82</sup>

$K_I^c$				
<i>Cpd</i>	<i>hCA I<sup>a</sup></i> ( $\mu\text{M}$ )	<i>hCA II<sup>a</sup></i> ( $\mu\text{M}$ )	<i>hCA IX<sup>a,b</sup></i> (nM)	<i>hCA XII<sup>a,b</sup></i> (nM)
<i>umbelliferone<sup>d</sup></i>	58.4	>100	482	754
<b>32<sup>d</sup></b>	>100	>100	8030	>100000
<b>33<sup>d</sup></b>	>100	>100	8015	>100000
<b>34<sup>d</sup></b>	>100	>100	73.0	61.9
<b>35<sup>d</sup></b>	>100	>100	58.2	61.7
<b>36<sup>d</sup></b>	>100	>100	7800	6540
<b>37<sup>d</sup></b>	>100	>100	7400	>100000
<b>38<sup>d</sup></b>	>100	>100	7580	>100000
<b>39<sup>d</sup></b>	>100	>100	>100000	>100000
<b>40<sup>d</sup></b>	>100	>100	>100000	>100000
<b>41<sup>d</sup></b>	>100	>100	>100000	77700
<b>42<sup>d</sup></b>	>100	>100	78.3	60.9
<b>43<sup>d</sup></b>	>100	>100	70.8	1.0
<b>44<sup>d</sup></b>	>100	>100	56.7	0.98
<b>45<sup>d</sup></b>	>100	>100	61.2	8.8
<b>46<sup>d</sup></b>	>100	>100	72.3	22.4
<b>47<sup>d</sup></b>	>100	>100	63.9	31.5
<b>48<sup>d</sup></b>	>100	>100	37.8	26.3
<b>49<sup>d</sup></b>	>100	>100	46.7	33.2
<b>50<sup>d</sup></b>	>100	>100	50.2	38.4

<sup>a</sup> h ) human. <sup>b</sup> Catalytic domain. <sup>c</sup> Errors in the range of  $\pm 5\%$  of the reported data from three different assays.

<sup>d</sup> Preincubation of 6 h between enzyme and inhibitor.

The following structure-activity relationship (SAR) observations could be drawn from data in Table 3.4.

1. The coumarins possessing 6,7-disubstituted moieties, of types **32-33** and **36-41**, showed very weak or total lack of CA inhibitory activity against all investigated isoforms. Thus, only **32** and **33** were micromolar hCA IX inhibitors; **36** was a micromolar inhibitor of hCA IX and XII, whereas all other compounds generally showed inhibition constants  $> 100 \mu\text{M}$  against all investigated isoforms. Definitely, this substitution pattern leads to a total loss of CA inhibitory properties to the compounds incorporating it.
2. Compounds **34,35** as well as **42-50**, isomeric to the previously discussed ones, but possessing the substituents in the 7,8 positions of the coumarin ring, showed a totally different inhibition profile. Thus, all these compounds were ineffective as hCA I and II inhibitors, with  $K_{\text{IS}} > 100 \mu\text{M}$ , similar to the lead molecule umbelliferone. This was a desirable feature for CAI, in order to target isoforms involved in pathological processes, and not hCA I and especially hCA II (which is the physiologically dominant isoform), whose inhibition may be deleterious and lead to side effects of such a drug.<sup>1,19</sup>
3. The tumor-associated hCA IX was inhibited by umbelliferone in the submicromolar range ( $K_{\text{I}}$  of 482 nM), as discussed above, but most of its derivatives **34,35** and **42-50** were much better inhibitors, with  $K_{\text{IS}}$  in the range of 37.8 – 78.3 nM. Thus, for the compounds obtained after the Fries rearrangement, the activity increased from the acetyl **34** to the propionyl **35** derivatives. In the case of the ethers **42-47**, activity increased from the C1 to the C3 derivative (the *n*-propyl derivative **44** was the best hCA IX inhibitor for their acetyl subseries), to decrease then again for the benzyl and adamantylethyl derivatives **46** and **47**. However the ethyl and adamantylethyl derivatives had quite similar derivatives, proving that SAR (which generally for this class of CAIs is very much sensitive to small modifications in the scaffold of the inhibitor) was less sharp for these two derivatives differing quite a lot by the presence of such a bulky group in **47** (compared to **43**). However, for the other derivatives investigated here the reverse was true, with small modifications leading to a sharp increase or decrease of activity (compare **34** and **35**, **43** and **44**, **44** and **45**, respectively). For the propionyl derivatives **48-50**, activity was even more increased compared to the corresponding acetyl derivatives **42-44**, with

inhibition constants in the range of 37.8 – 50.2 nM. The best hCA IX inhibitor was **48**, with a  $K_i$  of 37.8 nM.

4. The same behavior as that observed for hCA IX was also detected for the inhibition of the second tumor-associated isoform, hCA XII with coumarins **34,35** and **42-50** investigated here. Thus, the lead umbelliferone was a moderate hCA XII inhibitor, with a  $K_i$  of 754 nM, whereas the new compounds reported here possessing the 7,8-disubstitution pattern, behaved as much more effective inhibitors, with  $K_i$ s in the range of 0.98 – 61.9 nM. It was the first detection of subnanomolar inhibition with a coumarin derivative a very interesting finding (many sulfonamides with subnanomolar inhibition of various CA isozymes are known).<sup>1,102</sup> The following SAR was evidenced for these new hCA XII inhibitors. The two key intermediates **34** and **35** had the same potency as hCA XII inhibitors ( $K_i$ s of 61.7 – 61.9 nM), irrespective whether an acetyl or propionyl moiety was present in the 8 position of the coumarin ring. This behavior is different from that observed with these two compounds against hCA IX, as discussed above. The ethers **42-50** showed on the other hand enhanced inhibitory properties compared to the parent phenols from which they were prepared. Thus, the methoxy derivatives **42** and **48** were better inhibitors than the parent phenols **34** and **35**, but the increase in activity was not highly significant ( $K_i$ s of 60.9 nM for **42** and of 26.3 nM for **48** have been measured). However for the acetyl series, the increase of the aliphatic chain in the ether moiety from one (in compound **42**) to two and three carbon atoms led to an impressive increase in the hCA XII inhibitory activity, the compounds **43** and **44** having inhibition constants of 1 nM and of 0.98 nM, respectively. Further increasing the length of the aliphatic chain, as in **45**, or introduction of the benzyl or adamantylethyl moieties, as in **46** and **47**, led to a decrease in activity, but these compounds were still among the best hCA XII coumarin CAIs reported so far, with  $K_i$ s of 8.8 – 341.5 nM. For the propionyl series, the activity remained good enough but the compounds **49** and **50** were less active compared to the corresponding acetyl derivatives **43** and **44**.

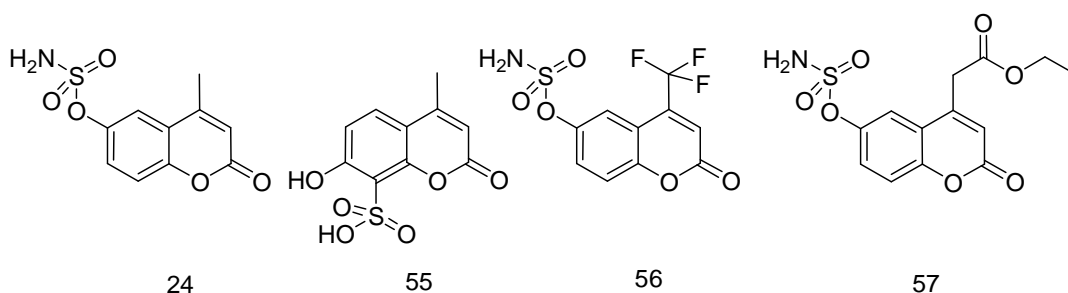
SAR for the inhibition of hCA IX and XII was complex but the main features associated with low nanomolar inhibitors have been delineated. So, starting from consideration on natural compound **1**, synthesis of 7,8 disubstituted derivatives type **42-50**, led to the discovery of inhibitors acting in the low nanomolar range, with fivefold selectivity towards hCA XII compared to the off-target hCA I and II.

### 3.3 Assaying heterogenous coumarinic compounds

In order to increase SAR data on this class of compounds, in particular towards hCA IX and hCA XII isoforms, I evaluated the inhibitory activity of very different coumarinic patterns, synthesized by Trapencieris' groups. To gain an easier approach to the data analysis I divided such compounds in six classes comprehending: sulfonamido/sulfonate derived coumarins, hydroxamate derived coumarins, methoxy substituted coumarins, pyrrolecoumarins, coumarins showing one or more hydroxyl moiety, heterocyclic analogs of coumarins.

In Table 3.5 are shown inhibition data for sulfonamido/sulfonate derivatives **54-57** against mammalian isoforms hCAIX and hCA XII, compared to the two housekeeping, offtarget isoforms hCA I and II.

**Table 3.5.** Inhibition of Mammalian Isozymes CA I, II, IX and XII with Coumarins **54-57** by a Stopped-Flow, CO<sub>2</sub> Hydration Assay Method.<sup>82</sup>



$K_I$ (nM) <sup>c</sup>				
<i>Compound</i>	<i>hCA I</i> <sup>a</sup>	<i>hCA II</i> <sup>a</sup>	<i>hCA IX</i> <sup>a,b</sup>	<i>hCA XII</i> <sup>a,b</sup>
<b>54</b> <sup>d</sup>	485	372	370	80.2
<b>55</b> <sup>d</sup>	754	821	608	81.9
<b>56</b> <sup>d</sup>	8.7	7.3	43.5	8.2
<b>57</b> <sup>d</sup>	9.5	8.0	34.7	64.1

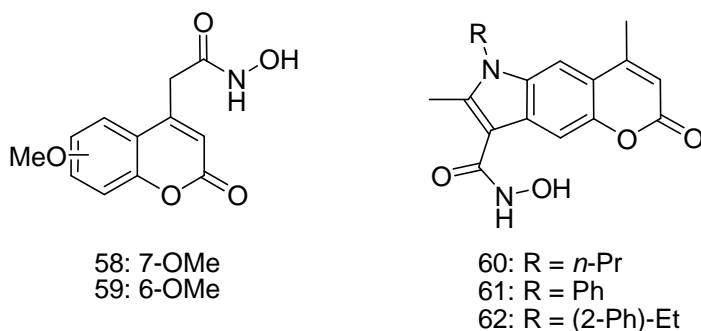
<sup>a</sup> h ) human. <sup>b</sup> Catalytic domain. <sup>c</sup> Errors in the range of  $\pm 5\%$  of the reported data from three different assays. <sup>d</sup> Preincubation of 6 h between enzyme and inhibitor.

In particular, the aim of this first study was to confirm the need to avoid the presence of the sulfonamido moiety or its bioisosteres, in order to develop isoform selectivity for this kind of scaffold; indeed all reported compounds acted as effective inhibitors all over the four isoforms, with a loss in selectivity towards them. As expected, the sulfonamido/sulfonate moiety exerted an inhibitory activity much more potent than the one showed by the coumarin moiety itself, lowering the  $K_I$ s values to the range of nM (from 7.3 to 821 nM). In a recent elegant X-Ray crystallographic study, Wagner *et al.* described some adducts

of sulfonamido-coumarinyl derivatives within hCA II active site.<sup>103</sup> It was shown the expected direct interaction between the sulfonamido moiety and the metal ion, whereas the coumarinyl tail was not hydrolyzed, but interacted with other residues of the active site, in particular Phe131. This was in accordance with these first results: the loss in selectivity of derivatives **54-57** was related to the sulfonamido moiety coordination on the catalytic zinc; the inhibitory activity of such molecules could not be ascribed to the not hydrolyzed coumarin ring,

In Table 3.6 are shown  $K_I$  values for hydroxamic derivatives **58-62**. In particular compounds **58, 59** presented a methyl-hydroxamic moiety in position 4 of the heterocycle, while compounds **60-62**, *N*-substituted pyrrolecoumarins, presented an hydroxamic portion in position 8.

**Table 3.6.** Inhibition of Mammalian Isozymes CA I, II, IX and XII with Coumarins **58-62** by a Stopped-Flow, CO<sub>2</sub> Hydration Assay Method.<sup>82</sup>



$K_I$ ( $\mu\text{M}$ ) <sup>c</sup>				
<i>Compound</i>	<i>hCA I</i> <sup>a</sup>	<i>hCA II</i> <sup>a</sup>	<i>hCA IX</i> <sup>a,b</sup>	<i>hCA XII</i> <sup>a,b</sup>
<b>58</b> <sup>d</sup>	43.7	>100	0.93	0.226
<b>59</b> <sup>d</sup>	80.1	>100	0.965	0.156
<b>60</b> <sup>d</sup>	91.5	>100	9.21	43.7
<b>61</b> <sup>d</sup>	66.0	>100	9.20	50.4
<b>62</b> <sup>d</sup>	59.4	>100	7.34	9.60

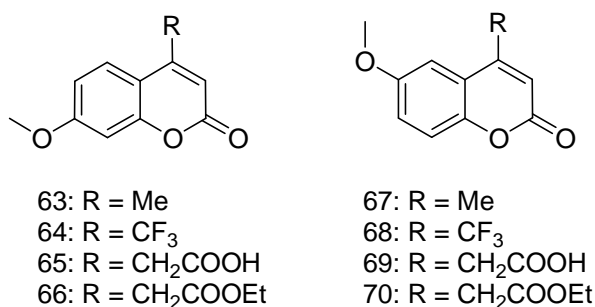
<sup>a</sup> h ) human. <sup>b</sup> Catalytic domain. <sup>c</sup> Errors in the range of  $\pm 5\%$  of the reported data from three different assays. <sup>d</sup> Preincubation of 6 h between enzyme and inhibitor.

In this case I tested scaffold presenting an hydroxamate moiety as zinc-binding group. With the elimination of the sulfonamido moiety there was a relevant decrease in inhibitory activity of these compounds, with  $K_I$  values in the range of  $\mu\text{M}$ . Thus, hydroxamic acids, even if capable to bind directly to the catalytic zinc, do not represented so effective substituent in inhibiting CAs, assembled on these coumarinic scaffolds. In

general compounds **58** and **59** showed a better activity profile, compared to tricyclic derivatives **60-62**, quite poor inhibitors of hCA IX and XII; indeed they showed  $K_I$  values in high nM range, with an important decrease in activity towards hCA I and II.

From this point we focused on type **58**, **59** scaffolds: 6- or 7-methoxy, 4-substituted coumarins **63-70**. From the early studies on compounds **1-3**, methoxy group emerged as an important tool for coumarins regarding CAs inhibition; it appeared of some relevance to investigate how the position of this substituent, on the heterocycle, could modulate the inhibitory activity itself. In this case, assays have been conducted on scaffold presenting methyl, trifluoromethyl, acetic acid or ethyl acetate in position 4 of the ring. In Table 3.7 are reported inhibition data for compound **63-70**.

**Table 3.7.** Inhibition of Mammalian Isozymes CA I, II, IX and XII with Coumarins **63-70** by a Stopped-Flow, CO<sub>2</sub> Hydration Assay Method.<sup>82</sup>



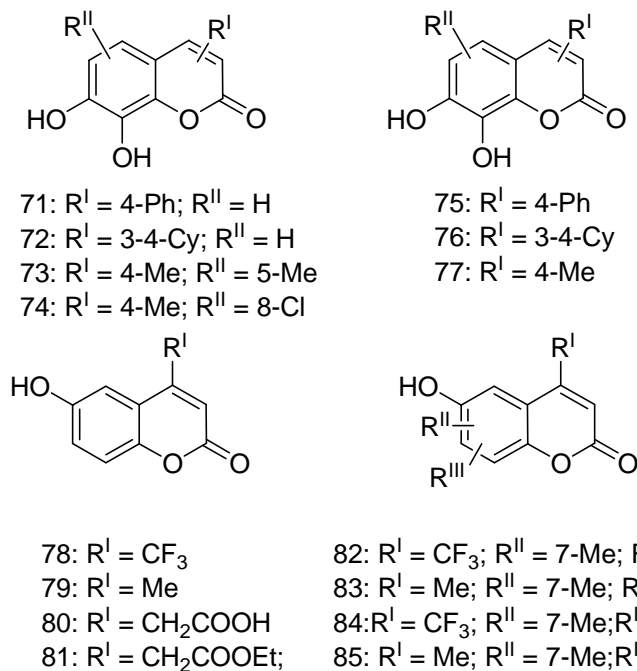
$K_I$ ( $\mu\text{M}$ ) <sup>c</sup>				
Compound	hCA I <sup>a</sup>	hCA II <sup>a</sup>	hCA IX <sup>a,b</sup>	hCA XII <sup>a,b</sup>
<b>63</b> <sup>d</sup>	3.34	0.103	0.126	0.309
<b>64</b> <sup>d</sup>	4.15	10.23	0.260	0.367
<b>65</b> <sup>d</sup>	13.6	>100	0.759	0.315
<b>66</b> <sup>d</sup>	77.1	>100	0.930	0.226
<b>67</b> <sup>d</sup>	40.6	>50	0.261	0.323
<b>68</b> <sup>d</sup>	>50	>50	0.423	0.274
<b>69</b> <sup>d</sup>	43.5	>50	0.235	0.278
<b>70</b> <sup>d</sup>	4.38	>100	0.481	0.845

<sup>a</sup> h ) human. <sup>b</sup> Catalytic domain. <sup>c</sup> Errors in the range of  $\pm 5\%$  of the reported data from three different assays. <sup>d</sup> Preincubation of 6 h between enzyme and inhibitor.

7-methoxy-substituted compounds showed a better profile in activity all over the four isoforms, except for **66**; in particular derivatives **63** and **64** maintained activity even towards hCAII, that was coherent with data shown in Table 3.2 for compound **3**; the only difference was a threefold activity increase towards the two tumor-associated isoforms,

duced to the presence of methyl or trifluoromethyl moiety in position 4. An enlargement in size of this group led to a decrease, or to total loss, in activity versus hCAII, keeping  $K_I$  values for hCA IX and XII in the range of high  $\mu\text{M}$ . Despite of this increment in activity, compared to compound **3**, the selectivity profile of derivatives **63-66** did not meet our requirements to be ascribed as interesting lead. The same arguments for compounds **67-70** which showed a lower, but always comparable, activity towards the four isoforms. To summarize the only interesting considerations, raising from this study, are the following:

1. Not elaborated, 6- or 7- methoxy-substituted coumarinic scaffolds were able to preserve activity towards hCAII.
2. Little changes in substitution pattern, like the addition of methyl or trifluoromethyl moieties, in certain positions, can dramatically increase the activity towards certain CA isoforms for this kind of derivatives.

**Table 3.8.** Inhibition of Mammalian Isozymes CA I, II, IX and XII with Coumarins **71-85** by a Stopped-Flow, CO<sub>2</sub> Hydration Assay Method.<sup>82</sup>

<b>K<sub>I</sub> (μM)<sup>c</sup></b>				
<b>Compound</b>	<b>hCA I<sup>a</sup></b>	<b>hCA II<sup>a</sup></b>	<b>hCA IX<sup>a,b</sup></b>	<b>hCA XII<sup>a,b</sup></b>
<b>71<sup>d</sup></b>	3.50	13.12	0.273	0.287
<b>72<sup>d</sup></b>	4.13	6.65	0.346	0.234
<b>73<sup>d</sup></b>	4.22	9.27	0.202	0.293
<b>74<sup>d</sup></b>	6.39	>100	629	908
<b>75<sup>d</sup></b>	3.93	15.6	0.204	0.280
<b>76<sup>d</sup></b>	3.96	12.45	0.138	0.297
<b>77<sup>d</sup></b>	4.21	16.60	0.215	0.269
<b>78<sup>d</sup></b>	>50	>50	0.335	0.360
<b>79<sup>d</sup></b>	40.1	>50	0.203	0.287
<b>80<sup>d</sup></b>	>50	>50	0.173	0.325
<b>81<sup>d</sup></b>	6.31	>100	312	816
<b>82<sup>d</sup></b>	47.1	>50	0.402	0.305
<b>83<sup>d</sup></b>	>50	>50	0.220	0.291
<b>84<sup>d</sup></b>	>50	>50	0.410	0.283
<b>85<sup>d</sup></b>	>50	>50	0.173	0.325

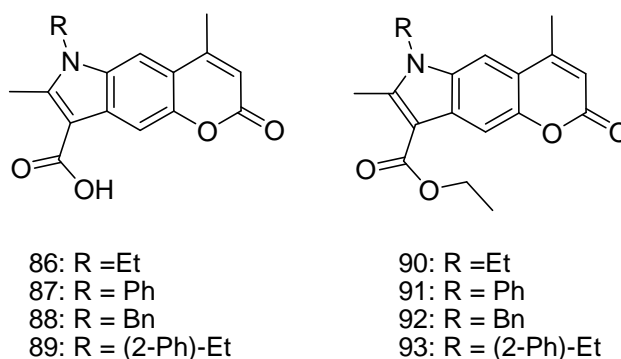
<sup>a</sup> h ) human. <sup>b</sup> Catalytic domain. <sup>c</sup> Errors in the range of ±5% of the reported data from three different assays. <sup>d</sup> Preincubation of 6 h between enzyme and inhibitor.

Thus, I proceeded considering scaffolds **71-85** presenting free hydroxyl moieties on the heterocycle. In particular such molecules possessed one or more hydroxyl groups in various position of the ring (position 6, 7 or 7 and 8 of the ring), a substituent in position 4 and one or more different moieties, not always present, in other positions, like 5, 7 or 8 of the ring. In Table 3.8 are shown inhibition data for compound **71-85**.

This series of compounds did not show an increment in selectivity towards the two tumor-associated hCA isoforms; maybe emerged a little decrease, from this point of view, comparing such derivatives with the profile of compounds **73-80** shown above. In general all these compounds maintained a certain activity towards all the four considered isoforms;  $K_I$  values towards hCA I remained in the range of medium  $\mu\text{M}$ , except for compounds **78-79** and **82-85**; hCA II was inhibited in the range of medium  $\mu\text{M}$  by compounds **71-73** and **75-77**, all other derivatives did not show interesting affinity for such enzyme; the inhibition profiles towards hCA IX and XII were comparable with the ones of compounds **63-70** showing methoxy, but not free hydroxyl, moieties; this except for compounds **74** and **81** ( $K_I$  values of 629  $\mu\text{M}$  and 312  $\mu\text{M}$  respectively for hCA IX; 908 and 816  $\mu\text{M}$  respectively for hCA XII).

Considering 6-hydroxyl substituted derivatives **78-85**, insertion of various moieties on the heterocycle did not modulate the activity profile of such derivatives; the one and only exception was for compound **81** which presented ethyl acetate moiety in position 4 leading to a better inhibitory activity towards hCA I ( $K_I$  of 6.31  $\mu\text{M}$ ) but to a total loss in activity towards the other three considered isoforms ( $K_{Is} > 100 \mu\text{M}$ ). The same argument for 7-substituted compounds **71-77**: maybe they showed a little enhanced activity towards hCA II, but not relevant differences arose, among these derivatives, in hCA IX and XII inhibition; the only consideration was for compound **74** showing a chlorine moiety in position 8, presenting a **81**-like inhibition profile.

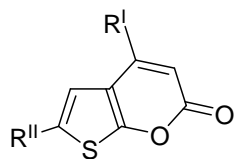
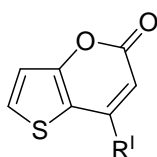
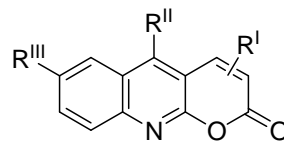
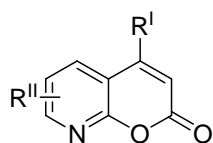
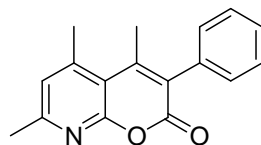
In Table 3.9 are presented  $K_I$  values for other *N*-substituted pyrrolecoumarins **86-93**. Such derivatives were related to compounds **60-62** shown above, differing from these by the lack of hydroxamic moiety in position 8 of the heterocycle, replaced by carboxylic or ethyl carboxylate groups.

**Table 3.9.** Inhibition of Mammalian Isozymes CA I, II, IX and XII with Coumarins **86-93** by a Stopped-Flow, CO<sub>2</sub> Hydration Assay Method.<sup>82</sup>

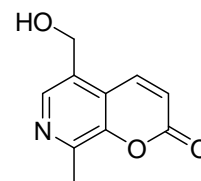
$K_I$ ( $\mu\text{M}$ ) <sup>c</sup>				
<i>Compound</i>	<i>hCA I</i> <sup>a</sup>	<i>hCA II</i> <sup>a</sup>	<i>hCA IX</i> <sup>a,b</sup>	<i>hCA XII</i> <sup>a,b</sup>
<b>86<sup>d</sup></b>	93.8	>100	15.0	12.7
<b>87<sup>d</sup></b>	81.2	>100	0.959	5.70
<b>88<sup>d</sup></b>	46.5	>100	0.923	0.145
<b>89<sup>d</sup></b>	79.2	>100	11.3	15.2
<b>90<sup>d</sup></b>	>100	>100	8.36	9.35
<b>91<sup>d</sup></b>	89.7	>100	9.60	58.1
<b>92<sup>d</sup></b>	56.3	>100	0.934	0.285
<b>63<sup>d</sup></b>	59.5	>100	0.749	0.287

<sup>a</sup> h ) human. <sup>b</sup> Catalytic domain. <sup>c</sup> Errors in the range of  $\pm 5\%$  of the reported data from three different assays. <sup>d</sup> Preincubation of 6 h between enzyme and inhibitor.

In general, 8-carboxy-substituted compounds **86-89** and 8-ethyl carboxylate-substituted derivatives **90-93**, presented analog inhibitory profile over the considered hCAs, with poor activity towards hCA I and II and  $K_I$  values for hCA IX and XII variable from low to high micromolar range. However it was worth noting that, in comparison with their hydroxamic analogs **60-62**, derivatives **86-93** showed a better selectivity profile towards the two targeted isoforms hCA IX and XII. Here, once more, the proof that the replacement of a suitable zinc coordinating group like the hydroxamic acid, with milder functions (carboxylic acids or esters), arose the possibility to meet our aim.

**Table 3.10.** Inhibition of Mammalian Isozymes CA I, II, IX and XII with Coumarins **94-115** by a Stopped-Flow, CO<sub>2</sub> Hydration Assay Method.<sup>82</sup> <sup>a</sup> h ) human. <sup>b</sup> Catalytic domain. <sup>c</sup> Errors in the range of ±5% of the reported data from three different assays. <sup>d</sup> Preincubation of 6 h between enzyme and inhibitor.94: R<sup>I</sup> = Me; R<sup>II</sup> = H95: R<sup>I</sup> = CH<sub>2</sub>COOEt; R<sup>II</sup> = H96: R<sup>I</sup> = CF<sub>3</sub>; R<sup>II</sup> = H97: R<sup>I</sup> = CH<sub>2</sub>COOH; R<sup>II</sup> = H98: R<sup>I</sup> = Me; R<sup>II</sup> = Me99: R<sup>I</sup> = Me100: R<sup>I</sup> = CH<sub>2</sub>COOEt101: R<sup>I</sup> = CF<sub>3</sub>102: R<sup>I</sup> = CH<sub>2</sub>COOH103: R<sup>I</sup> = H; R<sup>II</sup> = OH; R<sup>III</sup> = H104: R<sup>I</sup> = 4-Me; R<sup>II</sup> = OH; R<sup>III</sup> = H105: R<sup>I</sup> = 4-CF<sub>3</sub>; R<sup>II</sup> = OH; R<sup>III</sup> = H106: R<sup>I</sup> = 3-Ph; R<sup>II</sup> = H; R<sup>III</sup> = 7-OMe107: R<sup>I</sup> = 3-*o*-To; R<sup>II</sup> = H; R<sup>III</sup> = 7-OMe108: R<sup>I</sup> = H; R<sup>II</sup> = 7-OH109: R<sup>I</sup> = Me; R<sup>II</sup> = 7-OH110: R<sup>I</sup> = CF<sub>3</sub>; R<sup>II</sup> = 7-OH111: R<sup>I</sup> = CH<sub>2</sub>COOMe; R<sup>II</sup> = 7-OH112: R<sup>I</sup> = Me; R<sup>II</sup> = 5-OH113: R<sup>I</sup> = CF<sub>3</sub>; R<sup>II</sup> = 5-OH

114



115

<b>K<sub>I</sub> (μM)<sup>c</sup></b>				
<b>Compound</b>	<b>hCA I<sup>a</sup></b>	<b>hCA II<sup>a</sup></b>	<b>hCA IX<sup>a,b</sup></b>	<b>hCA XII<sup>a,b</sup></b>
<b>94<sup>d</sup></b>	>100	>100	0.388	0.796
<b>95<sup>d</sup></b>	>100	>100	0.314	0.589
<b>96<sup>d</sup></b>	>100	>100	0.256	0.611
<b>97<sup>d</sup></b>	>100	>100	0.292	0.759
<b>98<sup>d</sup></b>	81.8	>100	0.959	5.70
<b>99<sup>d</sup></b>	>100	>100	0.202	0.388
<b>100<sup>d</sup></b>	>100	>100	0.173	0.510
<b>101<sup>d</sup></b>	>100	>100	0.298	0.722
<b>102<sup>d</sup></b>	>100	>100	0.365	0.384
<b>103<sup>d</sup></b>	>100	>100	0.749	0.657
<b>104<sup>d</sup></b>	>100	45.2	0.490	6.14
<b>105<sup>d</sup></b>	60.7	28.4	0.208	3.19
<b>106<sup>d</sup></b>	>100	>100	7.23	8.52
<b>107<sup>d</sup></b>	>100	>100	6.95	9.58
<b>108<sup>d</sup></b>	9.37	35.9	0.174	0.478
<b>109<sup>d</sup></b>	42.7	33.9	0.113	3.67
<b>110<sup>d</sup></b>	60.7	28.4	0.208	3.19
<b>111<sup>d</sup></b>	9.22	61.3	0.367	5.91
<b>112<sup>d</sup></b>	>100	>100	0.731	0.683
<b>113<sup>d</sup></b>	>100	>100	0.760	0.601
<b>114<sup>d</sup></b>	>100	25.4	0.495	7.78
<b>115<sup>d</sup></b>	30.4	76.5	0.243	7.35

At the end of this initial screening, I considered coumarin-like scaffolds **94-115**. These compounds differed from the series described until now for the variation in the heterocycle ring: the benzenic ring of benzopyrone was substituted by thiophene, quinoline or pyridine heterocycles. The reason to test these derivatives was to verify if changes in the intimate heterocycle structure, correlated with various substitution patterns, were responsible for a relevant modulation in selectivity profile towards the same four CA isoforms. In Table 3.10 are presented  $K_I$  values for “coumarin-like” structures **94-115**. The trend of this series reflected the ones of other compounds shown earlier: poor activity towards the offtarget hCA I and II,  $K_I$  values in the range of  $\mu\text{M}$  towards the tumor-associated hCA IX and XII. More in detail, hCA I was not so relevantly affected by derivatives **94-115** ( $K_I$  values in the high  $\mu\text{M}$  range), except for **108** and **111**, two pyrano-pyridine-2-one derivatives showing a free hydroxyl moiety ( $K_I$  of 9.37  $\mu\text{M}$  and 9.22  $\mu\text{M}$  respectively). The same inhibition profile for the dominant isoform hCA II: just three compounds **105**, **110** and **114** presented  $K_I$ s of 28.4  $\mu\text{M}$ , 28.4, 25.4  $\mu\text{M}$  respectively; the other compounds did not show affinity for such isoform. Activity towards hCA IX and XII remained in the low micromolar range for all the series, except for **106** and **107** which showed a lower activity ( $K_I$  of 7.23  $\mu\text{M}$  and 6.95  $\mu\text{M}$  respectively for CA IX and 8.52  $\mu\text{M}$  and 9.58  $\mu\text{M}$  respectively for CA XII). Even in this case no particular selective scaffold arose from the series, but it was possible to summarize results from this initial screening as follows:

1. Insertion of zinc binding groups on coumarinic scaffolds leads to a loss in selectivity towards the various isoforms. In particular, in presence of a sulfonamido moiety, the responsible for inhibition activity is not the hydrolysis product of the coumarinic scaffold but the sulfonamide itself.<sup>103</sup> This resolves in a nanomolar range inhibition profile characterized by a poor or absent selectivity attitude.
2. On the other hand, the hydroxamic moiety, another common zinc binding group,<sup>104</sup> was not so effective towards CAs, built on these kind of compounds. The effect was to decrease the inhibition to micromolar range and, nevertheless, despite this decrease in activity, no particular increase in selectivity could be observed.
3. With coumarinic scaffolds it is possible to develop selectivity on particular isoforms, with no activity towards the two housekeeping off-target hCA I and hCA II. This is a very important peculiarity that distinguishes this class of compounds from the more studied and common sulfonamides, making it an promising “weapon” to exploit towards particular CA isoforms. However, this important

selectivity profile has not been shown by the totality of the studied compounds: there is also for coumarins the possibility to maintain activity towards hCA II (e. g. compound **63**).

4. Little variations on the coumarinic substitution pattern can lead to changes in the activity profile (e. g., compounds **2** and **3**); this fact could be explained in terms of substrate arrangement inside the enzyme. As shown by chrystallographic studies,<sup>51</sup> coumarins do not interact directly with the catalytic zinc ion, but exert their action interacting only with allosteric zones. Thus, even not relevant variations in terms of ring substitution can modulate the approach of the substrate and the way it “moves” inside the enzyme cavity.
5. The replacement of benzene ring with an heterocycle moiety did not affect in terms of variations, the activity profile in comparison with the one showed by usual coumarins.

At the end of this screening, however, several compounds showing interesting selectivity towards the two tumor-associated CA isoforms were found out. However such derivatives were not satisfactory in terms of inhibitory activity, showing  $K_i$  values for these two enzymes in the range of submicromolar, such results didn't prompt me to continue in this research line.

### 3.4 “Click Chemistry” coumarins

Finally, I synthesized a series of 6- and 7-triazolyphenyl halogeno substituted coumarins, **123-132**, using a “click chemistry” approach. This kind of strategy has been already used for other types of CAs inhibitors, like sulfonamides, sulfamates and it arose derivatives with interesting inhibitory profiles. Further, this approach, cause of reactions properties, allows to synthesize very diversified libraries of compounds. In particular I considered structures type **B** and **C**, shown in Chart 3.4.

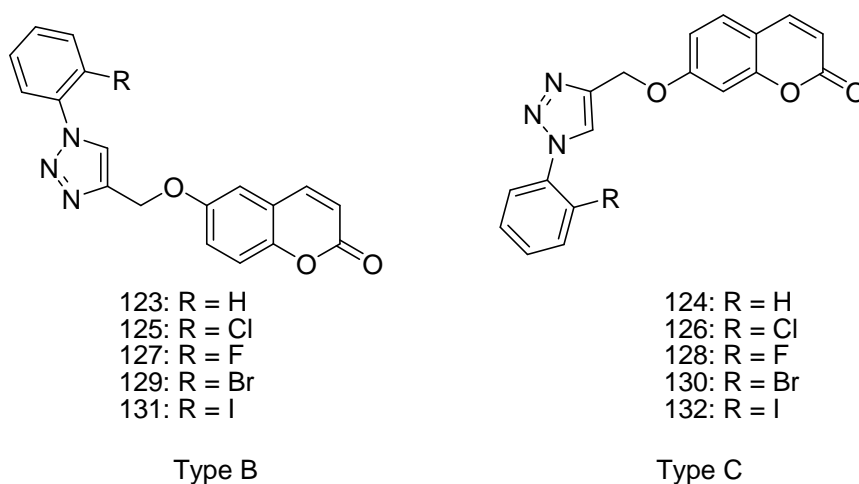
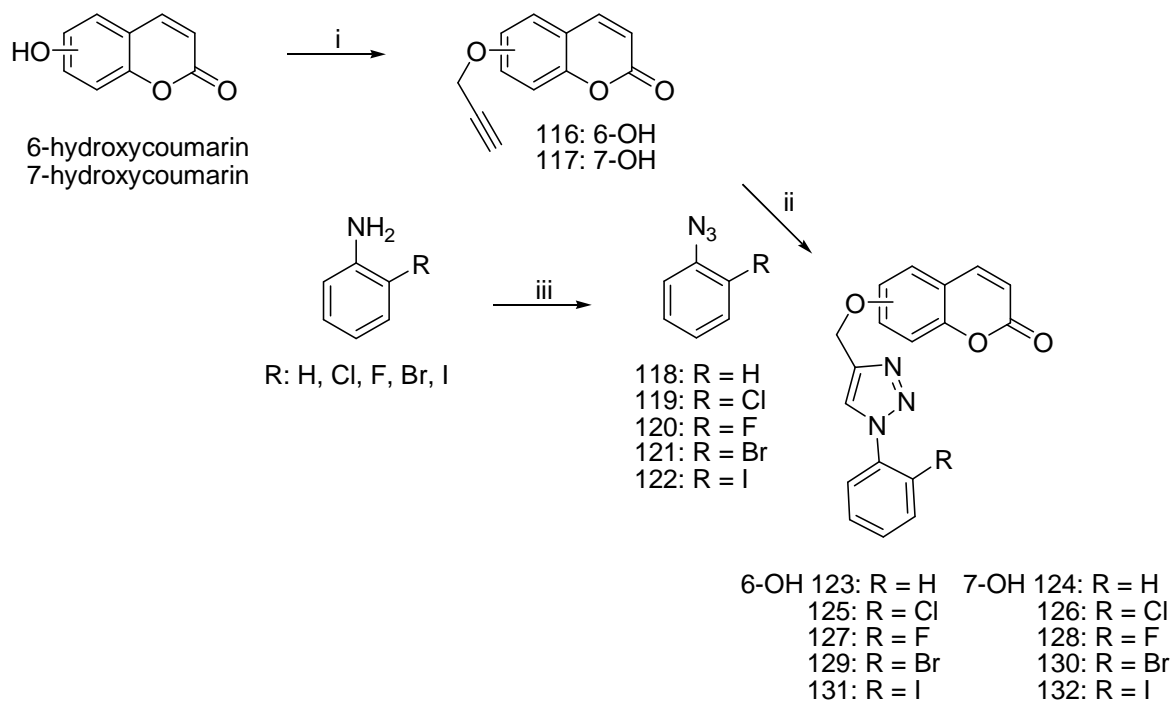


Chart 3.4. Structures type **B** and **C** of “click chemistry” compounds **123-132**.

For the synthesis of such derivatives (Scheme 3.5) I started from 6- and 7-hydroxy coumarins reacted under sonication with propargyl alcohol, in Mitsunobu conditions, to give ether compounds **116** and **117**. These were converted to triazolyphenyl derivatives **123-132** reacting with freshly prepared phenylazides **118-122** through a Huisgen’s 1,3 dipolar cycloaddition Cu(0) nanosized catalyzed, in presence of tetramethylammonium chloride. Phenylazides were obtained starting from the correspondent anilines with a diazotization/azidation process using sodium nitrite and sodium azide in a mixture of acetic acid/water.



i: Propargyl alcohol, PPh<sub>3</sub>, DIAD, dry THF, sonication; ii: Cu<sup>0</sup> nanosized, TMACl, H<sub>2</sub>O/tBuOH, r.t.  
iii 1) NaNO<sub>2</sub>, AcOH/H<sub>2</sub>O 2) NaN<sub>3</sub>.

**Scheme 3.5.** Synthesis of derivatives **116-132**.

Compounds **125**, **128**, **130** and **131** have been chosen from this series for *in vitro* assay, together with other three derivatives, shown in Chart 3.5, synthesized by Carta.

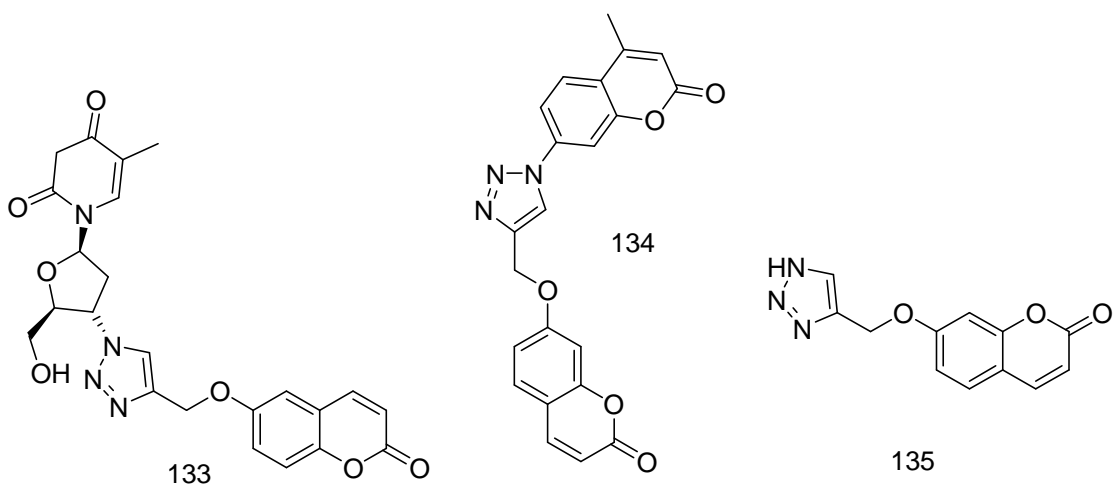


**Chart 3.5.** Structures of derivatives **133-135**.

In Table 3.11 are presented  $K_I$  values for derivatives **125**, **128**, **130**, **131**, **133-135** over the four isoforms usually considered so far.

**Table 3.11.** Inhibition of Mammalian Isozymes CA I, II, IX and XII with Coumarins **94-115** by a Stopped-Flow, CO<sub>2</sub> Hydration Assay Method.<sup>82</sup>

$K_I$ ( $\mu\text{M}$ ) <sup>c</sup>				
<i>Compound</i>	<i>hCA I<sup>a</sup></i>	<i>hCA II<sup>a</sup></i>	<i>hCA IX<sup>a,b</sup></i>	<i>hCA XII<sup>a,b</sup></i>
<b>125<sup>d</sup></b>	>100000	>100000	7.5	48.6
<b>128<sup>d</sup></b>	117	>100000	7.5	18.7
<b>130<sup>d</sup></b>	40.6	>100000	6.8	27.0
<b>131<sup>d</sup></b>	57.6	>100000	6.4	40.8
<b>133<sup>d</sup></b>	87.8	913	9.3	49.9
<b>134<sup>d</sup></b>	15400	>100000	8.6	46.5
<b>135<sup>d</sup></b>	>100000	>100000	9.1	70.4

<sup>a</sup> h ) human. <sup>b</sup> Catalytic domain. <sup>c</sup> Errors in the range of  $\pm 5\%$  of the reported data from three different assays. <sup>d</sup> Preincubation of 6 h between enzyme and inhibitor.

Considered compounds showed no activity over hCA II, except for compound **133**; they presented a nice profile over the two tumor-associated isoforms, but many of them conserved affinity towards hCA I. In particular the most interesting considerations arose from derivatives **125** and **135**, which exerted a micromolar range activity towards hCA IX and XII ( $K_I$ s from 6.4 to 70.4  $\mu\text{M}$ ), with lower activity over the offtarget isoenzymes. Is not easy to explain such behaviour, probably due to the dimension of halogen atom and to its electronegativity. Compound **133** showed the best activity profile towards all the four considered isoforms, with a loss in selectivity.

### 3.5 Conclusions

Coumarins showed to be an interesting chemotype to develop selectivity towards particular CA isoforms. The time-dependant mechanism of action, with no interactions on the catalytic zinc and their capacity to orientate in several conformations within the active site are features showed, to far, only by this class, among all CAIs. From compound **1** has been synthesized a series of 8-acyl, 7 ether-substituted coumarins showing impressive ability in selective inhibition. From the “click chemistry” approach emerged interesting derivatives acting as selective inhibiting substrates, exerting their activity in the micromolar range. Further developments urge to be realized using this approach that could reveal new synthetic derivatizations, useful to increase selectivity towards precise isoforms.



## CHAPTER FOUR

### *Studies on $\beta$ -Carbonic Anhydrases*

#### **4.1 Kinetic characterization and inhibition studies of the most active $\beta$ -Carbonic Anhydrase from *Mycobacterium tuberculosis*, mtCA 2**

##### **4.1.1 Introduction**

The widely spread human pathogen *Mycobacterium tuberculosis* contains three  $\beta$ -carbonic anhydrase genes in its genome, that is, Rv1284 (encoding for a protein we named mtCA 1), Rv3588c, shown to be essential for bacteria growth *in vivo*,<sup>105</sup> (encoding for mtCA 2) and Rv3273 (encoding for a third enzyme, mtCA 3).<sup>13,29,106</sup> The catalytic activity and inhibition studies with a range of sulfonamides and one sulfamate of two of these enzymes, that is, mtCA 1 and mtCA 3 have been recently reported,<sup>107,108,106</sup> whereas Covarrubias *et al.* reported the X-ray crystal structure of mtCA 1 and mtCA2.<sup>13,29</sup> CAs belonging to the  $\beta$ -class<sup>1</sup> are indeed found in many pathogenic organisms such as fungi (*Candida albicans*, *Candida glabrata* and *Cryptococcus neoformans* among others)<sup>109-114</sup> and bacteria (*Helicobacter pylori*, *Arthrobacter aurescens*, *Leptospira borgpetersenii*, *Legionella pneumophila* and *Haemophilus influenzae*)<sup>4,115,116,54,117</sup> but they lack from mammals, in which only  $\alpha$ -CAs are present.<sup>1</sup> Thus, inhibition of such  $\beta$ -CAs started to be considered<sup>4,106-116</sup> as a new possible approach for designing anti-infectives (antifungal or antibacterial agents) possessing a different mechanism of action compared to the classical pharmacological agents in clinical use for a long period, for which pathogenic fungi and bacteria developed various degrees of resistance.<sup>118-121</sup> The drug resistance problem of antifungals and antibiotics represents a serious medical problem.<sup>122</sup> In this context, *M. tuberculosis* infection is one of the worst example, as multi-drug resistant and extensively multi-drug resistant tuberculosis (TB) is present in many countries.<sup>123</sup> Such drug-resistant mycobacteria show a continuously reduced susceptibility to the clinically used drugs, all of which were developed 30–40 years ago.<sup>124,125</sup> There is actually a huge interest for novel anti-TB drugs, possessing alternative mechanisms of action compared to the clinically used antibiotics.<sup>124,125</sup>

##### **4.1.2 Structure and function of mtCA 2**

The fundamental structure unit in Rv3588c is a dimer<sup>29</sup> composed by the interaction of two single subunits around a crystallographic 2-fold axis;<sup>29</sup> each subunit consists of a

five stranded  $\beta$ -sheet, in which strands 1–4 are parallel and ordered 2-1-3-4. The fifth strand is anti-parallel and connected to the fourth by a short reverse turn. The  $\beta$ 1- $\beta$ 2 loop is short and irregular, the  $\beta$ 2- $\beta$ 3 connection includes a regular  $\alpha$ -helix ( $\alpha$ 2) packing on the surface of the sheet, the  $\beta$ 3- $\beta$ 4 loop is much longer, containing four helices in Rv3588c. One of these helices packs on the sheet near  $\beta$ 4 in both proteins. The remaining portion of the loop stretches across the surface of the dimer to interact with the 2-fold related helix linking  $\beta$ 2 and  $\beta$ 3. Figure 4.1 represents the structures of Rv3588c single subunit (A) and its dimeric form (B).<sup>29</sup>

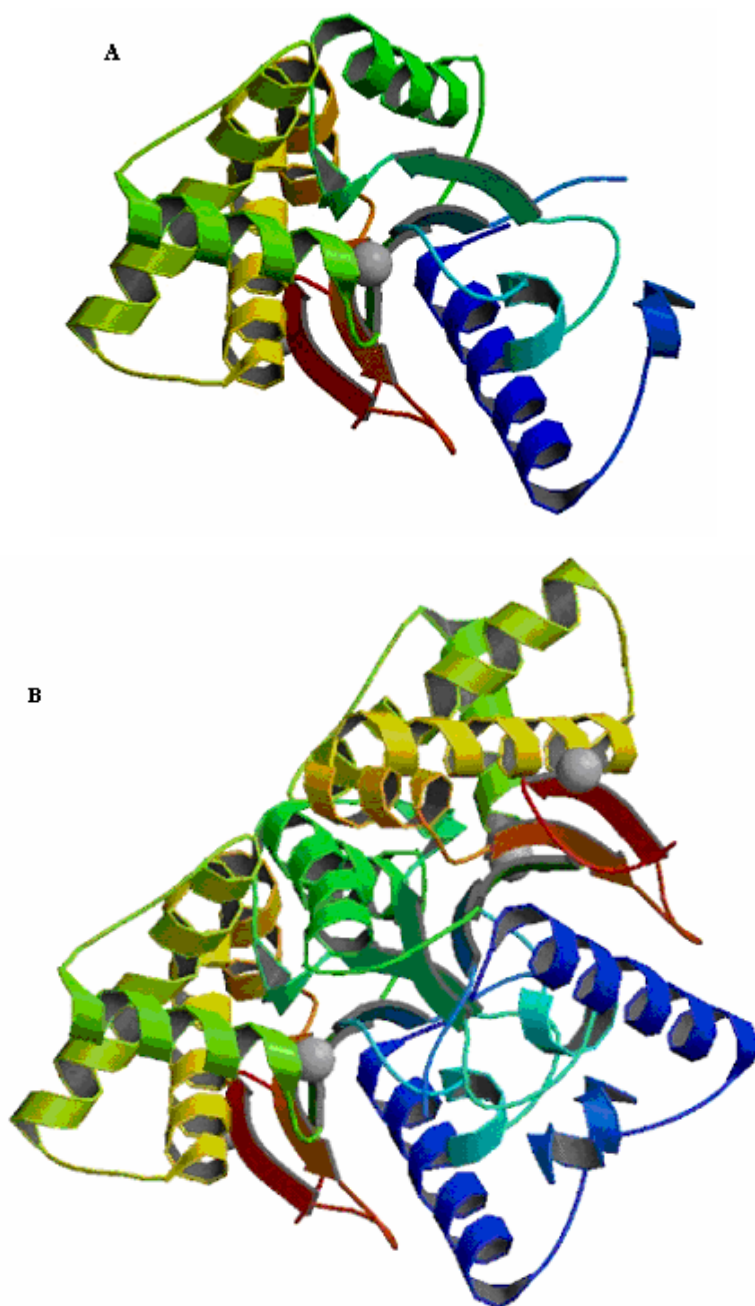


**Figure 4.1.** Overall structures of Rv3588c. Ribbon diagrams illustrate the single subunit structure (A) and the dimeric form (B).

Surprisingly, the thiocyanate complex of the same enzyme crystallizes as a dimer of dimers<sup>13</sup> in the asymmetric unit with classic 2-2-2 symmetry. The tetramerization interface of Rv3588c is stabilized by a large network of salt bridges in which positively charged residues (mostly Arg) outnumber negatively charged residues (Asp and Glu). Dynamic light scattering studies<sup>13</sup> show that the tetrameric form of the enzyme dissociates into dimers as the pH is lowered from pH 8.4 to 7.5, and that this quaternary structure change is associated with changes in zinc ligation sphere. It is possible that Rv3588 requires high pH for tetramerization in order to maximize the neutralization of excess positive charge in the tetramerization interface.<sup>13</sup> The active site of a  $\beta$ -CA lies near a switch point at the C-terminal edge of its parallel  $\beta$ -sheet, as has been observed for other  $\alpha/\beta$  proteins.<sup>126</sup> Considering the coordination sphere around the catalytic ion and the orientation of the nearby aminoacidic residues, Rv3588c adopts, in its monomeric form, a type II  $\beta$ -CA structure.<sup>5</sup> Such frame presents a pseudo-tetrahedral coordination shell composed entirely of protein ligands: Cys51, Asp53, His104 and Cys107. In particular, the active site residue Asp53 displaces the water molecule and coordinates directly to the zinc ion, thus breaking a potential salt link to Arg55 (Figure 4.2).

In complex with thiocyanate, so in its tetrameric form, the enzyme adopts an alternate type I  $\beta$ -CA structure. The nitrogen atom of thiocyanate bonds to the zinc ion and displaces Asp53, which in turn interacts with Arg55 to form the Asp-Arg dyad that is characteristic of type I  $\beta$ -CAs. This condition renders one of the zinc coordination positions available for coordination by exogenous ligands, in this case the hydroxide form of a water molecule, deputated for the CO<sub>2</sub> hydration. The carboxylate shift of Asp53 is accompanied by major backbone changes mainly of residues Ser54 and Val56. The side chain of Ser54 flips to point in the opposite direction with atomic shifts of up to 8 Å. In concert, Val56 undergoes an equally dramatic change, whereas the side chain of Arg55 undergoes relatively small shifts. The result of these molecular gymnastics is the creation of a salt link between Asp53 and Arg55.

To sum up, the real significance of the two Rv3588 structures is that they suggest that type II  $\beta$ -CAs are able to adopt two different conformations in solution, mediated by a reorientation, called “carboxylate shift” of the active site Asp from acting as a zinc ligand to forming a dyad with the active site Arg residue. At pH 7.5 the protein is in its dimeric inactive form, with the zinc coordination shell totally occupied by aminoacidic ligands (one of them is Asp53); at pH 8.4 the protein rearranges in its tetrameric, catalytically

active form, with Asp53 shifted towards interaction with Arg55, leaving one zinc coordination position free for exogenous ligands.

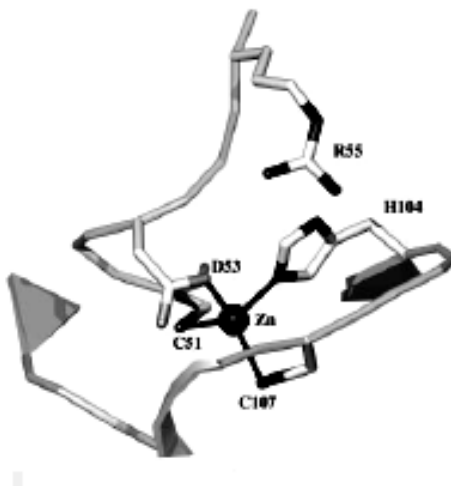


**Figure 4.2.** Active site of Rv3588c. Residues involved in metal coordination are shown with *ball-and-stick models*, with the hydrogen bonds mentioned in the text indicated by black dotted lines.

#### 4.1.3 Kinetic investigation and inhibition studies

Covarrubias *et al.*<sup>29</sup> reported that mtCA 2 has catalytic activity as CO<sub>2</sub> hydrase, so, considering the interest in  $\beta$ -CAs as possible new drug targets, I proceeded here with the characterization and inhibition studies, with a panel of sulfonamides/sulfamates, of mtCA 2. This enzyme has been reported and characterized crystallographically by Covarrubias *et al.*<sup>13,29</sup> but its kinetic parameters, as well as inhibition, has not been investigated for the moment. I performed a kinetic investigation of purified mtCA 2, prepared as described earlier by one of our groups,<sup>29</sup> comparing its kinetic parameters ( $K_{cat}$  and  $K_{cat}/K_M$ ) with those of thoroughly investigated  $\alpha$ -CAs, such as the cytosolic, ubiquitous human isozymes hCA I and II,<sup>1</sup> as well the other two mycobacterial enzymes, mtCA 1 and mtCA 3<sup>106,108</sup> investigated earlier (Table 4.1). As CAs are susceptible to be inhibited by sulfonamides,<sup>19,82,127,128,106</sup> data of Table 4.1 also present the inhibition constant of these enzymes with acetazolamide (AAZ), a clinically used drug.<sup>1</sup>

**Table 4.1.** Kinetic parameters for the CO<sub>2</sub> hydration<sup>82</sup> reaction catalyzed by the  $\alpha$ -hCA isozymes I, II at 20 °C and pH 7.5 in 10 mM HEPES buffer, and the three *Mycobacterium tuberculosis* enzymes Rv1284 (mtCA 1), Rv3273 (mtCA 3) and Rv3588c (mtCA 2) at 20 °C, pH 8.3 in 20 mM Tris–HCl buffer and 20 mM NaCl and their inhibition data with acetazolamide AAZ.

Isoenzyme	Activity level	$K_{cat}$ (s <sup>-1</sup> )	$K_{cat}/K_M$ (M <sup>-1</sup> s <sup>-1</sup> )	$K_I$ (AAZ) (nM)
<i>hCA II</i>	Moderate	$2.0 \times 10^5$	$5.0 \times 10^7$	250
<i>hCA II</i>	Very high	$1.4 \times 10^6$	$1.5 \times 10^8$	12
<i>mtCA 1</i>	Moderate	$3.9 \times 10^5$	$3.7 \times 10^7$	480
<i>mtCA 3</i>	Moderate	$4.3 \times 10^5$	$4.0 \times 10^7$	104
<i>mtCA 2</i>	High	$9.8 \times 10^5$	$9.3 \times 10^7$	9.8

Data of Table 4.1 show that mtCA 2 has the highest catalytic activity for the physiologic reaction among the three mycobacterial enzymes mtCA 1–3, with kinetic parameters in the same range as those for  $\alpha$ - or  $\beta$ -CAs investigated earlier, such as hCA I and II.<sup>4,19,67,70,129,130,127,128</sup> Indeed, mtCA 2 has a  $k_{cat}$  of  $9.8 \times 10^5$  s<sup>-1</sup>, and  $K_{cat}/K_M$  of  $9.3 \times 10^7$  M<sup>-1</sup> s<sup>-1</sup>, being thus 2.5 times more active than mtCA 1, and 2.3 times more active than mtCA 3 as a catalyst for the physiological reaction. Only the human isoforms hCA II was slightly more active (1.6 times) a catalysts for CO<sub>2</sub> hydration compared to mtCA 2 among the enzymes shown in Table 4.1,

Tables 4.2 and 4.3 show mtCA2 inhibition data with a panel of sulfonamides and one sulfamate (obtained for the CO<sub>2</sub> hydration reaction catalyzed by CAs),<sup>82</sup> some of which are clinically used drugs,<sup>1</sup> such as acetazolamide **AAZ**, methazolamide **MZA**, ethoxzolamide **EZA**, dichlorophenamide **DCP**, dorzolamide **DZA**, brinzolamide **BRZ**, benzolamide **BZA**, topiramate **TPM**, sulpiride **SLP**, indisulam **IND**, zonisamide **ZNS**, celecoxib **CLX**, valdecoxib **VLX**, sulthiame **SLT** and saccharin **SAC**. The simpler derivatives **136-157** were also included in the study as they represent the most extensively used scaffolds for designing potent or isoform-selective CAIs (Chart 4.1).<sup>131-134,106</sup>



**Table 4.2.** Inhibition of hCA II, and *M. tuberculosis* enzymes mtCA 1–3 with sulfonamides **136-157** and 15 clinically used derivatives **AAZ-SAC**.

$K_I$ *				
<i>Compound</i>	<i>hCA II<sup>a</sup> (nM)</i>	<i>mtCA I<sup>b</sup> (<math>\mu</math>M)</i>	<i>mtCA 3<sup>c</sup> (<math>\mu</math>M)</i>	<i>mtCA 2<sup>d</sup> (<math>\mu</math>M)</i>
<b>136</b>	295	9.23	6.24	33.7
<b>137</b>	240	9.84	7.11	29.6
<b>138</b>	495	7.93	7.83	28.4
<b>139</b>	320	4.92	7.02	38.9
<b>140</b>	170	8.69	7.33	30.7
<b>141</b>	160	9.56	3.42	29.1
<b>142</b>	60	8.74	7.90	28.9
<b>143</b>	110	7.52	1.51	27.7
<b>144</b>	40	0.186	7.32	31.6
<b>145</b>	70	7.71	5.81	32.4
<b>146</b>	63	8.10	2.35	29.6
<b>147</b>	75	1.72	21.7	32.5
<b>148</b>	60	11.54	7.63	2.09
<b>149</b>	19	12.65	7.92	2.38
<b>150</b>	2	0.905	3.10	0.978
<b>151</b>	46	0.612	2.21	3.21
<b>152</b>	50	0.853	0.170	2.29
<b>153</b>	33	0.750	0.091	2.63
<b>154</b>	12	7.48	7.60	45.2
<b>155</b>	80	9.56	7.82	38.3
<b>156</b>	125	5.51	2.51	34.5
<b>157</b>	133	8.21	7.40	39.2
<b>AAZ</b>	12	0.481	0.104	0.009
<b>MZA</b>	14	0.781	0.562	0.66
<b>EZA</b>	8	1.03	0.594	0.027
<b>DCP</b>	38	0.872	0.611	2.01
<b>DZA</b>	9	0.744	0.137	0.099
<b>BRZ</b>	3	0.839	0.201	0.127
<b>BZA</b>	9	0.810	0.338	0.467
<b>TPM</b>	10	0.612	3.02	0.474
<b>SLP</b>	40	2.30	7.92	0.266
<b>IND</b>	15	0.097	7.84	0.717
<b>ZNS</b>	35	28.68	0.208	0.876
<b>CLX</b>	21	10.35	7.76	0.713
<b>VLX</b>	43	12.97	7.81	0.682
<b>SLT</b>	9	5.16	6.72	0.664
<b>SAC</b>	5950	7.96	7.15	0.792

<sup>a</sup> Human recombinant isozyme, stopped-flow CO<sub>2</sub> hydrase assay method, pH 7.5, 20 mM Tris–HCl buffer.<sup>82</sup><sup>b,c</sup> Bacterial recombinant enzymes, at 20 °C, pH 8.3 in 20 mM Tris–HCl buffer and 20 mM NaCl, from Refs. 106,108. Data of isoform II are from Ref. 67 whereas data of mtCA 1 and 3 from Refs. 106,108.<sup>d</sup> Bacterial recombinant enzyme, at 20 °C, pH 8.3 in 20 mM Tris–HCl buffer and 20 mM NaCl, this work.

\* Errors in the range of 5–10% of the shown data, from three different assays.

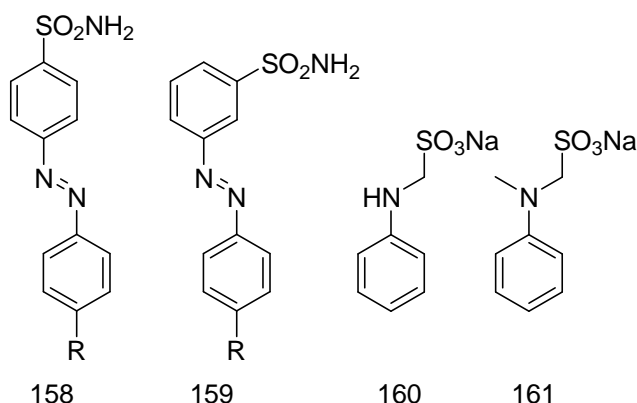
Data for the inhibition of the dominant human isoform hCA II<sup>1</sup> as well as those of the other two *M. tuberculosis* enzymes, mtCA 1 and mtCA 3,<sup>106,108</sup> are also included, in Table 4.2, with these compounds for comparison reasons.

The following SAR can be observed from data of Table 4.2:

1. A number of the investigated derivatives, such as **136-147** and **154-157** showed modest mtCA 2 inhibitory activity, with activity in the micromolar range, and inhibition constants of 27.7–45.2  $\mu\text{M}$ . It may be observed that these compounds are either simple 2- or 4-substituted benzenesulfonamides incorporating amino, alkylamino, carboxyalkyl, carboxyl or hydroalkyl moieties (**136-141** and **155-157**), halogeno-substituted sulfanilamides (**142-145**) or benzene-1,3-disulfonamide derivatives (**146** and **147**). Generally, all these compounds were more effective mtCA 1 and mtCA 2 inhibitors ( $K_{\text{I}}$ s in the low micromolar or even submicromolar range, Table 4.2).
2. Activity in the low micromolar range has been observed for six of the investigated derivatives: **148**, **149**, **151-153** and **DCP**, with  $K_{\text{I}}$ s in the range of 2.01–3.21  $\mu\text{M}$ . These compounds are either heterocyclic derivatives (**148** and **149**, the acetazolamide and methazolamide precursors), sulfanilyl- sulfonamides **151** and **152**, as well as the pyrimidyl-substituted benzenesulfonamide **153**. Dichlorophenamide **DCP** is the only disulfonamide having this interesting and rather effective mtCA 2 inhibitory activity (compared to the structurally related **146** and **147** discussed above, which showed a much weaker inhibitory activity). It may be observed that the elongation of the inhibitor molecule **140** and **141** by means of a sulfanilyl moiety, such as in **151** and **152**, leads to a roughly 10 times increase of the inhibitory power of the corresponding sulfonamide against mtCA 2.
3. Submicromolar mtCA 2 inhibitory activity has been observed for a rather large number of derivatives, such as **150**, **MZA** and **BRZ-SAC**, which showed  $K_{\text{I}}$ s in the range of 127–978 nM. Compound **150** is structurally related to **151** and **152** discussed above, but it has the acetazolamide head, whereas most other compounds are heterocyclic sulfonamides in clinical use, except **TPM** which is a sulfamate. These data clearly show that many chemotypes lead to effective, submicromolar mtCA 2 inhibitors. Many of these compounds also effectively inhibit the other two mycobacterial CAs as well as hCA II.
4. Very effective mtCA 2 inhibitors were acetazolamide **AAZ** ( $K_{\text{I}}$  of 9 nM), etoxzolamide **EZA** ( $K_{\text{I}}$  of 27 nM) and dorzolamide **DZA** ( $K_{\text{I}}$  of 99 nM). These are

very encouraging data, as we detected CAIs with an affinity <100 nM for mtCA 2, but on the other hand, all these compounds are very potent inhibitors of most mammalian (host) CA isoforms,<sup>1</sup> which make them less appropriate for developing inhibitors targeting specifically  $\beta$ -CAs.

Thus, my purpose was to detect compounds which may have better affinity for mtCA 2 but at the same time behave as weaker hCA II inhibitors than the clinically used drugs **AAZ**, **EZA** or **DZA** discussed above. In a recent study by Carta *et al.* it was demonstrated that several diazenylbenzenesulfonamides act as weak-moderate inhibitors of the ubiquitous, house-keeping human isoforms hCA I and II.<sup>135</sup> Thus, by using this observation and data reported in Table 4.2, showing that compounds with an elongated tail geometry such as **150-152** possess good (low micromolar) mtCA 2 inhibitory activity, I decided to investigate a series of recently reported<sup>136</sup> diazenylbenzenesulfonamides **158** and **159**, as well as their precursors **160** and **161**, derived from sulfanilamide or metanilamide, prepared by Carta.<sup>135</sup> The mtCA 2 data with the new compounds were indeed quite interesting, as the following SAR was observed.

**Table 4.3.** Inhibition of CAs of human (hCA II) and mycobacterial CAs mtCA 1–3 with sulfonamides **158** and **159**, the sulfonates **160** and **161**, by a stopped-flow CO<sub>2</sub> hydrase assay.<sup>82</sup>

$K_I$ ( $\mu\text{M}$ )*					
<i>Cpd</i>	<i>R</i>	<i>hCA II</i> <sup>a</sup>	<i>mtCA 1</i> <sup>b</sup>	<i>mtCA 3</i> <sup>b</sup>	<i>mtCA 2</i> <sup>c</sup>
<b>158a</b>	<i>OH</i>	0.665	9.27	12.40	0.678
<b>158b</b>	<i>NH<sub>2</sub></i>	0.106	7.20	8.78	0.955
<b>158c</b>	<i>NHMe</i>	0.093	7.69	9.18	0.346
<b>158d</b>	<i>NMe<sub>2</sub></i>	0.638	6.86	30.7	5.48
<b>158e</b>	<i>NHCH<sub>2</sub>SO<sub>3</sub>Na</i>	0.105	6.78	8.90	0.059
<b>158f</b>	<i>N(Me)CH<sub>2</sub>SO<sub>3</sub>Na</i>	0.104	8.71	9.03	0.045
<b>159a</b>	<i>OH</i>	0.106	8.97	9.23	6.48
<b>159b</b>	<i>NH<sub>2</sub></i>	0.088	7.00	8.68	1.98
<b>159d</b>	<i>NMe<sub>2</sub></i>	0.105	7.54	9.36	2.13
<b>159e</b>	<i>NHCH<sub>2</sub>SO<sub>3</sub>Na</i>	0.107	7.51	9.45	6.56
<b>159f</b>	<i>N(Me)CH<sub>2</sub>SO<sub>3</sub>Na</i>	0.109	63	7.4	6.90
<b>160</b>	-	58.3	8.67	8.90	42.9
<b>161</b>	-	63.6	7.86	9.11	54.0

<sup>a</sup> Human recombinant isozyme, stopped-flow CO<sub>2</sub> hydrase assay method, pH 7.5, 20 mM Tris–HCl buffer.<sup>82</sup>

<sup>b</sup> Bacterial recombinant enzymes, at 20 °C, pH 8.3 in 20 mM Tris–HCl buffer and 20 mM NaCl, from Ref. 134.

<sup>c</sup> Bacterial recombinant enzyme, at 20 °C, pH 8.3 in 20 mM Tris–HCl buffer and 20 mM NaCl, this work.

\* Errors in the range of 5–10% of the shown data, from three different assays.

First, all the para-substituted azo dyes **158** were much more effective mtCA 2 inhibitors compared to the corresponding meta-substituted derivatives **159**. Thus, the metanilamide derivatives are less effective than the sulfanilamide ones. For the sulfanilamide derivatives **159**, the dimethylamino-substituted compound was the least effective mtCA 2 inhibitor ( $K_I$  of 5.48  $\mu\text{M}$ ), whereas the compounds possessing OH, NHMe and NH<sub>2</sub> moieties as substituents to the benzenediazenium system were better inhibitors, with  $K_I$ s of 346–955 nM. Thus, a very small structural change in the molecule of these compounds (e.g., an additional methyl moiety in the amino, methylamino or dimethylamino compounds **158b**–

**d**, leads to drastic changes of inhibitory activity). But the best activity has been observed for the aminomethylene sodium sulfonate derivative **158e** and the corresponding *N*-methylated analogue **158f**, which showed inhibition constants in the low nanomolar range ( $K_{IS}$  of 45–59 nM). The precursors sulfonates **160** and **161** were on the other hand very weak mtCA 2 inhibitors. It is also important to note that these two compounds show some selectivity as mtCA 2 versus hCA II inhibitors, with selectivity ratios for inhibiting the parasite over the host enzyme of 1.8–2.2. Thus, this drug design strategy may be considered a good one (for the *para*-substituted derivatives) in obtaining effective (low nanomolar) and selective mtCA 2 inhibitors. The meta-substituted compounds **159a**, **159b**, **159d-f** were less effective mtCA 2 inhibitors, with  $K_{IS}$  of 1.98–6.90  $\mu$ M.

#### 4.1.4 Conclusions

In conclusion, is reported here the kinetic characterization and the first inhibition studies of the third CA from the widespread human pathogen *M. tuberculosis*, mtCA 2, encoded by the gene Rv3588c, which has been shown to possess the highest catalytic activity for CO<sub>2</sub> hydration ( $K_{cat}$  of  $9.8 \times 10^5 \text{ s}^{-1}$ , and  $K_{cat}/K_M$  of  $9.3 \times 10^7 \text{ M}^{-1} \text{ s}^{-1}$ ) among the three CAs encoded in the genome of this pathogen. A series of sulfonamides/sulfamates was assayed for their interaction with mtCA 2, whereas some diazenylbenzenesulfonamides were newly synthesized from sulfanilamide/metanilamide by diazotization followed by coupling with amines or phenols. Several low nanomolar mtCA 2 inhibitors have been detected among which acetazolamide, ethoxzolamide and some 4- diazenylbenzenesulfonamides ( $K_{IS}$  of 9–59 nM). As this gene is essential for the growth of *M. tuberculosis*, inhibition of this enzyme may be relevant for the design of anti-TB drugs possessing a novel mechanism of action.

## 4.2 Substituted phenyl-1*H*-indole-5-sulfonamides: new $\beta$ -CAs strong inhibitors

### 4.2.1 Studies on *mtCA 1* and *mtCA 3*

In preliminary works<sup>106-108</sup> have been reported the cloning and kinetic characterizations of two of *M. tuberculosis*  $\beta$ -CAs: Rv1284<sup>108</sup> (*mtCA 1*, essential for the growth/virulence of this bacteria) and Rv3273<sup>106</sup> (*mtCA 3*, not essential). Molecular biology data, based on mutagenesis studies in strain H37Rv<sup>137</sup> and up-regulation of the encoding genes under the starvation conditions used to model persistent bacteria,<sup>138</sup> suggested that inhibition of mycobacterial  $\beta$ -CAs may be used for drug design campaigns aiming to find antimycobacterial agents.

Although it was showed that Rv1284<sup>108</sup> and Rv3273<sup>106</sup> can be inhibited by many types of sulfonamides or sulfamates, the best inhibitors detected so far showed only medium potency, with the best Rv1284 inhibitors possessing  $K_{iS}$  in the range of 100-200 nM and the best Rv3273 inhibitors having  $K_{iS}$  in the range of 90-500 nM, as shown above in Table 4.2. Furthermore, the best such compounds possessed simple scaffolds (e.g., 3-bromosulfanilamide **144** and indisulam **IND** were the most effective Rv1284 inhibitors, whereas acetazolamide **AAZ** and 2-amino-pyrimidin-4-yl-sulfanilamide **153** were the best Rv3273 inhibitors, Chart 4.2), which are not easily amenable to derivatization. Thus, I decided to explore different scaffolds incorporating the sulfamoyl zinc-binding groups (ZBGs) for the design of  $\beta$ -CA inhibitors targeting these mycobacterial enzymes.

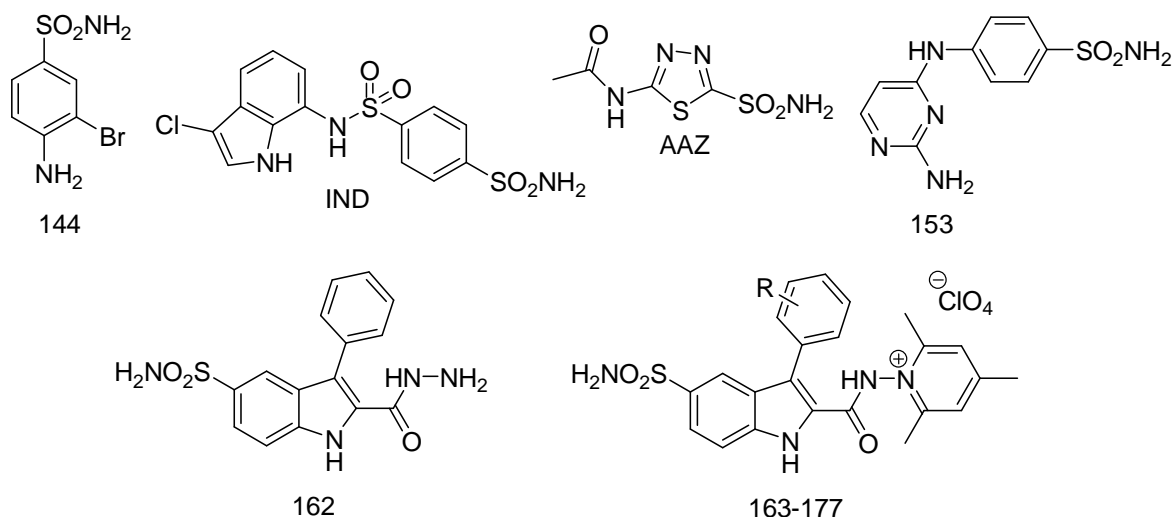


Chart 4.2. Sulfonamidic  $\beta$ -CAs inhibitors.

Recently has been reported the excellent inhibitory activity against various mammalian CA isozymes (belonging to the  $\alpha$ -CA genetic family)<sup>1</sup> of a series of 2-(hydrazinocarbonyl)-3-aryl-1*H*-indole-5-sulfonamides, synthesized by Guzel.<sup>139,140</sup> Considering this X-ray crystal structure of the hCA II–**162** adduct as starting point<sup>140</sup> and the good inhibitory activity of this class of sulfonamides against many  $\alpha$ -CA isoforms,<sup>2,140,139</sup> I decided to investigate whether this scaffold may also lead to effective  $\beta$ -CA inhibitors targeting the mycobacterial enzymes.

Inhibition data of the two  $\beta$ -CAs of *M. tuberculosis*, encoded by the genes Rv1284 and Rv3273, are shown in Table 4.4. Data of Table 4.4 also present the inhibitory activity against two physiologically relevant host CA isozymes (hCA I and II) of the new compounds **162-177** reported here (Chart 4.2), as the search of pathogen-selective CAIs is an important aspect in the design of new applications for this class of pharmacological agents. Inhibition data with the best mycobacterial CAIs detected so far,<sup>106,108</sup> i.e., compounds **144**, **IND**, **AAZ**, **153** are also shown in Table 4.4 for comparison reasons.

**Table 4.4.** Inhibition of CA Human Isoforms hCA I, II, and Mycobacterial Enzymes Rv1284 and Rv3273 with Sulfonamides **162-177**, and **144**, **IND**, **AAZ**, **153** as standards. <sup>a</sup> Errors in the range of 5-10% of the shown data, from three different assays, by a CO<sub>2</sub> hydration stopped flow assay. <sup>b</sup> Human, recombinant isozymes, pH 7.5, 20 mM TRIS-HCl buffer. <sup>c</sup> Bacterial recombinant enzyme, at 20 °C, pH 8.3 in 20 mM TRIS-HCl buffer and 20 mM NaCl.

<b>K<sub>I</sub> (nM)<sup>a</sup></b>					
<b>Cpd</b>	<b>R</b>	<b>hCA I<sup>b</sup></b>	<b>hCA II<sup>b</sup></b>	<b>mtCA I<sup>c</sup></b>	<b>mtCA 3<sup>c</sup></b>
<b>162</b>		7.5	7.2	48	31
<b>163</b>	<i>H</i>	9.0	71	6.5	7.0
<b>164</b>	2- <i>F</i>	8.5	91	9.3	6.9
<b>165</b>	3- <i>F</i>	11.3	3380	7.6	6.0
<b>166</b>	4- <i>F</i>	7.6	65	9.7	6.5
<b>167</b>	2- <i>Cl</i>	25.1	100	35.3	6.7
<b>168</b>	3- <i>Cl</i>	113	1800	31.8	6.6
<b>169</b>	4- <i>Cl</i>	3.2	77	20.9	0.96
<b>170</b>	2- <i>Br</i>	43.4	38	25.1	1.01
<b>171</b>	3- <i>Br</i>	30.8	74	3.2	0.97
<b>172</b>	4- <i>Br</i>	12.3	85	5.2	0.96
<b>173</b>	2- <i>Me</i>	10.5	106	0.98	6.8
<b>174</b>	3- <i>Me</i>	110	104	1.5	7.8
<b>175</b>	4- <i>Me</i>	5.1	68	0.97	3.6
<b>176</b>	3- <i>OMe</i>	8.6	2840	0.92	1.8
<b>177</b>	<i>F</i> <sub>5</sub>	9.7	0.93	0.93	0.88
<b>144</b>		6500	40	186	7320
<b>IND</b>		31	15	97	7840
<b>AAZ</b>		250	12	481	104
<b>153</b>		109	33	750	91

The following should be noted regarding the inhibition data of Table 4.4:

1. Rv1284 was effectively inhibited by the lead molecule **162** possessing a new indolesulfonamide scaffold, with a  $K_I$  of 48 nM, thus already two times a better Rv1284 CAI as compared to the best such compound detected so far, indisulam **IND** ( $K_I$  of 97 nM). Probably this new scaffold fitted better within the Rv1284 active site compared to the scaffolds of derivatives investigated earlier for the inhibition of this enzyme. However, the pyridinium derivatives **163-177**, were much more effective CAIs as compared to **162** or any other sulfonamide/sulfamate investigated earlier.<sup>108</sup> Thus, the new class of sulfonamides reported here showed inhibition constants in the range of 0.92-35.3 nM against Rv1284. The least effective derivatives were **167-170**, which, presenting  $K_I$ s in the range of 20.9-35.3 nM, were anyhow much more effective Rv1284 CAIs compared to compounds **144** and **IND** investigated previously ( $K_I$ s of 97-186 nM). These least effective CAIs incorporate 2-, 3-, 4-chloro and 2-bromophenyl moieties in position 3 of the indolesulfonamide scaffold. Another group of the new derivatives, among which **163-166**, **171**, **172**, and **174**, showed an enhanced inhibitory activity toward Rv1284, with  $K_I$ s in the range of 1.5-9.7 nM. These compounds incorporated the following substitution patterns at the 3-phenyl moiety of the indolesulfonamide scaffold: unsubstituted phenyl; 2-, 3-, and 4-fluorophenyl, 3-bromo- and 4-bromophenyl and 3-tolyl. The remaining derivatives **173** and **175-177** were subnanomolar inhibitors of Rv1284, with  $K_I$ s of 0.92-0.98 nM. They incorporate 2- and 4-tolyl, 3-methoxyphenyl, and perfluorophenyl moieties in the 3 position of the indolesulfonamide scaffold. Thus, not only the 2-(hydrazinocarbonyl)-3-substituted-phenyl-1*H*-indole-5-sulfonamide derivatives led to highly effective Rv1284 CAIs but the pyridinium derivatives obtained from this lead molecule showed a very interesting SAR, with the nature of the group substituting the 3-phenyl ring strongly influencing the enzyme inhibitory activity.
2. Rv3273 was also highly inhibited by **162** and its pyridinium derivatives **163-177** investigated here, with  $K_I$ s in the range of 0.88-31 nM. **162** was the least effective such CAI ( $K_I$  of 31 nM) although being at least a 3 times better inhibitor compared to compounds **AAZ** and **153** investigated earlier<sup>106</sup> and found to be the most effective inhibitors of this mycobacterial CA. All substitution patterns presented in the pyridinium derivatives **163-177** were highly effective in inducing excellent Rv3273 inhibitory properties, as the entire class of compounds showed a compact

behavior of very potent CAIs, with inhibition constants  $<8$  nM. Thus, the unsubstituted compound **163**, its 2-, 3-, 4-fluoro, 2- and 3-chloro, 2-, 3-, and 4-methyl, as well as 3-methoxy derivatives, showed  $K_{IS}$  of 1.8-8.0 nM, whereas the remaining compounds were even better CAIs, with inhibition constants in the range of 0.88-1.01 nM. These last derivatives incorporated 4-chlorophenyl, 2-, 3-, and 4-bromophenyl, and perfluorophenyl moieties in position 3 of the indolesulfonamide scaffold. It should be noted that the simple sulfonamides **144**, **IND**, **AAZ**, **153** investigated earlier,<sup>106</sup> as Rv3273 inhibitors are several orders of magnitude weaker CAIs as compared to the compounds investigated here.

3. Compounds **163-117** were also investigated as inhibitors of two human CAs, the cytosolic isoforms hCA I and II. Against the cytosolic isoform hCA I, the new pyridinium sulfonamides **163-177** generally showed good inhibitory activity, with  $K_{IS}$  in the range of 3.2-113 nM, being thus more active than the clinically used sulfonamide acetazolamide **AAZ** and having a similar activity to indisulam **IND**, a compound in clinical development as an anticancer agent.<sup>1</sup> Most of the new derivatives **163-177**, similarly to the lead **162**, were in fact low nanomolar hCA I inhibitors ( $K_{IS}$  in the range 3.2-30.8 nM), except for **168**, **170**, and **174**, which were less active ( $K_{IS}$  in the range 43.4-113 nM). SAR was thus rather flat except for the three less active compounds mentioned earlier, proving that most of the substitution patterns present in the phenyl ring in position 3 were beneficial for the hCA I inhibitory properties of these compounds.
4. Although the lead **162** showed excellent hCA II inhibitory activity ( $K_I$  of 7.2 nM), the derivatives **163-177** reported here were generally much less effective inhibitors of this ubiquitous isoform, with  $K_{IS}$  in the range of 38-3380 nM, except for the pentafluorophenyl derivative **177**, which was a subnanomolar hCA II inhibitor ( $K_I$  of 0.93 nM). These data were indeed very interesting, as they proved that the substitution pattern of the phenyl moiety in the pyridinium salts **163-177** was crucial for their hCA II inhibitory activity. Thus, a very active compound has been detected (**177**), together with moderate inhibitors (such as **163**, **164**, **166**, **167**, **169-175**,  $K_{IS}$  in the range 38-106 nM), as well as three very ineffective inhibitors (**5**, **8**, and **16**, possessing  $K_{IS}$  in the range 1800-3380 nM). It should be noted that all these ineffective hCA II inhibitors had the substituent of the phenyl moiety in the meta-position, probably provoking a clash with some amino acid residues present in the hCA II active site, as already documented earlier in literature.<sup>43</sup> However, in the

absence of detailed structural data for this class of inhibitors this remains a hypothesis to be checked. The pentafluorophenyl derivative **177** on the other hand, was 7.7 times more effective as a hCA II inhibitor as compared to the lead **162**, and it would be also of great interest to resolve its high resolution X-ray crystal structure in adduct with hCA II for understanding the elements leading to this excellent inhibitory activity.

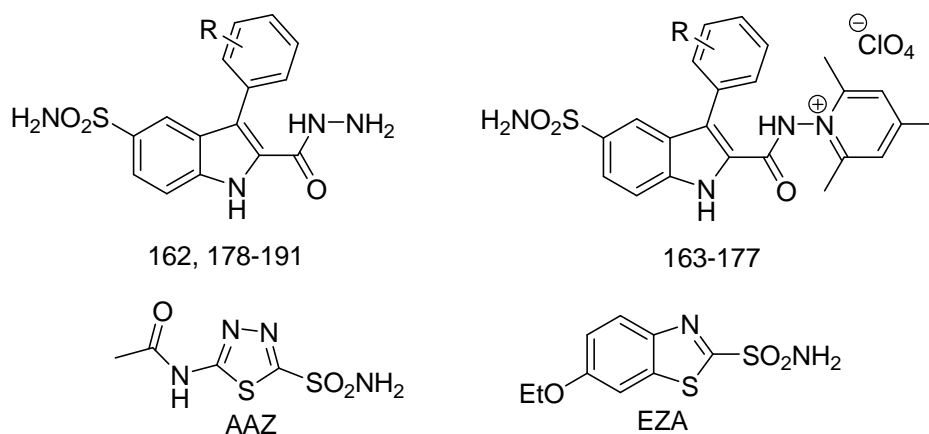
5. Many of the new sulfonamides reported here showed a much better inhibition of the mycobacterial  $\beta$ -CAs Rv1284 and Rv3273 than for the host enzymes hCA I and II. Furthermore, many of these compounds showed appreciable inhibition of only hCA I, an enzyme whose physiologic function is not well understood but seems to be marginal,<sup>1</sup> whereas the physiologically dominant hCA II showed a weak inhibition with these compounds (except one of them, **177**). Thus, these finding was important not only for detecting low nanomolar and subnanomolar inhibitors of the two mycobacterial CAs but also because these compounds showed a much higher affinity for these  $\beta$ -CAs than for hCA II. Thus, the selectivity ratios for the inhibition of the pathogen over the host enzymes were indeed very favorable for the potential use of these compounds for *in vivo* antimycobacterial studies.

In conclusion, the  $\beta$ -CAs encoded by the genes Rv1284 and Rv3273 of *Mycobacterium tuberculosis*, which show appreciable catalytic activity for the physiological reaction, were inhibited by sulfonamides; in particular among the variously substituted series of 2-(hydrazinocarbonyl)-3-aryl-1*H*-indole-5-sulfonamides, compounds **162-177** were highly effective, low nanomolar or subnanomolar inhibitors of the two mycobacterial enzymes, having a good affinity for the host enzyme hCA I but much lower inhibitory properties against the major, physiologically dominant isoform hCA II. These new compounds were several orders of magnitude better mycobacterial CAIs compared to sulfonamides/sulfamates investigated earlier.

#### 4.2.2 Studies on $\beta$ -CAs from *Cryptococcus neoformans* and *Candida albicans*

In the search for antiinfectives possessing a different mechanism of action, compared to the classical antibiotic/antifungal drugs,<sup>106-111,114,115,141,131</sup> I considered  $\beta$ -CAs from the fungal pathogens *Cryptococcus neoformans* (Can 2)<sup>142,143</sup> and *Candida albicans* (CaNce103)<sup>113</sup> that can be inhibited by sulfonamides, as recently emerged.<sup>111</sup> Up to now only simple sulfonamide scaffolds have been investigated as well as the 20 clinically used sulfonamides, among which acetazolamide **AZA** and ethoxzolamide **EZA**, for the inhibition of these enzymes, finding very few effective inhibitors against the fungal enzymes.<sup>111</sup> Indeed, **AZA** was a good Can2 inhibitor (with a  $K_I$  of 10 nM) whereas it had a more modest activity against CaNce103 (with a  $K_I$  of 132 nM).<sup>111</sup> **EZA** was even less effective, with  $K_I$ s of 87 nM against Can2 and 1070 nM against CaNce103, respectively. Thus, in the search for more effective sulfonamide compounds targeting the fungal pathogenic enzymes Can2 and CaNce103, I considered the series, synthesized by Guzel, of compounds shown earlier, presenting excellent activity towards  $\beta$ -CAs from *M. tuberculosis*, enlarged in this study, with other derivatives; in particular I considered the phenyl-1H-indole-5-sulfonamides **162**, **178-191** and their trimethylpyridinium salts analogs **163-177** shown in Table 4.5. Inhibition data with such derivatives, as well as the standard drugs **AZA** and **EZA** against Can2 and CaNce103, as well as the offtarget hCA I and II are presented in Table 4.5.

**Table 4.5.** Inhibition of human  $\alpha$ -CA (hCA) isozymes I and II and fungal  $\beta$ -CAs from *C. neoformans* (Can2) and *C. albicans* (CaNce103) with sulfonamides **162**, **178-191** and **163-177**, acetazolamide (**AZA**) and ethoxzolamide (**EZA**) as standards.<sup>82</sup>



$K_I$ (nM) <sup>*</sup>					
<i>Cpd</i>	<i>R</i>	<i>hCA I<sup>a</sup></i>	<i>hCA II<sup>a</sup></i>	<i>Can2<sup>b</sup></i>	<i>CaNce103<sup>b</sup></i>
<b>162</b>	<i>H</i>	7.5	7.2	72	85
<b>178</b>	<i>2-Me</i>	107	11.6	9.2	78
<b>179</b>	<i>3-Me</i>	730	48.4	9.1	43
<b>180</b>	<i>4-Me</i>	104	60.5	10.5	52
<b>181</b>	<i>2-F</i>	621	36.0	7.9	47
<b>182</b>	<i>3-F</i>	116	8.6	7.2	54
<b>183</b>	<i>4-F</i>	108	15.5	8.6	61
<b>184</b>	<i>2-Cl</i>	640	38.8	8.0	45
<b>185</b>	<i>3-Cl</i>	311	9.2	7.4	52
<b>186</b>	<i>4-Cl</i>	112	11.6	70	55
<b>187</b>	<i>2-Br</i>	110	48.5	62	81
<b>188</b>	<i>3-Br</i>	510	54.1	93	87
<b>189</b>	<i>4-Br</i>	659	40.8	118	94
<b>190</b>	<i>3-OMe</i>	342	7.4	12.0	128
<b>191</b>	<i>F<sub>5</sub></i>	110	7.0	103	7.5
<b>163</b>	<i>H</i>	9.0	71	16.5	42
<b>164</b>	<i>2-F</i>	8.5	91	16.2	19
<b>165</b>	<i>3-F</i>	11.3	3380	8.3	24
<b>166</b>	<i>4-F</i>	7.6	65	8.7	21
<b>167</b>	<i>2-Cl</i>	25.1	100	15.4	33
<b>168</b>	<i>3-Cl</i>	113	1800	4.4	31
<b>169</b>	<i>4-Cl</i>	3.2	77	3.1	29
<b>170</b>	<i>2-Br</i>	43.4	38	12.1	45
<b>171</b>	<i>3-Br</i>	30.8	74	14.3	48
<b>172</b>	<i>4-Br</i>	12.3	85	10.9	53
<b>173</b>	<i>2-Me</i>	10.5	106	6.5	62
<b>174</b>	<i>3-Me</i>	110	104	6.1	64
<b>175</b>	<i>4-Me</i>	5.1	68	5.9	41
<b>176</b>	<i>3-OMe</i>	8.6	2840	8.3	119
<b>177</b>	<i>F<sub>5</sub></i>	9.7	0.93	60.1	5.1
<b>AAZ</b>	-	250	12	10	132
<b>EZA</b>	-	25	8	87	1070

\* Errors in the range of  $\pm 5\%$  of the reported data from three different assays by a stopped-flow CO<sub>2</sub> hydration method.<sup>82</sup>

The following SAR can be drawn by considering data of Table 4.5:

1. Against Can2, the indolesulfonamides **162** and **178-191** showed good inhibitory activity, with  $K_I$ s in the range of 7.2–118 nM, making this entire sulfonamide class among the best sulphonamide Can2 inhibitors detected so far. Thus, the lead compound **162**, and derivatives **186-189** and **191** showed medium- high potency as Can2 inhibitors, with inhibition constants in the range of 62–118 nM. These derivatives incorporated the 4-chloro, 2-, 3- and 4-bromo as well as

pentafluorophenyl moieties (together with the lead **162**). In contrast, the remaining derivatives, incorporating methyl-, fluoro-, 2-/3-chloro- and methoxy-substituted phenyl moieties in the position 3 of the indole ring, of types **178-185**, and **190**, showed a much stronger Can2 inhibitory effect, with  $K_{IS}$  in the range of 7.2–10.5 nM. Thus, the nature of the group substituting the 3-phenyl ring present in compounds **1** and **2** strongly influences the Can2 inhibitory activity, with the methyl-, methoxy-, fluoro- and chloro-substituted derivatives showing a better activity (around 10-fold) compared to the lead **162** or the bromosubstituted compounds **187-189**. The position of the substituent of the phenyl ring was somehow less influential on the inhibitory activity (except for the chloro-derivatives **184-186**, case in which the 4-chlorosubstituted compound **186** was around 8.7–9.4 times a weaker inhibitor compared to the 2- or 3-chlorosubstituted isomers **184** and **185**). Indeed, the 2-, 3- or 4-methyl-substituted compounds **178-180**, or the 2-, 3- or 4-fluoro-substituted compounds **181-183**, respectively, showed comparable Can2 inhibitory activities. The pyridinium-substituted sulfonamides **163-177** showed similar activity with the corresponding series of sulfonamides just described. However they were better Can2 inhibitors compared to the corresponding carbohydrazides **162**, **178-191**, with inhibition constants in the range of 4.4–60.1 nM. Again the best Can2 inhibitor was a chlorine-substituted derivative, **168**, whereas the least effective one the pentafluorophenyl derivative **177**. Overall, this subseries of positively-charged sulfonamides showed excellent inhibitory capacity against the fungal enzyme Can2. It should be also mentioned that the most active compounds among the indolesulfonamides investigated here showed a better activity than acetazolamide **AZA**, the most effective Can2 inhibitor detected before this study.<sup>111</sup>

2. CaNce103 was slightly less susceptible to be inhibited by the tested indolesulfonamides, compared to Can2, a situation already observed with other classes of sulfonamides.<sup>111</sup> Thus, derivatives **162**, **178-191** showed  $K_{IS}$  of 7.5–128 nM for the inhibition of CaNce103, being more effective CAIs compared to **AZA** ( $K_I$  of 132 nM, the best sulfonamide inhibitor detected before this study) or **EZA** ( $K_I$  of 1070 nM). The 3-methoxysubstituted derivative **190** was the least effective CaNce103 inhibitor in this series, with a  $K_I$  of 128 nM, whereas the pentafluorophenyl- substituted one, **191**, the most effective inhibitor ( $K_I$  of 7.5 nM). This is one of the best CaNce103 inhibitors detected so far, with efficiency

17.6 times better than that of **AZA**, and also possessing a quite hydrophobic character due to the presence of the pentafluorophenyl moiety. This was a positive feature indeed, as sulfonamides are normally insufficiently lipophilic to penetrate the cell walls and membranes of some bacteria or fungi,<sup>141</sup> a fact which is attributed to the highly polar nature of the sulfonamidic group. The remaining derivatives, of types **162** and **178-189**, showed a rather flat SAR, and were only moderately inhibitory against CaNce103, with inhibition constants of 43–94 nM. Both the substitution pattern and the nature of the 3-substituted phenyl moieties influence the CaNce103 inhibitory activity of this series of indolesulfonamides. Thus, the lead **162** was moderately active ( $K_I$  of 85 nM) and all substitution patterns at the 3-phenyl moiety (except the bromophenyl ones, present in **187-189**) led to an increase of the CaNce103 inhibitory power. Actually, the bromophenyl derivatives **187-189** showed similar (**187** and **188**) or slightly diminished (**189**) CaNce103 inhibitory activity compared to **162**. For the halogenosubstituted compounds, the 2-halogeno derivative was a better CaNce103 inhibitor compared to the corresponding 3-halogeno substituted compound, which in turn was a better inhibitor compared to the 4-halogeno substituted derivative. For the methyl substituted compounds, the best CaNce103 inhibitor was the 3-substituted compound **179**. Thus, minor structural changes in the scaffold of compounds 2 strongly influence the CaNce103 inhibitory activity for this series of derivatives. The compounds **163-177**, bearing the trimethylpyridinium moiety instead of the terminal amino one present in **178-191**, were also effective CaNce103 inhibitors, with inhibition constants in the range of 5.1–119 nM. SAR for these positively-charged derivatives was rather similar to the corresponding carbohydrazides from which they were prepared, with the pentafluorophenyl derivative **177** being the most effective CaNce103 inhibitor reported so far ( $K_I$  of 5.1 nM) and the 3-methoxy-substituted one **176** the least effective ( $K_I$  of 119 nM). Generally, all the positively charged, trimethylpyridinium derivatives **163-177** were better CaNce103 inhibitors compared to the corresponding noncharged derivatives analogs.

3. The investigated sulfonamides were generally less effective hCA I inhibitors ( $K_{IS}$  of 110–730 nM) except for the lead **162**, which was a very potent hCA I inhibitor ( $K_I$  of 7.5 nM), but most of them were highly effective hCA II inhibitors ( $K_{IS}$  of 7.2–60.5 nM). However, some interesting selectivity ratios for the inhibition of the fungal over the host enzymes have been observed for some of the investigated

sulfonamides. Thus, compound **179** had a selectivity ratio of 5.1 for inhibiting Can2 over hCA II, and of 80.2 for inhibiting Can2 over hCA I. This is the first example of a fungal pathogenic CA-selective inhibitor (over the off-target hCA II). Similar features were also observed for **184**, with selectivity ratios of 4.8 (Can2 over hCA II) and 80 (Can2 over hCA I). However, no CaNce103 selective inhibitors (over hCA II) have been detected so far, in this as in other studies.<sup>111</sup>

### 4.3 Conclusions

In conclusion, the  $\beta$ -CAs encoded by the genes Rv1284 and Rv3273 of *Mycobacterium tuberculosis*, showing appreciable catalytic activity for the physiological reaction, were inhibited by sulfonamides; in particular among the variously substituted series of 2-(hydrazinocarbonyl)-3-aryl-1*H*-indole-5-sulfonamides, compounds **162-177** were highly effective, low nanomolar or subnanomolar inhibitors of the two mycobacterial enzymes, having a good affinity for the host enzyme hCA I but much lower inhibitory properties against the major, physiologically dominant isoform hCA II. These new compounds were several orders of magnitude better mycobacterial CAIs compared to sulfonamides/sulfamates investigated earlier.

Both  $\beta$ -CAs from the fungal pathogens *C. neoformans* (Can 2) and *C. albicans* (CaNce103), were potently inhibited by these sulfonamides, with inhibition constants in the range of 4.4–118 nM against Can2, and of 5.1–128 against CaNce103, respectively. SAR was rather well defined, with minor structural changes in the 3-substituted phenyl moiety being the main contributors to the enzyme inhibitory activity. Some of the investigated sulfonamides also showed acceptable selectivity ratios for inhibiting Can2 over the host, human enzymes hCA I and II.



## CHAPTER FIVE

### *Inhibition studies on mitochondrial CA VA and VB with sulfonamides*

#### 5.1 CAIs as potential anti-obesity drugs

Among the  $\alpha$ -CA isoforms found in animals, two CA isozymes, VA and VB, are present in mitochondria.<sup>66,144</sup> These isozymes are involved in several biosynthetic processes, such as ureagenesis,<sup>144</sup> gluconeogenesis<sup>145</sup> and lipogenesis, in vertebrates (for example, rodents) and in invertebrates (for example, the locust).<sup>146-149</sup> The provision of enough substrate bicarbonate, in several biosynthetic processes involving pyruvate carboxylase (PC), acetyl-CoA carboxylase (ACC) and carbamoyl phosphate synthetases I and II, is assured mainly by the catalytic reaction involving the mitochondrial isozymes CA VA and VB, probably assisted by the high activity cytosolic isozyme CA II (Figure 5.1).<sup>150</sup>

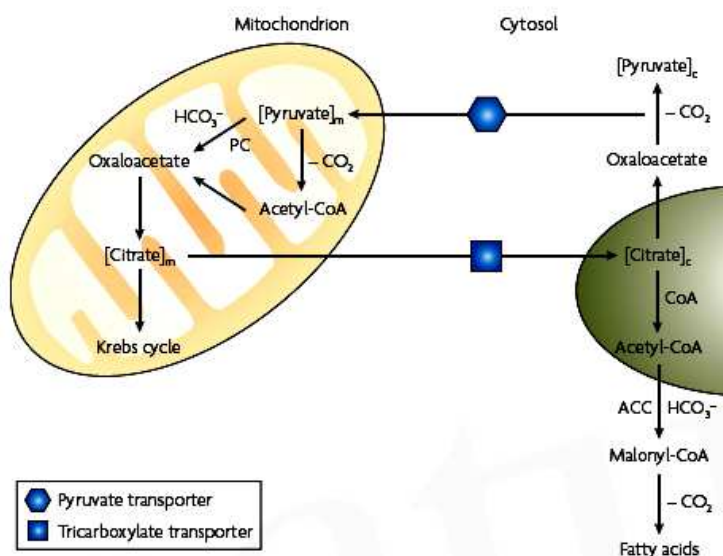


**Figure 5.1.** Fatty-acid biosynthesis and the role of carbonic anhydrase isozymes.

Mitochondrial pyruvate carboxylase (PC) is needed for the efflux of acetyl groups from the mitochondria to the cytosol where fatty-acid biosynthesis takes place.<sup>64,150</sup> Pyruvate is carboxylated to oxaloacetate in the presence of bicarbonate under the catalytic influence of the mitochondrial isozymes CA VA and/or CA VB. The mitochondrial membrane is impermeable to acetyl-CoA, which reacts with oxaloacetate, leading to the formation of citrate, which is then translocated to the cytoplasm by means of the tricarboxylic acid transporter. As oxaloacetate is unable to cross the mitochondrial membrane, its decarboxylation regenerates pyruvate, which can then be transported into the mitochondria by means of the pyruvate transporter. The acetyl-CoA thus generated in the cytosol is in fact used for *de novo* lipogenesis, by carboxylation in the presence of acetyl-CoA carboxylase (ACC) and bicarbonate, with formation of malonyl-CoA, the conversion between  $CO_2$  and bicarbonate being assisted by CA II. Subsequent steps involving the sequential transfer of acetyl groups lead to longer-chain fatty acids. Therefore, CA isozymes are critical to the entire process of fatty-acid biosynthesis: VA and/or VB within the mitochondria (to provide enough substrate to PC), and CA II within the cytosol (for providing sufficient substrate to ACC).

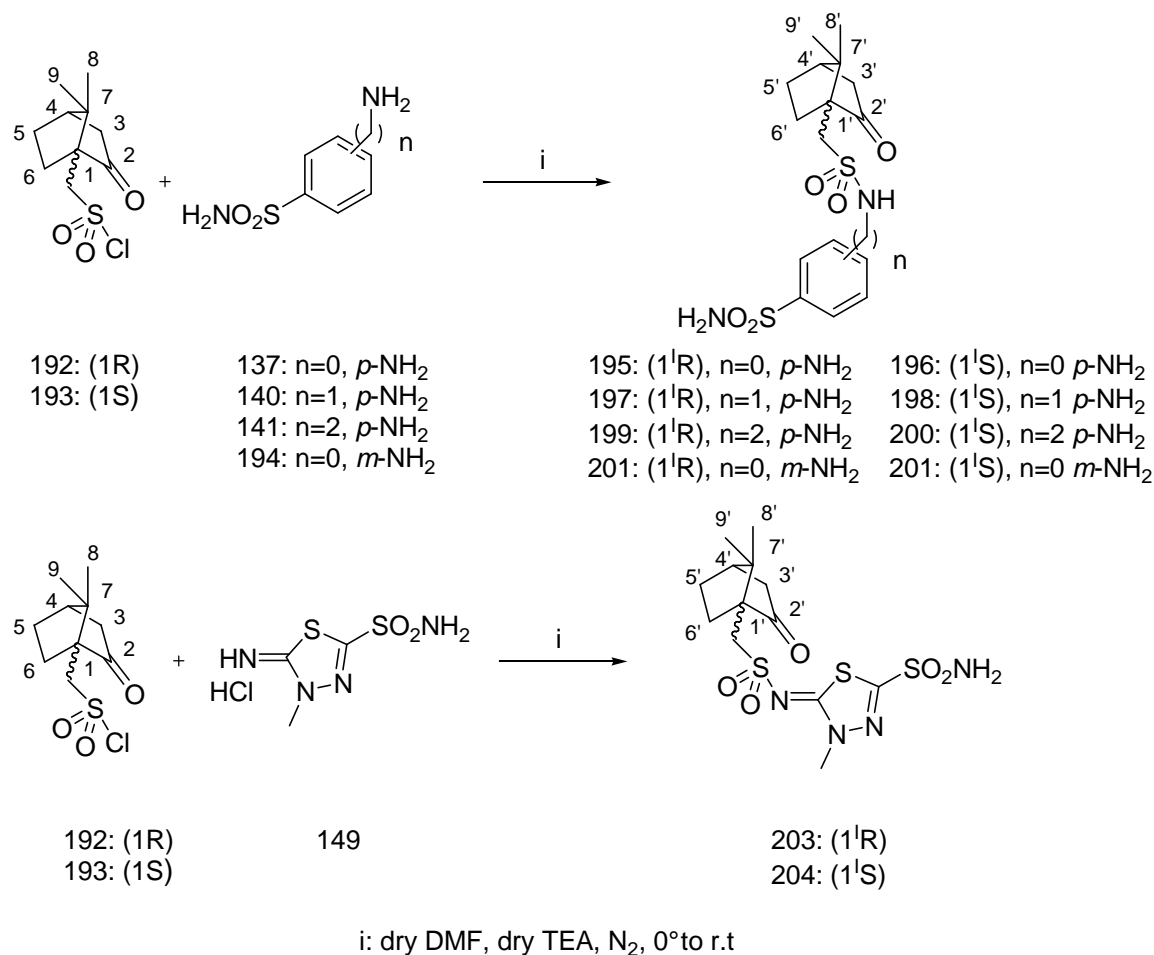
Several studies have provided evidence that CAIs have potential as anti-obesity drugs, which might be due to their effects on CA isozymes. Topiramate (TPM) is an anti-epileptic drug possessing potent anticonvulsant effects due to a multifactorial mechanism of action: blockade of sodium channels and kainate/AMPA ( $\alpha$ -amino-3-hydroxy-5-methyl-4-isoxazole propionic acid) receptors, CO<sub>2</sub> retention secondary to inhibition of the red blood cell and brain CA isozymes, as well as enhancement of GABA ( $\gamma$ -aminobutyric acid)-ergic transmission.<sup>40</sup> A side effect of this drug observed in obese patients was the loss of body weight, although no pharmacological explanation of this phenomenon has been provided.<sup>151</sup> Furthermore, Topiramate was shown to reduce energy and fat gain in lean (*Fa/?*) and obese (*fa/fa*) Zucker rats.<sup>151</sup> It was recently demonstrated that Topiramate is also a potent inhibitor of several CA isozymes, such as II, VA, VB, VI, VII, XII and XIII, and the X-ray crystal structure of its complex with human CA II has been determined, revealing the molecular interactions that explain the high affinity of this compound for the CA active site.<sup>40</sup>

Zonisamide (ZNS) is another anti-epileptic drug used as adjunctive therapy for refractory partial seizures.<sup>64,41,152</sup> It has multiple mechanisms of action, and exhibits a broad spectrum of anticonvulsant activity. Similar to Topiramate, recent clinical studies have demonstrated additional potential for therapeutic use for neuropathic pain, bipolar disorder, migraine, obesity, eating disorders and Parkinson's disease.<sup>64</sup> Zonisamide is an aliphatic sulfonamide, which also potently inhibits cytosolic and mitochondrial CAs involved in lipogenesis.<sup>41</sup> Furthermore, Zonisamide in conjunction with a reduced-calorie diet (deficit of 500 kcal per day), resulted in an additional mean 5 kg (11-pound) weight loss compared with diet alone in obese female patients.<sup>152</sup> Thus, inhibition of mitochondrial isoforms CA VA and VB, probably in conjunction with that of the ubiquitous cytosolic isoform CA II, may represent targets for novel anti-obesity drugs that reduce lipogenesis by inhibiting CAs.<sup>150</sup>

## **5.2 (R)-/(S)-10-Camphorsulfonyl-substituted aromatic/heterocyclic sulfonamides selectively inhibit mitochondrial over cytosolic carbonic anhydrases**

Sulfonamides<sup>1,7,19,153,154,98,130</sup> and sulfamates<sup>1,19,155,156,40</sup> are among the most potent CAIs reported up to now against all the physiologically relevant CA isozymes, including the mitochondrial ones CA VA and VB.<sup>1,19,66,144</sup> Thus, I decided to explore new series of aromatic as well as heterocyclic sulfonamides which should also incorporate lipophilic

moieties, in order to endow them with good membrane permeability and thus access to mitochondria, where these isoforms are located. I have considered the reactions of (1*R*)-(-)-10-camphorsulfonyl chloride **192** and (1*S*)-(+)-10-camphorsulfonyl chloride **193** with aromatic/heterocyclic sulfonamides incorporating amino or imino moieties, as a facile way to generate such new compounds (Scheme 5.1).



**Scheme 5.1:** Synthesis of sulfonamide derivatives **195-204**.

Indeed, reaction of sulfonyl chlorides **192** and **193** with amino/imino-sulfonamides **137**, **140**, **141**, **194** afforded a series of chiral new sulfonamides of type **195-204**, which incorporated the highly lipophilic camphorsulfonyl moieties. Such derivatizations (the “tail approach”) have been investigated earlier extensively by my research group,<sup>74,157,158</sup> being shown that they may lead to effective CAIs.

The new sulfonamides reported here, of types **195-204**, as well as the classical CAIs in clinical use **AAZ-ZNS**, have been assayed<sup>82</sup> for the inhibition of four physiologically relevant CA isoforms, the cytosolic, off-target hCA I and II, as well as the mitochondrial hCA VA and hCA VB (Table 5.1).

**Table 5.1.** hCA I, II, VA and VB inhibition data with sulfonamides **195-204** and the standard inhibitors **AAZ- ZNS**, by a stopped-flow, CO<sub>2</sub> hydration assay method.<sup>82</sup> Data for the standard inhibitors are from ref.<sup>1</sup>

<b>K<sub>I</sub> (nM)<sup>*</sup></b>				
<b>Compound</b>	<b>hCA I<sup>a</sup></b>	<b>hCA II<sup>a</sup></b>	<b>hCA VA<sup>b</sup></b>	<b>hCA VB<sup>b</sup></b>
<b>195</b>	1241	1207	17.1	26.4
<b>196</b>	3130	1165	68.6	30.0
<b>197</b>	920	1563	16.6	40.3
<b>198</b>	1042	2459	27.5	67.3
<b>199</b>	4964	963	64.5	36.2
<b>200</b>	5513	2254	33.2	54.1
<b>201</b>	9711	78.9	35.3	38.4
<b>202</b>	81.5	2304	48.7	44.3
<b>203</b>	5246	1773	5.9	7.8
<b>204</b>	4382	398	21.0	7.3
<b>AAZ</b>	250	12	63	54
<b>MZA</b>	50	14	65	62
<b>EZA</b>	25	8	25	19
<b>DCP</b>	1200	38	630	21
<b>TPM</b>	250	10	63	30
<b>ZNS</b>	56	35	20	6033

<sup>a</sup> Full length, cytosolic recombinant isoform; <sup>b</sup> Full length, mitochondrial recombinant enzyme.

\* Errors in the range of  $\pm$  5-10 % of the reported value, from 3 different assays.

The following should be observed regarding CA inhibition data with these compounds:

1. Sulfonamides **195-204** incorporating the lipophilic moieties of the *R*- and *S*-10-camphorsulfonyl type, behaved as weak inhibitors of the cytosolic, slow isoform hCA I, with inhibition constants in the micromolar range ( $K_{IS}$  of 0.92–9.71  $\mu$ M). Only one of these derivatives, **202**, showed more efficient inhibition of this isoform, with  $K_I$  of 81.5 nM. It was interesting to note the huge difference in inhibitory power between the two enantiomers **201** and **202**, with the last one being approximately 120 times a better hCA I inhibitor compared to the other. Thus, the nature of the moiety on which the sulfonamide group was grafted (aromatic or heterocyclic) as well as the spacer between this moiety and the camphorsulfonyl group, did not influence markedly the activity of these compounds. It was however difficult to explain the rather good inhibitory activity of **202**, but a recent work showed a very variable binding pattern within the enzyme active site even for structurally very similar congeners belonging to the sulfonamides.<sup>159</sup> It may be observed, on the other hand, that the clinically used derivatives **AAZ-ZNS** showed

more potent inhibitory activities against these isoforms, with inhibition constants in the range of 25 nM-1.2  $\mu$ M.

2. A rather similar inhibition pattern with compounds **195-204** (as for hCA I) has been also observed against isoform hCA II. Thus, weak inhibition, in the micromolar range ( $K_{IS}$  of 0.96–2.45  $\mu$ M) was observed for all these compounds except **201** and **204**, more effective hCA II inhibitors ( $K_{IS}$  of 78.9–398 nM). Again, important differences of activity have been observed for diverse enantiomers of the same sulfonamide (e.g., **201** versus **202**, or **203** versus **204**), and this has been documented by crystallographic work on different classes of chiral sulfonamides.<sup>160,140</sup> The clinically used derivatives were on the other hand low nanomolar inhibitors of this isoform, with  $K_{IS}$  in the range of 8-38 nM.
3. The mitochondrial isoform hCA VA was much more susceptible to inhibition by compounds **195-204** compared to the cytosolic ones discussed above. Indeed,  $K_{IS}$  in the range of 5.9 – 68.6 nM have been measured for these derivatives. SAR was here more intriguing compared to the inhibition of the cytosolic isoforms. Thus, generally the *R* enantiomer was more effective as a hCA VA inhibitor compared to the corresponding *S*-enantiomer (except for the pair **199-200** where the reverse was true). The most effective inhibitor was thus the heterocyclic derivative **203** ( $K_I$  of 5.9 nM), which is the most effective hCA VA inhibitor reported to far. Its enantiomer, **204**, was a 3.5 times weaker inhibitor, being anyhow equipotent to **ZNS**, one of the best hCA VA inhibitors among the clinically used drugs.
4. The second mitochondrial isoform, hCA VB was also significantly inhibited by sulfonamides **195-204**, with inhibition constants in the range of 7.3–67.3 nM, two orders of magnitude better than the inhibition of the cytosolic isoforms hCA I and II discussed above. Again the best inhibitors were the heterocyclic sulfonamides **203** and **204**, and generally the *R* enantiomer was more active compared to the corresponding *S* one, as for the inhibition of hCA VA discussed above (the only exception is the pair **203-204**).
5. The selectivity ratios for the inhibition of the mitochondrial over the cytosolic isoforms, for the new compounds reported here, were very good. For example, **203**, a low nanomolar hCA VA and VB inhibitor, had a selectivity ratio of 889 for the inhibition of hCA VA over hCA I, and of 300.5 for the inhibition of hCA VA over hCA II. The selectivity ratios for the inhibition of hCA VB over hCA I and of hCA VB over hCA II were of 672 and 227, respectively. For ethoxzolamide **EZA**, one

of the best classical mitochondrial CA inhibitors, these parameters were of 1 (hCA VA over hCA I), 0.32 (hCA VA over hCA II); 1.31 (hCA VB over hCA I) and 0.42 (hCA VB over hCA II), respectively. Thus, most of the classical sulfonamides/sulfamates were much better hCA I/II inhibitors than hCA VA/VB inhibitors, whereas exactly the reverse was true for the new sulfonamides **195-204** reported here.

In conclusion, the new derivatives, synthesized by reaction of the sulfonyl chlorides with amino/imino-containing sulfonamides, were investigated for the inhibition of CA I, II, VA and VB. The new sulfonamides selectively inhibited the mitochondrial isozymes hCA VA and VB over the cytosolic, offtarget ones hCA I and II, with inhibition constants in the low nanomolar range (5.9–68.6 nM). The nature, chirality and position of the groups substituting the sulfonamide greatly influenced the CA inhibitory properties.



## CHAPTER SIX

### *Experimental section*

#### 6.1 Chemistry

Nuclear magnetic ( $^1\text{H}$ ,  $^{13}\text{C}$ ,  $^{19}\text{F}$ , COSY, DEPT, HSQC and HMBC) spectra determined in  $\text{DMSO-}d_6$  and  $\text{CDCl}_3-d$  and were recorded using a Bruker Advance III 400 MHz instrument. The chemical shifts ( $\delta$  scale) are reported in parts per million (ppm) and the coupling constants ( $J$ ) are expressed in hertz (Hz). Splitting patterns are designated as follows: s, singlet; d, doublet; t, triplet; q, quadruplet; m, multiplet; dd, doubledoublet. For all new compounds DEPT, COSY, HSQC and HMBC were routinely used to definitely assign the signals of  $^1\text{H}$  and  $^{13}\text{C}$ . Infrared (IR) spectra were recorded on a Perkin–Elmer Spectrum R XI spectrometer as solids on KBr plates and are expressed in  $\nu$  ( $\text{cm}^{-1}$ ). Melting points (mp) were measured in open capillary tubes, unless otherwise stated, using a Büchi Melting Point B-540 melting point apparatus and are uncorrected. Polarimetric measurements were performed on a Perkin-Elmer 343 polarimeter at  $20^\circ\text{C}$  in 0.1 N NaOH ( $\lambda=589$  nm) solutions. Electron ionization mass spectra (30eV) were recorded in positive or negative mode on a Water MicroMass ZQ spectrometer. Thin layer chromatography (TLC) was carried out on Merck Silica Gel 60 F254 aluminum backed plates. Elution of the plates was carried out using ethyl acetate/*n*-Hexane or MeOH/DCM systems. Visualization was achieved with UV light at 254 nm, by dipping into a 0.5% aqueous potassium permanganate solution, by Hanessian's stain solution and heating with a hot air gun or by exposure to iodine. Flash column chromatography was carried out using Merck SilicaGel 60Å, 230-400 mesh, (obtained from Aldrich Chemical Co.) as stationary phase. The crude product was introduced into the column as a solution in the same elution solvent system, alternatively as a powder obtained by mixing the crude product with the same weight of silica gel in acetone and then removing the solvent in vacuo at room temperature, or dissolved into a minimum amount of DCM or carbon tetrachloride. All moisture or air sensitive reactions were carried out in oven-dried glassware under a positive pressure of nitrogen or argon using standard syringe/septa techniques to transfer solutions. All the inert gases used (nitrogen and argon) were passed through jacket columns fitted with activated silica gel containing cobalt(II) chloride adsorbed as humidity indicator. umbelliferone, aliphatic acids **28**, **29**, **51**, sulfanyl chlorides **192**,**193** and all the sulfonamides used for synthesis are commercially available from Sigma–Aldrich (Milan, Italy), and were used

without further purification. All other solvents and chemicals were used as supplied from Aldrich Chemical Co., Acros, Fisher, Alfa Aesar or Lancaster Synthesis. All CA isozymes were recombinant ones produced and purified in our laboratory as described earlier.<sup>7,130,154,98</sup>

## 6.2 CA Inhibition Assays

An SX.18MV-R Applied Photophysics stopped-flow instrument has been used for assaying the CA catalyzed CO<sub>2</sub> hydration activity.<sup>82</sup> Phenol red (at a concentration of 0.2 mM) has been used as indicator, working at the absorbance maximum of 557 nm, with 10-20 mM Hepes (pH 7.5, for  $\alpha$ -CAs) or Tris (pH 8.3 for  $\beta$ -CAs) as buffers, and 20 mM Na<sub>2</sub>SO<sub>4</sub> (for  $\alpha$ -CAs) or 20 mM NaCl for  $\beta$ -CAs (for maintaining constant the ionic strength), following the initial rates of the CA-catalyzed CO<sub>2</sub> hydration reaction for a period of 10-100 s. The CO<sub>2</sub> concentrations ranged from 1.7 to 17 mM for the determination of the kinetic parameters and inhibition constants. For each inhibitor, at least six traces of the initial 5-10% of the reaction have been used for determining the initial velocity. The uncatalyzed rates were determined in the same manner and subtracted from the total observed rates. Stock solutions of inhibitor (0.1 mM) were prepared in distilled-deionized water and dilutions up to 0.01 nM were done thereafter with distilled-deionized water. Inhibitors and enzyme solutions were preincubated together for 15 min in case of sulfonamidic/sulfamatic inhibitors, or for 15 min to 72 h at room temperature (15 min) or 4 °C (all other incubation times), in case of (thio)coumarinic inhibitors, prior to assay in order to allow for the formation of the E-I complex or for the eventual active site mediated hydrolysis of the inhibitor. Data reported for (thio)coumarins show the inhibition after 6 h incubation, which led to the completion of the *in situ* hydrolysis of the (thio)coumarin and formation of the hydroxy/mercapto-cinnamic acid.<sup>51</sup>

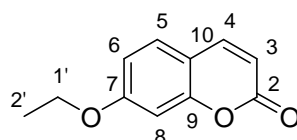
The inhibition constants were obtained by nonlinear leastsquares methods using PRISM 3, as reported earlier<sup>4,9,51,73,132</sup> and represent the mean from at least three different determinations.

## 6.3 Synthesis

### 6.3.1 General procedure for preparation of ether derivatives 6-10<sup>95</sup>

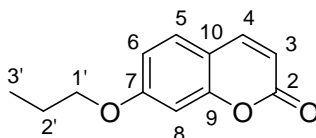
Reaction of umbelliferone (7-hydroxycoumarin) with alkyl halides was done in Williamson conditions. In a round bottom flask, at 0°C and under nitrogen atmosphere, to a suspension in dry DMF (2 ml) of sodium hydride (60% mineral oil dispersion) (1.2 mmol), previously washed with *n*-Hexane, umbelliferone (1.0 mmol) was carefully added. After five minutes a solution of the appropriate alkyl halide (1.0 mmol) in dry DMF (1.0 ml) was added dropwise. The mixture was left stirring at r.t until it was complete (monitoring by TLC); then it was quenched with crushed ice (2 g) extracted with ethyl acetate (5 ml), washed with brine (5 x 5 ml). The collected organic phase was dried on anhydrous Na<sub>2</sub>SO<sub>4</sub>, filtered and evaporated under vacuum. The crude was purified by silica gel column chromatography using *n*-Hexane/ethyl acetate mixture as eluent, affording compounds 6-10 as white solids in medium yields.

#### 7-ethoxy-2H-chromen-2-one (6)



Compound **6** was synthesized by reacting umbelliferone (0.2 g, 1.0 eq) with bromoethane (0.09 ml, 1.0 eq.), in presence of sodium hydride 60% mineral oil dispersion following the general procedure mentioned above. The crude was purified by silica gel column chromatography eluting with 20% AcOEt in *n*-Hexane to afford compound **6** as white solid in 45% yield. m.p: 90.5-92.5 °C; silica gel TLC *R<sub>f</sub>* 0.29 (AcOEt/*n*-Hex 20%, v/v);  $\nu_{\max}$  (KBr) cm<sup>-1</sup>, 2918 (C-H), 1721 (C=O), 1609 (C=C), 1522 (aromatic), 1226 (C-O);  $\delta_{\text{H}}$  (400MHz, DMSO-*d*<sub>6</sub>) 1.37 (3H, t, *J* 7.2, 2'-H<sub>3</sub>), 4.15 (2H, q *J* 7.2, 1'-H<sub>2</sub>), 6.30 (1H, d *J* 9.6, 3-H), 6.95 (1H, dd *J* 8.8, 2.2, 6-H), 6.98 (1H, d *J* 2.2, 8-H), 7.63 (1H, d *J* 8.8, 5-H), 8.00 (1H, d *J* 9.6, 4-H);  $\delta_{\text{C}}$  (100 MHz, DMSO-*d*<sub>6</sub>) 162.6 (C-7), 161.2 (C-2), 159.2 (C-9), 145.2 (C-4), 130.3 (C-5), 113.5 (C-6), 113.2 (C-3), 113.1 (C-10), 101.9 (C-8), 64.9 (C-1'), 15.3 (C-2'); *m/z* (ESI+) 191.18 ([M+H]<sup>+</sup> 12%), 213.15 ([M+Na]<sup>+</sup> 25%), 403.17 ([2M+Na]<sup>+</sup> 100%).

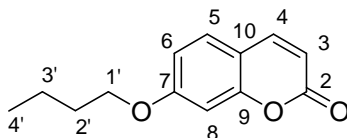
#### 7-propoxy-2H-chromen-2-one (7)



Compound **7** was synthesized by reacting umbelliferone (0.2 g, 1.0 eq) with 1-bromopropane (0.11 ml, 1.0 eq.), in presence of sodium hydride 60% mineral oil dispersion (0.06 g, 1.2 eq.) following the general procedure mentioned above. The crude was purified by silica gel column chromatography eluting with 20% AcOEt in *n*-Hexane to afford compound **7** as white solid in 40% yield. m.p: 66-68 °C; silica gel TLC *R<sub>f</sub>* 0.55 (AcOEt/*n*-Hex 20%, v/v);  $\nu_{\max}$  (KBr) cm<sup>-1</sup>, 2927 (C-H), 1718 (C=O), 1611 (C=C), 1525 (aromatic), 1218 (C-O);  $\delta_{\text{H}}$  (400MHz, DMSO-*d*<sub>6</sub>) 0.99 (3H, t *J* 6.8, 3'-H<sub>3</sub>), 1.75 (2H, m, 2'-H<sub>2</sub>), 4.04 (2H, t *J* 6.8, 1'-H<sub>2</sub>), 6.28 (1H, d *J* 9.4, 3-H), 6.94 (1H, dd *J* 8.4, 2.2, 6-H), 6.97 (1H, d *J* 2.2, 8-H), 7.62 (1H, d *J* 8.4, 5-H), 7.99 (1H, d, *J* 9.4, 4-H);  $\delta_{\text{C}}$  (100 MHz, DMSO-*d*<sub>6</sub>) 162.7 (C-7), 161.1 (C-2), 156.3 (C-9), 145.1 (C-4), 130.3 (C-5), 113.5 (C-6), 113.2 (C-

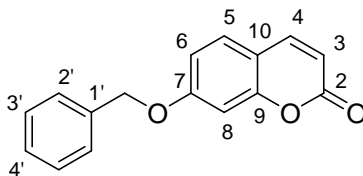
3), 113.1 (C-10), 101.9 (C-8), 70.6 (C-1'), 22.7 (C-2'), 11.1 (C-3');  $m/z$  (ESI+) 205.23 ([M+H]<sup>+</sup> 5%), 227.20 ([M+Na]<sup>+</sup> 100%), 241.19 (4).

### 7-butoxy-2H-chromen-2-one (8)

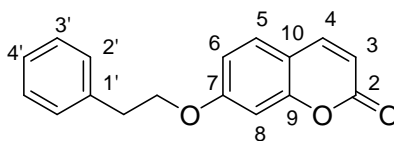


Compound **8** was synthesized by reacting umbelliferone (0.4 g, 1.0 eq) with 1-bromobutane (0.26 ml, 1.0 eq.), in presence of sodium hydride 60% mineral oil dispersion (0.12 g, 1.2 eq.) following the general procedure mentioned above. The crude was purified by silica gel column chromatography eluting with 14% AcOEt in *n*-Hexane to afford compound **8** as white solid in 45% yield. m.p: 60-62 °C; silica gel TLC  $R_f$  0.28 (AcOEt/*n*-Hex 14%, v/v);  $\nu_{\max}$  (KBr)  $\text{cm}^{-1}$ , 2915 (C-H), 1720 (C=O), 1608 (C=C), 1523 (aromatic), 1219 (C-O);  $\delta_{\text{H}}$  (400MHz, DMSO- $d_6$ ) 0.97 (3H, t  $J$  7.0, 4'-H<sub>3</sub>), 1.47 (2H, m, 3'-H<sub>2</sub>), 1.75 (2H, m, 2'-H<sub>2</sub>), 4.11 (2H, t  $J$  7.0, 1'-H<sub>2</sub>), 6.31 (1H, d  $J$  9.4, 3-H), 6.97 (1H, dd  $J$  8.4, 2.4, 6-H), 7.01 (1H, d  $J$  2.4, 8-H), 7.65 (1H, d  $J$  8.4, 5-H), 8.02 (1H, d  $J$  9.4, 4-H);  $\delta_{\text{C}}$  (100 MHz, DMSO- $d_6$ ) 162.8 (C-7), 161.2 (C-2), 156.3 (C-9), 145.2 (C-4), 130.4 (C-5), 113.6 (C-6), 113.3 (C-3), 113.1 (C-10), 102.0 (C-8), 68.9 (C-1'), 31.4 (C-2'), 19.5 (C-3'), 14.5 (C-4');  $m/z$  (ESI+) 219.21 ([M+H]<sup>+</sup> 7%), 241.19 ([M+Na]<sup>+</sup> 100%), 273.22 (4), 301.26 (12), 441.34 (5), 459.20 ([2M+Na]<sup>+</sup> 47%).

### 7-(benzyloxy)-2H-chromen-2-one (9)



Compound **9** was synthesized by reacting umbelliferone (0.4 g, 1.0 eq) with (bromomethyl)benzene (0.29 ml, 1.0 eq.), in presence of sodium hydride 60% mineral oil dispersion (0.12 g, 1.2 eq.) following the general procedure mentioned above. The crude was purified by silica gel column chromatography eluting with 25% AcOEt in *n*-Hexane to afford compound **9** as white solid in 40% yield. m.p: 93.5-95.5 °C; silica gel TLC  $R_f$  0.41 (AcOEt/*n*-Hex 25%, v/v);  $\nu_{\max}$  (KBr)  $\text{cm}^{-1}$ , 2919 (C-H), 1716 (C=O), 1614 (C=C), 1531 (aromatic), 1224 (C-O);  $\delta_{\text{H}}$  (400MHz, DMSO- $d_6$ ) 5.26 (2H, s, OCH<sub>2</sub>), 6.32 (1H, d  $J$  9.6, 3-H), 7.06 (1H, dd  $J$  8.8 2.6, 6-H), 7.11 (1H, d  $J$  2.6, 8-H), 7.46 (5H, m, 2'-H<sub>2</sub>, 3'-H<sub>2</sub>, 4'-H), 7.67 (1H, d  $J$  8.8, 5-H), 8.02 (1H, d  $J$  9.6, 4-H);  $\delta_{\text{C}}$  (100 MHz, DMSO- $d_6$ ) 162.4 (C-7), 161.2 (C-2), 156.3 (C-9), 145.2 (C-4), 137.2 (C-1'), 130.5 (C-5), 129.5 (C-3'), 129.0 (C-4'), 128.8 (C-2'), 113.9 (C-6), 113.5 (C-3), 113.4 (C-10), 102.6 (C-8), 70.8 (OCH<sub>2</sub>);  $m/z$  (ESI+) 205.23 (7), 253.24 ([M+H]<sup>+</sup> 70%), 275.22 ([M+Na]<sup>+</sup> 92%), 307.12 (5), 493.17 (15), 527.29 ([2M+Na]<sup>+</sup> 55%).

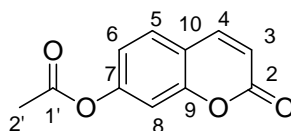
**7-phenethoxy-2H-chromen-2-one (10)**

Compound **10** was synthesized by reacting umbelliferone (0.4 g, 1.0 eq) with (2-bromoethyl)benzene (0.34 ml, 1.0 eq.), in presence of sodium hydride 60% mineral oil dispersion (0.12 g, 1.2 eq.) following the general procedure mentioned above. The crude was purified by silica gel column chromatography eluting with 17% AcOEt in *n*-Hexane to afford compound **10** as white solid in 50% yield. m.p: 84-86 °C; silica gel TLC  $R_f$  0.30 (AcOEt/*n*-Hex 17%, v/v);  $\nu_{\max}$  (KBr)  $\text{cm}^{-1}$ , 2936 (C-H), 1718 (C=O), 1628 (C=C), 1540 (aromatic), 1217 (C-O);  $\delta_{\text{H}}$  (400MHz, DMSO- $d_6$ ) 3.09 (2H, t  $J$  6.8, Ar-CH<sub>2</sub>), 4.34 (2H, t  $J$  6.8, OCH<sub>2</sub>), 6.31 (1H, d  $J$  9.6, 3-H), 6.96 (1H, dd  $J$  8.4, 2.4, 6-H), 7.02 (1H, d  $J$  2.4, 8-H), 7.31 (5H, m, 2'-H<sub>2</sub>, 3'-H<sub>2</sub>, 4'-H), 7.63 (1H, d  $J$  8.4, 5-H), 8.01 (1H, d  $J$  9.6, 4-H);  $\delta_{\text{C}}$  (100 MHz, DMSO- $d_6$ ) 162.5 (C-7), 161.2 (C-2), 156.3 (C-9), 145.2 (C-4), 138.9 (OCH<sub>2</sub>), 130.4 (C-5), 129.9 (C-3'), 129.2 (Ar-CH<sub>2</sub>), 127.3 (C-4'), 113.6 (C-6), 113.4 (C-3), 113.3 (C-10), 102.2 (C-8), 69.7 (C-1'), 35.6 (C-2');  $m/z$  (ESI+) 267.22 ([M+H]<sup>+</sup> 42%), 289.20 ([M+Na]<sup>+</sup> 100%), 321.17 (4), 357.07 (4), 393.21 (10), 413.36 (35), 441.47 (5), 507.23 (8), 555.27 ([2M+Na]<sup>+</sup> 55%).

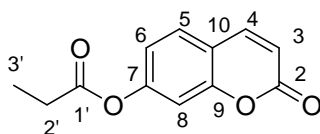
**6.3.2 Synthesis of compounds 32-50**<sup>99,100</sup>**6.3.2.1 General procedure for preparation of ester derivatives 30,31**

To a solution of umbelliferone (1.0 mmol) and acetic acid **28** or propionic acid **29** (1.0 mmol) in dry DMF (1.0 ml), cooled at 0° and under nitrogen atmosphere, was added dropwise a solution of DCC (1.2 mmol) and DMAP (0.05 mmol.) in dry DMF (1.0 ml). After five minutes the mixture was left stirring at room temperature.

When complete (monitoring by TLC), the reaction was quenched with crushed ice (2 g), filtered on celite, extracted with ethyl acetate (5 ml), washed with brine (5 x 5 ml). The collected organic phase was dried on anhydrous Na<sub>2</sub>SO<sub>4</sub>, filtered and evaporated under vacuum. The crude was purified by silica gel column chromatography using *n*-Hexane/ethyl acetate mixture as eluent. Further recrystallization in isopropilic alcohol afforded compounds **30,31** as white solids in high yields.

**2-oxo-2H-chromen-7-yl acetate (30)**

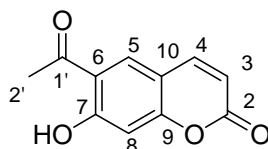
Compound **30** was synthesized by reacting umbelliferone (3.0 g, 1.0 eq) with glacial acetic acid **28** (1.05 ml, 1.0 eq.) following the general procedure mentioned above. The crude was purified by silica gel column chromatography eluting with 20% AcOEt in *n*-Hexane and then recrystallized from isopropilic alcohol to afford compound **30** as white solid in 85% yield. mp 141-143 °C; silica gel TLC  $R_f$  0.20 (AcOEt/*n*-Hex 20%, v/v);  $\nu_{\max}$  (KBr)  $\text{cm}^{-1}$ , 2928 (C-H), 1724 (C=O), 1618 (C=C), 1531 (aromatic), 1130 (O-CO);  $\delta_{\text{H}}$  (400 MHz, DMSO- $d_6$ ) 2.34 (3H, s, 2'-H<sub>3</sub>), 6.52 (1H, d  $J$  9.6, 3-H), 7.20 (1H, dd  $J$  8.4, 2.4, 6-H), 7.32 (1H, d  $J$  2.4, 8-H), 7.81 (1H, d  $J$  8.4, 5-H), 8.11 (1H, d  $J$  9.6, 4-H);  $\delta_{\text{C}}$  (100 MHz, DMSO- $d_6$ ) 169.7 (C-1'), 160.7 (C-2), 155.0 (C-7), 153.8 (C-9), 144.8 (C-4), 130.3 (C-5), 119.6 (C-6), 117.6 (C-3), 116.5 (C-10), 111.1 (C-8), 21.8 (C-2').

**2-oxo-2H-chromen-7-yl propionate (31)**

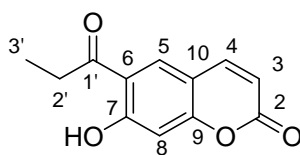
Compound **31** was synthesized by reacting umbelliferone (3.0 g, 1.0 eq) with propionic acid **29** (1.38 ml, 1.0 eq.) following the general procedure mentioned above. The crude was purified by silica gel column chromatography eluting with 20% AcOEt in *n*-Hexane and then recrystallized from isopropilic alcohol to afford compound **31** as white solid in 85% yield. mp 97-99 °C; silica gel TLC  $R_f$  0.25 (AcOEt/*n*-Hex 20%, v/v);  $\nu_{\max}$  (KBr)  $\text{cm}^{-1}$ , 2926 (C-H), 1721 (C=O), 1618 (C=C), 1522 (aromatic), 1112 (O-CO);  $\delta_{\text{H}}$  (400 MHz, DMSO- $d_6$ ) 1.18 (3H, t  $J$  7.2, 3'-H<sub>3</sub>), 2.68 (2H, q  $J$  7.2, 2'-H<sub>2</sub>), 6.52 (1H, d  $J$  9.6, 3-H), 7.20 (1H, dd  $J$  8.4, 2.4, 6-H), 7.32 (1H, d  $J$  2.4, 8-H), 7.81 (1H, d  $J$  8.4, 5-H), 8.11 (1H, d  $J$  9.6, 4-H);  $\delta_{\text{C}}$  (100 MHz, DMSO- $d_6$ ) 173.4 (C-1'), 160.7 (C-2), 155.0 (C-7), 153.9 (C-9), 144.8 (C-4), 130.3 (C-5), 119.6 (C-6), 117.6 (C-3), 116.5 (C-10), 111.0 (C-8), 27.8 (C-2'), 9.6 (C-3').

**6.3.2.2 General procedure for preparation of derivatives 32-35**

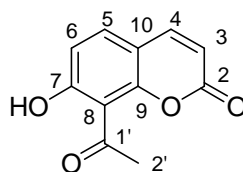
In an air opened round bottomed flask, a finely powdered mixture of esters **30** or **31** (1.0 mmol) and anhydrous aluminium chloride (4 mmol) was heated slowly in an oil bath, under nitrogen flow, from r.t to 180 °C. After four hours the reaction was complete (monitoring by TLC). The mixture was cooled and decomposed with crushed ice (20 g), extracted with AcOEt (20 ml), washed with brine (2 x 15 ml). The collected organic phase was dried on anhydrous Na<sub>2</sub>SO<sub>4</sub>, filtered and evaporated under vacuum. The crude was purified by silica gel column chromatography using *n*-Hexane/ethyl acetate mixture as eluent, affording compounds **32-35** as solids in low-medium yields.

**6-acetyl-7-hydroxy-2H-chromen-2-one (32)**

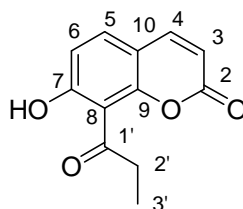
Compound **32** was synthesized by reacting 2-oxo-2H-chromen-7-yl acetate **30** (0.3 g, 1.0 eq) with anhydrous aluminium chloride (0.78 g, 4.0 eq.) following the general procedure mentioned above. The crude was purified by silica gel column chromatography eluting with 20% AcOEt in *n*-Hexane, to afford compound **32** as white solid in 35% yield. mp 173-175 °C; silica gel TLC  $R_f$  0.13 (AcOEt/*n*-Hex 20%, v/v);  $\nu_{\max}$  (KBr)  $\text{cm}^{-1}$ , 3071 (O-H), 2927 (C-H), 1736 (C=O), 1638 (C=C), 1521 (aromatic), 1192 (O-CO);  $\delta_{\text{H}}$  (400 MHz, DMSO- $d_6$ ) 2.71 (3H, s, 2'-H<sub>3</sub>), 6.38 (1H, d  $J$  9.4, 3-H), 6.93 (1H, s, 8-H), 8.07 (1H, d  $J$  9.4, 4-H), 8.37 (1H, s, 5-H);  $\delta_{\text{C}}$  (100 MHz, DMSO- $d_6$ ) 203.7 (C-1'), 164.3 (C-7), 160.5 (C-2), 159.2 (C-9), 145.2 (C-4), 133.9 (C-5), 119.7 (C-6), 114.2 (C-3), 112.6 (C-10), 104.7 (C-8), 29.1 (C-2').

**7-hydroxy-6-propionyl-2H-chromen-2-one (33)**

Compound **33** was synthesized by reacting 2-oxo-2H-chromen-7-yl propionate **31** (0.94 g, 1.0 eq) with anhydrous aluminium chloride (2.30 g, 4.0 eq.) following the general procedure mentioned above. The crude was purified by silica gel column chromatography eluting with 20% AcOEt in *n*-Hexane to afford compound **33** as pale yellow solid in 15% yield. mp 168-170 °C; silica gel TLC  $R_f$  0.15 (AcOEt/*n*-Hex 20%, v/v);  $\nu_{\max}$  (KBr)  $\text{cm}^{-1}$ , 3066 (O-H), 2921 (C-H), 1744 (C=O), 1632 (C=C), 1519 (aromatic), 1187 (O-CO);  $\delta_{\text{H}}$  (400 MHz, DMSO- $d_6$ ) 1.15 (3H, t  $J$  7.2, 3'-H<sub>3</sub>), 3.17 (2H, q  $J$  7.2, 2'-H<sub>2</sub>), 6.39 (1H, d  $J$  9.6, 3-H), 6.94 (1H, s, 8-H), 8.07 (1H, d  $J$  9.6, 4-H), 8.39 (1H, s, 5-H);  $\delta_{\text{C}}$  (100 MHz, DMSO- $d_6$ ) 206.1 (C-1'), 164.3 (C-7), 160.8 (C-2), 159.2 (C-9), 145.2 (C-4), 133.1 (C-5), 119.5 (C-6), 114.1 (C-3), 112.6 (C-10), 104.7 (C-8), 33.6 (C-2'), 8.9 (C-3').

**8-acetyl-7-hydroxy-2H-chromen-2-one (34)**

Compound **34** was synthesized by reacting 2-oxo-2H-chromen-7-yl acetate **30** (0.3 g, 1.0 eq) with anhydrous aluminium chloride (0.78 g, 4.0 eq.) following the general procedure mentioned above. The crude was purified by silica gel column chromatography eluting with 20% AcOEt in *n*-Hexane to afford compound **34** as pale green solid in 65% yield. mp 169-171 °C; silica gel TLC  $R_f$  0.27 (AcOEt/*n*-Hex 20%, v/v);  $\nu_{\max}$  (KBr)  $\text{cm}^{-1}$ , 3061 (O-H), 2927 (C-H), 1735 (C=O), 1615 (C=C), 1526 (aromatic), 1178 (O-C=O);  $\delta_{\text{H}}$  (400 MHz, DMSO- $d_6$ ) 2.65 (3H, s, 2'-H<sub>3</sub>), 6.33 (1H, d  $J$  9.4, 3-H), 6.95 (1H, d  $J$  8.6, 6-H), 7.70 (1H, d  $J$  8.6, 5-H), 8.03 (1H, d  $J$  9.4, 4-H);  $\delta_{\text{C}}$  (100 MHz, DMSO- $d_6$ ) 201.6 (C-1'), 160.8 (C-2), 160.4 (C-7), 153.4 (C-9), 145.6 (C-4), 132.8 (C-5), 115.7 (C-8), 114.4 (C-6), 112.7 (C-3), 112.1 (C-10), 33.4 (C-2').

**7-hydroxy-8-propionyl-2H-chromen-2-one (35)**

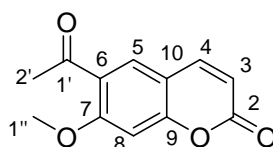
Compound **35** was synthesized by reacting 2-oxo-2H-chromen-7-yl propionate **31** (0.94 g, 1.0 eq) with anhydrous aluminium chloride (2.30 g, 4.0 eq.) following the general procedure mentioned above. The crude was purified by silica gel column chromatography eluting with 20% AcOEt in *n*-Hexane to afford compound **35** as pale yellow solid in 45% yield. mp 165-167 °C; silica gel TLC  $R_f$  0.32 (AcOEt/*n*-Hex 20%, v/v);  $\nu_{\max}$  (KBr)  $\text{cm}^{-1}$ , 3067 (O-H), 2940 (C-H), 1748 (C=O), 1617 (C=C), 1540 (aromatic), 1157 (O-C=O);  $\delta_{\text{H}}$

(400 MHz, DMSO- $d_6$ ) 1.13 (3H, t  $J$  7.2, 3'-H<sub>3</sub>), 2.94 (2H, q  $J$  7.2, 2'-H<sub>2</sub>), 6.30 (1H, d  $J$  9.6, 3-H), 6.93 (1H, d  $J$  8.6, 6-H), 7.66 (1H, d  $J$  8.6, 5-H), 8.02 (1H, d  $J$  9.6, 4-H);  $\delta_c$  (100 MHz, DMSO- $d_6$ ) 204.0 (C-1'), 160.5 (C-2), 159.6 (C-7), 152.8 (C-9), 145.5 (C-4), 131.8 (C-5), 116.7 (C-8), 114.1 (C-6), 112.7 (C-3), 112.1 (C-10), 38.3 (C-2'), 8.5 (C-3').

### 6.3.2.3 General procedure for preparation of derivatives 36-50

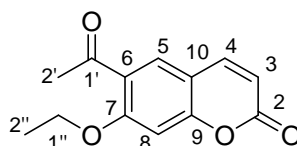
To a solution of one key intermediate **36-50** (1.0 mmol) in dry THF (5 ml), cooled at 0°C and under nitrogen atmosphere, was added triphenylphosphine (1.2 mmol), the appropriate aliphatic alcohol (1.0 mmol) and finally DIAD (1.2 mmol). The mixture was left stirring over night at room temperature, then quenched with crushed ice (2 g), extracted with AcOEt (10 ml) and washed with brine (2 x 10 ml). The collected organic phase was dried on anhydrous Na<sub>2</sub>SO<sub>4</sub>, filtered and evaporated under vacuum. The crude was purified by silica gel column chromatography using *n*-Hexane/ethyl acetate mixture as eluent, affording compounds **36-50** in medium-high yields.

#### 6-acetyl-7-methoxy-2H-chromen-2-one (36)



Compound **36** was synthesized by reacting 6-acetyl-7-hydroxy-2H-chromen-2-one **32** (0.06 g, 1.0 eq) with anhydrous methanol (0.01 ml, 1.0 eq.), in presence of triphenylphosphine (0.09 g, 1.2 eq.) and DIAD (0.07 ml, 1.2 eq.), following the general procedure mentioned above. The crude was purified by silica gel column chromatography eluting with 14% AcOEt in *n*-Hexane to afford compound **36** as a white solid in 60% yield; mp 182-184 °C. silica gel TLC  $R_f$  0.13 (AcOEt/*n*-Hex 14%, v/v);  $\nu_{\max}$  (KBr)  $\text{cm}^{-1}$ , 2928 (C-H), 1732 (C=O), 1646 (C=C), 1533 (aromatic), 1146 (O-CO);  $\delta_H$  (400 MHz, DMSO- $d_6$ ) 2.58 (3H, s, 2'-H<sub>3</sub>), 4.02 (3H, s, 1''-H<sub>3</sub>), 6.41 (1H, d  $J$  9.6, 3-H), 7.24 (1H, s, 8-H), 8.06 (1H, s, 5-H), 8.12 (1H, d  $J$  9.6, 4-H);  $\delta_c$  (100 MHz, DMSO- $d_6$ ) 198.0 (C-1'), 162.3 (C-7), 160.6 (C-2), 158.5 (C-9), 145.2 (C-4), 131.4 (C-5), 126.0 (C-6), 114.4 (C-3), 112.9 (C-10), 101.3 (C-8), 57.7 (C-1''), 32.4 (C-2').

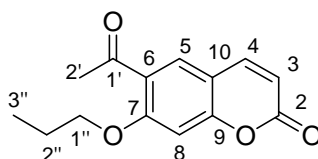
#### 6-acetyl-7-ethoxy-2H-chromen-2-one (37)



Compound **37** was synthesized by reacting 6-acetyl-7-hydroxy-2H-chromen-2-one **32** (0.05 g, 1.0 eq) with absolute ethanol (0.01 ml, 1.0 eq.), in presence of triphenylphosphine (0.08 g, 1.2 eq.) and DIAD (0.076 ml, 1.2 eq.), following the general procedure mentioned above. The crude was purified by silica gel column chromatography eluting with 14% AcOEt in *n*-Hexane to afford compound **37** as a white solid in 60% yield. mp 164-166 °C; silica gel TLC  $R_f$  0.16 (AcOEt/*n*-Hex 14%, v/v);  $\nu_{\max}$  (KBr)  $\text{cm}^{-1}$ , 2935 (C-H), 1732 (C=O), 1622 (C=C), 1533 (aromatic), 1240 (C-O), 1107 (O-C=O);  $\delta_H$  (400 MHz, DMSO- $d_6$ ) 1.47 (3H, t  $J$  6.8, 2''-H<sub>3</sub>), 2.60 (3H, s, 2'-H<sub>3</sub>), 4.29 (2H, q  $J$  6.8, 1''-H<sub>2</sub>), 6.39 (1H, d  $J$  9.6, 3-H), 7.20 (1H, s, 8-H), 8.04 (1H, s, 5-H), 8.11 (1H, d  $J$  9.6, 4-H);  $\delta_c$  (100 MHz,

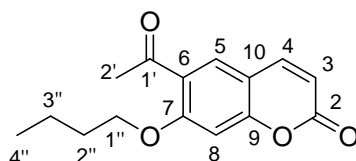
DMSO-*d*<sub>6</sub>) 198.0 (C-1'), 161.6 (C-7), 160.6 (C-2), 158.4 (C-9), 145.3 (C-4), 131.4 (C-5), 125.9 (C-6), 114.4 (C-3), 112.8 (C-10), 101.7 (C-8), 66.1 (C-1''), 32.6 (C-2'), 15.4 (C-2'').

### 6-acetyl-7-propoxy-2H-chromen-2-one (38)

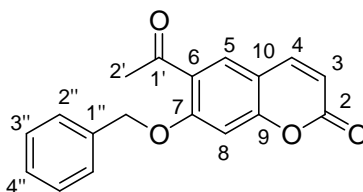


Compound **38** was synthesized by reacting 6-acetyl-7-hydroxy-2H-chromen-2-one **32** (0.08 g, 1.0 eq) with *n*-propanol (0.03 ml, 1.0 eq.), in presence of triphenylphosphine (0.13 g, 1.2 eq.) and DIAD (0.09 ml, 1.2 eq.), following the general procedure mentioned above. The crude was purified by silica gel column chromatography eluting with 17% AcOEt in *n*-Hexane to afford compound **38** as white solid in 70% yield. mp 131-133 °C; silica gel TLC *R*<sub>f</sub> 0.22 (AcOEt/*n*-Hex 17%, v/v);  $\nu_{\max}$  (KBr)  $\text{cm}^{-1}$ , 2943 (C-H), 1728 (C=O), 1646 (C=C), 1569 (aromatic), 1284 (C-O), 1102 (O-C=O);  $\delta_{\text{H}}$  (400 MHz, DMSO-*d*<sub>6</sub>) 1.07 (3H, t *J* 6.8, 3''-H<sub>3</sub>), 1.87 (2H, m, 2''-H<sub>2</sub>), 2.61 (3H, s, 2'-H<sub>3</sub>), 4.20 (2H, t *J* 6.8, 1''-H<sub>2</sub>), 6.39 (1H, d *J* 9.6, 3-H), 7.20 (1H, s, 8-H), 8.05 (1H, s, 5-H), 8.11 (1H, d *J* 9.6, 4-H);  $\delta_{\text{C}}$  (100 MHz, DMSO-*d*<sub>6</sub>) 197.9 (C-1'), 161.7 (C-7), 160.7 (C-2), 158.5 (C-9), 145.3 (C-4), 131.5 (C-5), 125.8 (C-6), 114.3 (C-3), 112.8 (C-10), 101.6 (C-8), 71.8 (C-1''), 32.5 (C-2'), 22.7 (C-2''), 11.5 (C-3'').

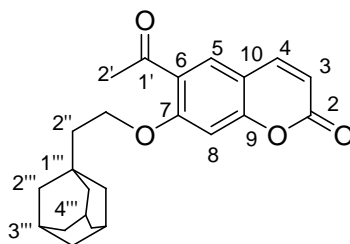
### 6-acetyl-7-butoxy-2H-chromen-2-one (39)



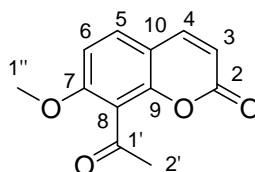
Compound **39** was synthesized by reacting 6-acetyl-7-hydroxy-2H-chromen-2-one **32** (0.05 g, 1.0 eq) with *n*-butanol (0.03 ml, 1.0 eq.), in presence of triphenylphosphine (0.08 g, 1.2 eq.) and DIAD (0.06 ml, 1.2 eq.), following the general procedure mentioned above. The crude was purified by silica gel column chromatography eluting with 14% AcOEt in *n*-Hexane to afford compound **39** as white solid in 60% yield. mp 128-130 °C; silica gel TLC *R*<sub>f</sub> 0.16 (AcOEt/*n*-Hex 14%, v/v);  $\nu_{\max}$  (KBr)  $\text{cm}^{-1}$ , 2959 (C-H), 1739 (C=O), 1653 (C=C), 1521 (aromatic), 1284 (C-O), 1158 (O-C=O);  $\delta_{\text{H}}$  (400 MHz, DMSO-*d*<sub>6</sub>) 0.99 (3H, t *J* 6.8, 4''-H<sub>3</sub>), 1.52 (2H, m, 3''-H<sub>2</sub>), 1.84 (2H, m, 2''-H<sub>2</sub>), 2.60 (3H, s, 2'-H<sub>3</sub>), 4.24 (2H, t *J* 6.8, 1''-H<sub>2</sub>), 6.40 (1H, d *J* 9.6, 3-H), 7.23 (1H, s, 8-H), 8.05 (1H, s, 5-H), 8.11 (1H, d *J* 9.6, 4-H);  $\delta_{\text{C}}$  (100 MHz, DMSO-*d*<sub>6</sub>) 197.9 (C-1'), 161.7 (C-7), 160.6 (C-2), 158.5 (C-9), 145.2 (C-4), 131.5 (C-5), 125.9 (C-6), 114.4 (C-3), 112.8 (C-10), 101.7 (C-8), 70.0 (C-1''), 32.5 (C-2'), 31.31 (C-2''), 19.8 (C-3''), 14.6 (C-4'').

**6-acetyl-7-(benzyloxy)-2H-chromen-2-one (40)**

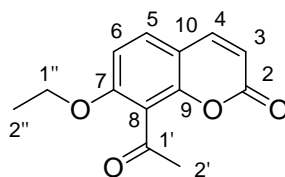
Compound **40** was synthesized by reacting 6-acetyl-7-hydroxy-2H-chromen-2-one **32** (0.05 g, 1.0 eq) with benzylic alcohol (0.02 ml, 1.0 eq.), in presence of triphenylphosphine (0.08 g, 1.2 eq.) and DIAD (0.06 ml, 1.2 eq.), following the general procedure mentioned above. The crude was purified by silica gel column chromatography eluting with 17% AcOEt in *n*-Hexane to afford compound **40** as white solid in 70% yield. mp 166-168 °C; silica gel TLC  $R_f$  0.26 (AcOEt/*n*-Hex 17%, v/v);  $\nu_{\max}$  (KBr)  $\text{cm}^{-1}$ , 2930 (C-H), 1734 (C=O), 1622 (C=C), 1534 (aromatic), 1235 (C-O), 1112 (O-C=O);  $\delta_{\text{H}}$  (400 MHz, DMSO- $d_6$ ), 2.56 (3H, s, 2'-H<sub>3</sub>), 5.39 (2H, s, OCH<sub>2</sub>), 6.41 (1H, d  $J$  9.6, 3-H), 7.34 (1H, s, 8-H), 7.44 (5H, m, 2''-H<sub>2</sub>, 3''-H<sub>2</sub>, 4''-H), 8.08 (1H, s, 5-H), 8.12 (1H, d  $J$  9.6, 4-H);  $\delta_{\text{C}}$  (100 MHz, DMSO- $d_6$ ) 197.9 (C-1'), 161.2 (C-7), 160.6 (C-2), 158.3 (C-9), 145.1 (C-4), 136.6 (C-1''), 131.5 (C-5), 129.5 (C-3''), 129.2 (C-4''), 128.9 (C-2''), 126.2 (C-6), 114.6 (C-3), 113.1 (C-10), 102.1 (C-8), 71.8 (OCH<sub>2</sub>), 32.5 (C-2').

**6-acetyl-7-(2''-(1'''-adamantyl)-ethoxy)-2H-chromen-2-one (41)**

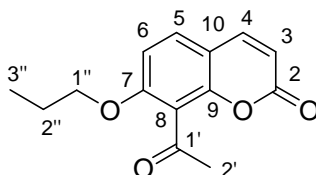
Compound **41** was synthesized by reacting 6-acetyl-7-hydroxy-2H-chromen-2-one **32** (0.05 g, 1.0 eq) with 2-(1-adamantyl)-ethanol **53** (0.04 g, 1.0 eq.), in presence of triphenylphosphine (0.08 g, 1.2 eq.) and DIAD (0.06 ml, 1.2 eq.), following the general procedure mentioned above. The crude was purified by silica gel column chromatography eluting with 14% AcOEt in *n*-Hexane to afford compound **41** as white solid in 75% yield. mp 175-177 °C; silica gel TLC  $R_f$  0.22 (AcOEt/*n*-Hex 14%, v/v);  $\nu_{\max}$  (KBr)  $\text{cm}^{-1}$ , 2899 (C-H), 1739 (C=O), 1615 (C=C), 1558 (aromatic), 1209 (C-O), 1098 (O-C=O);  $\delta_{\text{H}}$  (400 MHz, CDCl<sub>3</sub>- $d$ ) 1.61 (14H, m, 4'''-H<sub>6</sub>, 2'''-H<sub>6</sub>, 2''-H<sub>2</sub>), 1.99 (3H, m, 3'''-H<sub>3</sub>), 2.64 (3H, s, 2'-H<sub>3</sub>), 4.19 (2H, t  $J$  7.2, OCH<sub>2</sub>), 6.28 (1H, d  $J$  9.6, 3-H), 6.86 (1H, s, 8-H), 7.66 (1H, d  $J$  8.8, 4-H), 7.93 (1H, s, 5-H);  $\delta_{\text{C}}$  (100 MHz, CDCl<sub>3</sub>- $d$ ) 198.0 (C-1'), 161.7 (C-7), 160.6 (C-2), 158.4 (C-9), 143.7 (C-4), 131.2 (C-5), 125.8 (C-6), 114.4 (C-3), 112.4 (C-10), 100.8 (C-8), 66.1 (OCH<sub>2</sub>), 43.1 (C-2''), 42.9 (C-4'''), 37.3 (C-2'''), 32.4 (C-2'), 32.2 (C-1'''), 28.9 (C-3''').

**8-acetyl-7-methoxy-2H-chromen-2-one (42)**

Compound **42** was synthesized by reacting 8-acetyl-7-hydroxy-2H-chromen-2-one **34** (0.46 g, 1.0 eq) with anhydrous methanol (0.09 ml, 1.0 eq.), in presence of triphenylphosphine (0.75 g, 1.2 eq.) and DIAD (0.53 ml, 1.2 eq.), following the general procedure mentioned above. The crude was purified by silica gel column chromatography eluting with 50% AcOEt in *n*-Hexane to afford compound **42** as a white solid in 88% yield. mp 122-124 °C; silica gel TLC  $R_f$  0.32 (AcOEt/*n*-Hex 50%, v/v);  $\nu_{\max}$  (KBr)  $\text{cm}^{-1}$ , 2955 (C-H), 1717 (C=O), 1616 (C=C), 1521 (aromatic), 1265 (C-O), 1154 (*O*-C=O);  $\delta_{\text{H}}$  (400 MHz, DMSO- $d_6$ ) 2.54 (3H, s, 2'-H<sub>3</sub>), 3.94 (3H, s, 1''-H<sub>3</sub>), 6.37 (1H, d  $J$  9.6, 3-H), 7.21 (1H, d  $J$  8.8, 6-H), 7.81 (1H, d  $J$  8.8, 5-H), 8.06 (1H, d  $J$  9.6, 4-H);  $\delta_{\text{C}}$  (100 MHz, DMSO- $d_6$ ) 200.0 (C-1'), 160.3 (C-2), 159.0 (C-7), 151.2 (C-9), 145.2 (C-4), 131.4 (C-5), 119.3 (C-8), 114.0 (C-3), 113.6 (C-10), 109.6 (C-6), 57.5 (C-1''), 33.1 (C-2').

**8-acetyl-7-ethoxy-2H-chromen-2-one (43)**

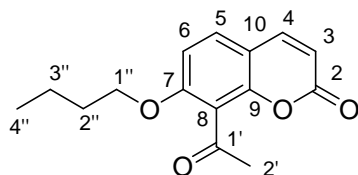
Compound **43** was synthesized by reacting 8-acetyl-7-hydroxy-2H-chromen-2-one **34** (0.2 g, 1.0 eq) with absolute ethanol (0.06 ml, 1.0 eq.), in presence of triphenylphosphine (0.31 g, 1.2 eq.) and DIAD (0.23 ml, 1.2 eq.), following the general procedure mentioned above. The crude was purified by silica gel column chromatography eluting with 33% AcOEt in *n*-Hexane to afford compound **43** as a white solid in 80% yield. mp 102-104 °C; silica gel TLC  $R_f$  0.22 (AcOEt/*n*-Hex 33%, v/v);  $\nu_{\max}$  (KBr)  $\text{cm}^{-1}$ , 2938 (C-H), 1718 (C=O), 1647 (C=C), 1522 (aromatic), 1246 (C-O), 1168 (*O*-C=O);  $\delta_{\text{H}}$  (400 MHz, DMSO- $d_6$ ) 1.37 (3H, t  $J$  6.8, 2''-H<sub>3</sub>), 2.54 (3H, s, 2'-H<sub>3</sub>), 4.24 (2H, q  $J$  6.8, 1''-H<sub>2</sub>), 6.36 (1H, d  $J$  9.6, 3-H), 7.18 (1H, d  $J$  8.8, 6-H), 7.77 (1H, d  $J$  8.8, 5-H), 8.05 (1H, d  $J$  9.6, 4-H);  $\delta_{\text{C}}$  (100 MHz, DMSO- $d_6$ ) 199.9 (C-1'), 160.3 (C-2), 158.4 (C-7), 151.2 (C-9), 145.1 (C-4), 131.3 (C-5), 119.6 (C-8), 113.9 (C-3), 113.5 (C-10), 110.3 (C-6), 65.7 (C-1''), 33.0 (C-2'), 15.3 (C-2'').

**8-acetyl-7-propoxy-2H-chromen-2-one (44)**

Compound **44** was synthesized by reacting 8-acetyl-7-hydroxy-2H-chromen-2-one **34** (0.2 g, 1.0 eq) with *n*-propanol (0.07 ml, 1.0 eq.), in presence of triphenylphosphine (0.31 g, 1.2 eq.) and DIAD (0.23 ml, 1.2 eq.), following the general procedure mentioned above. The crude was purified by silica gel column chromatography eluting with 33% AcOEt in *n*-

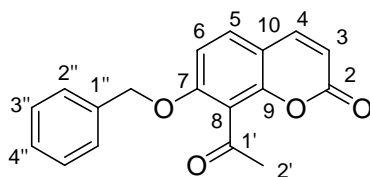
Hexane to afford compound **44** as a white solid in 70% yield. mp 79-81 °C; silica gel TLC  $R_f$  0.19 (AcOEt/*n*-Hex 33%, v/v);  $\nu_{\max}$  (KBr)  $\text{cm}^{-1}$ , 2972 (C-H), 1733 (C=O), 1635 (C=C), 1534 (aromatic), 1254 (C-O), 1165 (*O*-C=O);  $\delta_{\text{H}}$  (400 MHz, DMSO- $d_6$ ) 0.99 (3H, t  $J$  7.0, 3''-H<sub>3</sub>), 1.77 (2H, m, 2''-H<sub>2</sub>), 2.54 (3H, s, 2'-H<sub>3</sub>), 4.21 (2H, t  $J$  7.0, 1''-H<sub>2</sub>), 6.36 (1H, d  $J$  9.6, 3-H), 7.19 (1H, d  $J$  8.8, 6-H), 7.78 (1H, d  $J$  8.8, 5-H), 8.05 (1H, d  $J$  9.6, 4-H);  $\delta_{\text{C}}$  (100 MHz, DMSO- $d_6$ ) 200.9 (C-1'), 160.5 (C-2), 158.8 (C-7), 151.3 (C-9), 145.1 (C-4), 131.3 (C-5), 114.8 (C-8), 113.8 (C-3), 113.5 (C-10), 110.2 (C-6), 71.3 (C-1''), 33.0 (C-2''), 22.7 (C-2''), 11.2 (C-3'').

#### 8-acetyl-7-butoxy-2H-chromen-2-one (45)

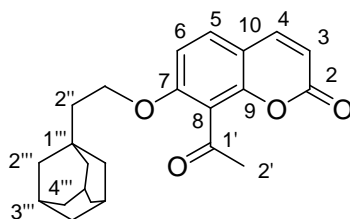


Compound **45** was synthesized by reacting 8-acetyl-7-hydroxy-2H-chromen-2-one **34** (0.2 g, 1.0 eq) with *n*-butanol (0.09 ml, 1.0 eq.), in presence of triphenylphosphine (0.31 g, 1.2 eq.) and DIAD (0.23 ml, 1.2 eq.), following the general procedure mentioned above. The crude was purified by silica gel column chromatography eluting with 25% AcOEt in *n*-Hexane to afford compound **45** as a white solid in 50% yield. mp 74-76 °C; silica gel TLC  $R_f$  0.22 (AcOEt/*n*-Hex 25%, v/v);  $\nu_{\max}$  (KBr)  $\text{cm}^{-1}$ , 2955 (C-H), 1720 (C=O), 1653 (C=C), 1522 (aromatic), 1270 (C-O), 1170 (*O*-C=O);  $\delta_{\text{H}}$  (400 MHz, DMSO- $d_6$ ) 0.96 (3H, t  $J$  7.0, 4''-H<sub>3</sub>), 1.44 (2H, m, 3''-H<sub>2</sub>), 1.74 (2H, m 2''-H<sub>2</sub>), 2.54 (3H, s, 2'-H<sub>3</sub>), 4.18 (2H, t  $J$  7.0, 1''-H<sub>2</sub>), 6.36 (1H, d  $J$  9.6, 3-H), 7.20 (1H, d  $J$  8.8, 6-H), 7.78 (1H, d  $J$  8.8, 5-H), 8.05 (1H, d  $J$  9.6, 4-H);  $\delta_{\text{C}}$  (100 MHz, DMSO- $d_6$ ) 199.8 (C-1'), 160.3 (C-2), 158.5 (C-7), 151.2 (C-9), 145.1 (C-4), 131.3 (C-5), 119.4 (C-8), 113.9 (C-3), 113.5 (C-10), 110.3 (C-6), 69.6 (C-1''), 33.0 (C-2''), 31.4 (C-2''), 19.5 (C-3''), 14.5 (C-4'').

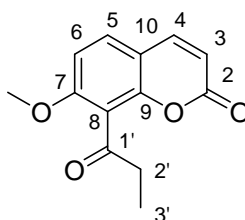
#### 8-acetyl-7-(benzyloxy)-2H-chromen-2-one (46)



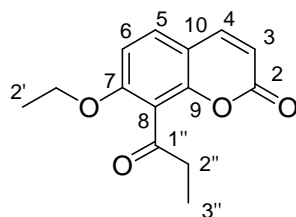
Compound **46** was synthesized by reacting 8-acetyl-7-hydroxy-2H-chromen-2-one **34** (0.2 g, 1.0 eq) with benzylic alcohol (0.10 ml, 1.0 eq.), in presence of triphenylphosphine (0.31 g, 1.2 eq.) and DIAD (0.23 ml, 1.2 eq.), following the general procedure mentioned above. The crude was purified by silica gel column chromatography eluting with 25% AcOEt in *n*-Hexane to afford compound **46** as a white solid in 98% yield. mp 116-118 °C; silica gel TLC  $R_f$  0.19 (AcOEt/*n*-Hex 25%, v/v);  $\nu_{\max}$  (KBr)  $\text{cm}^{-1}$ , 2951 (C-H), 1727 (C=O), 1653 (C=C), 1521 (aromatic), 1232 (C-O), 1166 (*O*-C=O);  $\delta_{\text{H}}$  (400 MHz, DMSO- $d_6$ ) 2.55 (3H, s, 2'-H<sub>3</sub>), 5.33 (2H, s, OCH<sub>2</sub>), 6.38 (1H, d  $J$  9.6, 3-H), 7.29 (1H, d  $J$  8.8, 6-H), 7.40 (5H, m, 2''-H<sub>2</sub>, 3''-H<sub>2</sub>, 4''-H) 7.78 (1H, d  $J$  8.8, 5-H), 8.05 (1H, d  $J$  9.6, 4-H);  $\delta_{\text{C}}$  (100 MHz, DMSO- $d_6$ ) 199.9 (C-1'), 160.2 (C-2), 158.0 (C-7), 151.2 (C-9), 145.1 (C-4), 136.9 (C-1''), 131.3 (C-5), 129.4 (C-3''), 129.0 (C-4''), 128.4 (C-2''), 119.8 (C-8), 114.1 (C-3), 113.8 (C-10), 110.8 (C-6), 71.2 (OCH<sub>2</sub>), 33.0 (C-2').

**8-acetyl-7-(2''-(1'''-adamantyl)-ethoxy)-2H-chromen-2-one (47)**

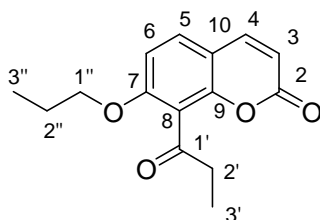
Compound **47** was synthesized by reacting 8-acetyl-7-hydroxy-2H-chromen-2-one **34** (0.07 g, 1.0 eq) with 2-(1-adamantyl)-ethanol **53** (0.06 g, 1.0 eq.), in presence of triphenylphosphine (0.11 g, 1.2 eq.) and DIAD (0.08 ml, 1.2 eq.), following the general procedure mentioned above. The crude was purified by silica gel column chromatography eluting with 20% AcOEt in *n*-Hexane to afford compound **47** as a white solid in 50% yield. mp 178-180 °C; silica gel TLC  $R_f$  0.16 (AcOEt/*n*-Hex 20%, v/v);  $\nu_{\max}$  (KBr)  $\text{cm}^{-1}$ , 2914 (C-H), 1728 (C=O), 1635 (C=C), 1533 (aromatic), 1259 (C-O), 1140 (*O*-C=O);  $\delta_{\text{H}}$  (400 MHz,  $\text{CDCl}_3$ -*d*) 1.65 (14H, m, 4'''-H<sub>6</sub>, 2'''H<sub>6</sub>, 2''-H<sub>2</sub>), 1.97 (3H, m, 3'''-H<sub>3</sub>), 2.59 (3H, s, 2'-H<sub>3</sub>), 4.13 (2H, t  $J$  7.2, OCH<sub>2</sub>), 6.25 (1H, d  $J$  9.6, 3-H), 6.86 (1H, d  $J$  8.8, 6-H), 7.42 (1H, d  $J$  8.8, 5-H), 7.61 (1H, d  $J$  9.6, 4-H);  $\delta_{\text{C}}$  (100 MHz,  $\text{CDCl}_3$ -*d*) 199.4 (C-1'), 160.2 (C-2), 158.6 (C-7), 151.6 (C-9), 143.4 (C-4), 129.8 (C-5), 120.0 (C-8), 114.0 (C-3), 113.0 (C-10), 108.9 (C-6), 65.8 (OCH<sub>2</sub>), 42.9 (C-2''), 42.8 (C-4'''), 37.3 (C-2'''), 32.7 (C-2'), 32.1 (C-1''') 28.9 (C-3''').

**7-methoxy-8-propionyl-2H-chromen-2-one (48)**

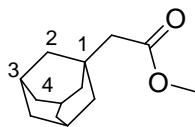
Compound **48** was synthesized by reacting 7-hydroxy-8-propionyl-2H-chromen-2-one **35** (0.10 g, 1.0 eq) with anhydrous methanol (0.02 ml, 1.0 eq.), in presence of triphenylphosphine (0.14 g, 1.2 eq.) and DIAD (0.11 ml, 1.2 eq.), following the general procedure mentioned above. The crude was purified by silica gel column chromatography eluting with 17% AcOEt in *n*-Hexane to afford compound **48** as a white solid in 60% yield. mp 102-104 °C; silica gel TLC  $R_f$  0.13 (AcOEt/*n*-Hex 17%, v/v);  $\nu_{\max}$  (KBr)  $\text{cm}^{-1}$ , 2946 (C-H), 1717 (C=O), 1646 (C=C), 1534 (aromatic), 1293 (C-O), 1162 (*O*-C=O);  $\delta_{\text{H}}$  (400 MHz, DMSO-*d*<sub>6</sub>) 1.11 (3H, t  $J$  7.2, 3'-H<sub>3</sub>), 2.84 (2H, q  $J$  7.2, 2'-H<sub>2</sub>), 3.92 (3H, s, OCH<sub>3</sub>), 6.37 (1H, d  $J$  9.6, 3-H), 7.20 (1H, d  $J$  8.8, 6-H), 7.80 (1H, d  $J$  8.8, 5-H), 8.07 (1H, d  $J$  9.6, 4-H);  $\delta_{\text{C}}$  (100 MHz, DMSO-*d*<sub>6</sub>) 203.0 (C-1'), 160.3 (C-2), 159.0 (C-7), 151.2 (C-9), 145.2 (C-4), 131.3 (C-5), 119.2 (C-8), 114.0 (C-3), 113.6 (C-10), 109.5 (C-6), 57.5 (OCH<sub>3</sub>), 38.4 (C-2'), 8.4 (C-3').

**7-ethoxy-8-propionyl-2H-chromen-2-one (49)**

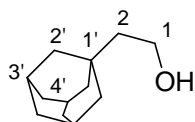
Compound **49** was synthesized by reacting 7-hydroxy-8-propionyl-2H-chromen-2-one **35** (0.03 g, 1.0 eq) with absolute ethanol (0.008 ml, 1.0 eq.), in presence of triphenylphosphine (0.04 g, 1.2 eq.) and DIAD (0.03 ml, 1.2 eq.), following the general procedure mentioned above. The crude was purified by silica gel column chromatography eluting with 20% AcOEt in *n*-Hexane to afford compound **49** as a white solid in 60% yield. mp 105-107 °C; silica gel TLC  $R_f$  0.13 (AcOEt/*n*-Hex 20%, v/v);  $\nu_{\max}$  (KBr)  $\text{cm}^{-1}$ , 2940 (C-H), 1715 (C=O), 1646 (C=C), 1534 (aromatic), 1297 (C-O), 1165 (*O*-C=O);  $\delta_{\text{H}}$  (400 MHz, DMSO- $d_6$ ) 1.24 (3H, t  $J$  7.2, 3''-H<sub>3</sub>), 1.34 (3H, t  $J$  6.8, 2'-H<sub>3</sub>), 2.83 (2H, q  $J$  7.2, 2''-H<sub>2</sub>), 4.21 (2H, q  $J$  6.8, OCH<sub>2</sub>), 6.36 (1H, d  $J$  9.6, 3-H), 7.18 (1H, d  $J$  8.8, 6-H), 7.77 (1H, d  $J$  8.8, 5-H), 8.05 (1H, d  $J$  9.6, 4-H);  $\delta_{\text{C}}$  (100 MHz, DMSO- $d_6$ ) 203.1 (C-1''), 160.3 (C-2), 158.4 (C-7), 151.3 (C-9), 145.2 (C-4), 131.2 (C-5), 119.4 (C-8), 113.9 (C-3), 113.5 (C-10), 110.3 (C-6), 65.7 (OCH<sub>2</sub>), 38.3 (C-2''), 15.2 (C-2'), 8.5 (C-3').

**8-propionyl-7-propoxy-2H-chromen-2-one (50)**

Compound **50** was synthesized by reacting 7-hydroxy-8-propionyl-2H-chromen-2-one **35** (0.03 g, 1.0 eq) with *n*-propanol (0.01 ml, 1.0 eq.), in presence of triphenylphosphine (0.04 g, 1.2 eq.) and DIAD (0.03 ml, 1.2 eq.), following the general procedure mentioned above. The crude was purified by silica gel column chromatography eluting with 20% AcOEt in *n*-Hexane to afford compound **50** as a white solid in 80% yield. mp 82-84 °C; silica gel TLC  $R_f$  0.12 (AcOEt/*n*-Hex 20%, v/v);  $\nu_{\max}$  (KBr)  $\text{cm}^{-1}$ , 2932 (C-H), 1747 (C=O), 1635 (C=C), 1534 (aromatic), 1287 (C-O), 1170 (*O*-C=O);  $\delta_{\text{H}}$  (400 MHz, DMSO- $d_6$ ) 0.98 (3H, t  $J$  7.2, 3''-H<sub>3</sub>), 1.13 (3H, t  $J$  7.4, 3'-H<sub>3</sub>), 1.74 (2H, m, 2''-H<sub>2</sub>), 2.83 (2H, q  $J$  7.4, 2'-H<sub>2</sub>), 4.13 (2H, t  $J$  7.2, 1''-H<sub>2</sub>), 6.36 (1H, d  $J$  9.6, 3-H), 7.19 (1H, d  $J$  8.8, 6-H), 7.77 (1H, d  $J$  8.8, 5-H), 8.06 (1H, d  $J$  9.6, 4-H);  $\delta_{\text{C}}$  (100 MHz, DMSO- $d_6$ ) 202.9 (C-1'), 160.3 (C-2), 158.5 (C-7), 151.3 (C-9), 145.2 (C-4), 131.2 (C-5), 119.4 (C-8), 113. (C-3), 113.5 (C-10), 110.2 (C-6), 71.2 (C-1''), 38.3 (C-2'), 22.7 (C-2''), 11.1 (C-3''), 8.4 (C-3').

**6.3.3 Procedure for preparation of alcohol 53<sup>101</sup>****Synthesis of 1-adamantane-acetic acid-methyl ester (52)**

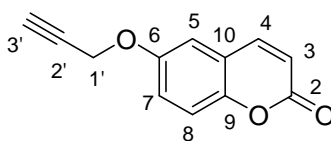
To a solution of 1-Adamantane-acetic acid **51** (0.5 g, 1.0 eq.) in dry methanol (10 ml), cooled at 0°C and under nitrogen atmosphere, was added dropwise thionyl chloride (0.28 ml, 1.5 eq.). The mixture was left stirring at room temperature. After one hour, when complete (monitoring by TLC), the reaction was evaporated under vacuum. The crude was purified by silica gel column chromatography eluting with 5% AcOEt in *n*-Hexane affording compound **52** as colorless oil in 90% yield. Silica gel TLC  $R_f$  0.67 (AcOEt/*n*-Hex 5%, v/v);  $\nu_{\max}$  (KBr)  $\text{cm}^{-1}$ , 2911 (C-H), 1712 (C=O), 1122 (O-C=O);  $\delta_{\text{H}}$  (400 MHz,  $\text{CDCl}_3$ -*d*), 1.63 (12H, m, 2-, 4-H<sub>12</sub>), 1.97 (3H, m, 3-H<sub>3</sub>), 2.07 (2H, s, CH<sub>2</sub>CO), 3.64 (3H, s, OCH<sub>3</sub>);  $\delta_{\text{C}}$  (100 MHz,  $\text{CDCl}_3$ -*d*) 172.6 (C=O), 51.4 (OCH<sub>3</sub>), 49.1 (CH<sub>2</sub>CO), 42.7 (C-2), 37.1 (C-4), 33.1 (C-1), 28.9 (C-3).

**Synthesis of 2-(1'-adamantyl)-ethanol (53)**

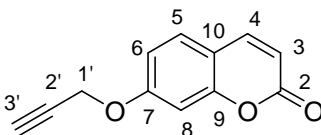
To a suspension of lithium aluminum hydride (0.25 g, 2.8 eq.) in dry THF (10 ml), cooled at 0°C and under nitrogen atmosphere, was added dropwise a solution of 1-adamantane-acetic acid-methyl ester **52** (0.48 g, 1.0 eq.) in dry THF (3 ml). The mixture was left stirring at room temperature. After three hour, when complete (monitoring by TLC), the reaction was quenched with careful addition of crushed ice and 1N KOH solution. The mixture was acidified with 1N HCl solution, extracted with AcOEt and washed with brine. The collected organic phase was dried on anhydrous Na<sub>2</sub>SO<sub>4</sub>, filtered and evaporated under vacuum. The crude was purified by silica gel column chromatography eluting with 9% AcOEt in *n*-Hexane affording compound **53** as white solid in 90% yield. m.p 71-73 °C; silica gel TLC  $R_f$  0.22 (AcOEt/*n*-Hex 9%, v/v);  $\nu_{\max}$  (KBr)  $\text{cm}^{-1}$ , 3293 (O-H), 2906 (C-H);  $\delta_{\text{H}}$  (400 MHz,  $\text{CDCl}_3$ -*d*), 1.27 (2H, m, 2-H<sub>2</sub>), 1.50 (6H, m, 2'-H<sub>6</sub>), 1.63 (6H, m, 4'-H<sub>6</sub>), 1.93 (3H, m, 3'-H<sub>3</sub>), 3.47 (2H, m, 1-H<sub>2</sub>), 4.22 (1H, t  $J$  5.2, OH);  $\delta_{\text{C}}$  (100 MHz,  $\text{CDCl}_3$ -*d*) 57.1 (C-1), 47.8 (C-2), 43.2 (C-2'), 37.6 (C-4'), 32.3 (C-1'), 28.9 (C-3').

**6.3.4 General procedure for synthesis of derivatives 123-132<sup>161,162</sup>****6.3.4.1 Preparation of ether compounds 116, 117<sup>161</sup>**

Reaction of 6-hydroxy or 7-hydroxycoumarin (1.0 g, 1.0 eq) and propargyl alcohol (1.0 eq) was carried out in Mitsunobu conditions at 0°C under sonication, in presence of triphenylphosphine (1.0 eq) and drop-wised diisopropylazodicarboxylate (1.1 eq) in dry THF as solvent (90 ml). The solution was sonicated at r.t. under a nitrogen atmosphere until starting material was consumed (TLC monitoring). Solvents were removed under *vacuo* to give a white solid that was recrystallized from MeOH to give compounds **116** and **117** as brown and colorless solids respectively, in medium yields.

**6-(prop-2'-ynoxy)-2H-chromen-2-one (116)**

Compound **116** was synthesised by reacting 6-hydroxycoumarin (0.8 g, 1.0 eq) with propargyl alcohol (0.28 ml, 1.0 eq.), in presence of triphenylphosphine (1.29 g, 1.0 eq.) and DIAD (0.97 ml, 1.0 eq.), following the general procedure mentioned above. The crude was recrystallized from MeOH to afford compound **116** as a brown solid in 50% yield. mp 202-204 °C; silica gel TLC  $R_f$  0.23 (AcOEt/*n*-Hex 10%, v/v);  $\nu_{\max}$  (KBr)  $\text{cm}^{-1}$ , 3302 (C≡C-H), 2167 (C≡CH), 1755 (C=O), 1674 (C=C), 1601 (aromatic), 1328 (C-O), 1199 (O-C=O);  $\delta_{\text{H}}$  (400 MHz, DMSO- $d_6$ ) 3.64 (1H, t,  $J$  2.4, 3'-H), 4.89 (2H, d,  $J$  2.4, 1'-H<sub>2</sub>), 6.54 (1H, d,  $J$  9.4, 3-H), 7.30 (1H, dd,  $J$  9.0, 3.0, 7-H), 7.38 (1H, d,  $J$  3.0, 5-H), 7.41 (1H, d,  $J$  9.0, 8-H), 8.06 (1H, d,  $J$  9.4, 4-H);  $\delta_{\text{C}}$  (100 MHz, DMSO- $d_6$ ) 161.1 (C-2), 154.3 (C-9), 149.2 (C-6), 144.8 (C-4), 120.9 (C-7), 120.0 (C-10), 118.3 (C-8), 117.7 (C-3), 113.3 (C-5), 79.8 (C-2'), 79.4 (C-3'), 57.0 (C-1').

**7-(prop-2'-ynoxy)-2H-chromen-2-one (117)**

Compound **117** was synthesised by reacting 7-hydroxycoumarin (0.8 g, 1.0 eq) with propargyl alcohol (0.28 ml, 1.0 eq.), in presence of triphenylphosphine (1.29 g, 1.0 eq.) and DIAD (0.97 ml, 1.0 eq.), following the general procedure mentioned above. The crude was recrystallized from MeOH to afford compound **117** as a white solid in 40% yield. mp 117-119 °C; silica gel TLC  $R_f$  0.20 (AcOEt/*n*-Hex 10%, v/v);  $\nu_{\max}$  (KBr)  $\text{cm}^{-1}$ , 3310 (C≡C-H), 2160 (C≡CH), 1715 (C=O), 1642 (C=C), 1584 (aromatic), 1301 (C-O), 1175 (O-C=O);  $\delta_{\text{H}}$  (400 MHz, DMSO- $d_6$ ) 3.69 (1H, t,  $J$  2.4, 3'-H), 4.97 (2H, d,  $J$  2.4, 1'-H<sub>2</sub>), 6.36 (1H, d,  $J$  9.6, 3-H), 7.03 (1H, dd,  $J$  8.5, 2.3, 6-H), 7.09 (1H, d,  $J$  2.3, 8-H), 7.69 (1H, d,  $J$  8.5, 5-H), 8.03 (1H, d,  $J$  9.6, 4-H);  $\delta_{\text{C}}$  (100 MHz, DMSO- $d_6$ ) 161.1 (C-2), 161.0 (C-7), 156.0 (C-9), 145.1 (C-4), 130.4 (C-5), 113.9 (C-3), 113.8 (C-10), 113.7 (C-6), 102.7 (C-8), 79.8 (C-3'), 79.4 (C-2'), 57.0 (C-1').

**6.3.4.2 General procedure for synthesis of phenylazides 118-122**<sup>162</sup>

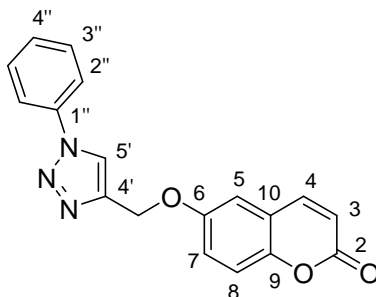
Halogenoaniline (0.3g, 1.0eq) was dissolved in a solution H<sub>2</sub>O/AcOH (1/2 v/v, 10 ml) at 0°C. NaNO<sub>2</sub> (1.4 eq) was slowly added and the resulting solution was stirred at the same temperature for 1h. Then NaN<sub>3</sub> (1.5 eq) was added portion-wise and the mixture was stirred at r.t. until starting material was consumed (TLC monitoring). The reaction was quenched with slush, extracted with ethyl acetate (2 x 20 ml) and the combined organic layers were washed with 5% NaHCO<sub>3</sub> (2 x 20 ml), dried over Na<sub>2</sub>SO<sub>4</sub>, filtered off and solvent evaporated in *vacuo* to afford the corresponding phenylazide which was used without further purification.

**6.3.4.3 General procedure for synthesis of triazolyl derivatives 123-132**<sup>162</sup>

Azide (1.0 eq) and alkyne (1.0 eq) were dissolved in *tert*-ButOH/H<sub>2</sub>O and then tetramethylammonium chloride (1.0 eq) and copper nanosize (5% mol) were added. The mixture was vigorously stirred at r.t. until starting material was consumed (TLC

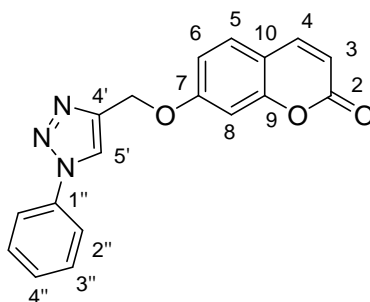
monitoring). Solvents were removed under *vacuo* (temperature has not to exceed 40 °C) and the brown residue was purified by silica gel column chromatography eluting with ethyl acetate in *n*-Hexane to afford compounds 123-132 as yellow solids in medium yields.

### 6-((1'-phenyl-1''H-1',2',3'-triazol-4'-yl)methoxy)-2H-chromen-2-one (123)

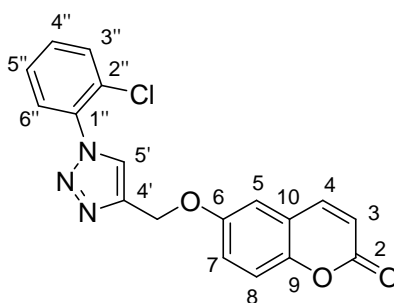


Compound **123** was synthesized by reacting azidobenzene **118** (0.52g, 1.1 eq) with 6-(prop-2-ynyloxy)-2H-chromen-2-one **116** (0.8g, 1.0 eq.), dissolved in *tert*-ButOH/H<sub>2</sub>O (1/1 v/v, 2.0 ml) in presence of tetramethylammonium chloride (0.04g, 1.0 eq) and copper nanosize (5 % mol), following the general procedure mentioned above. The crude was purified by silica gel column chromatography eluting with 33% ethyl acetate in *n*-hexane to afford **123** as a light brown solid in 40% yield. mp 154-156 °C; silica gel TLC *R<sub>f</sub>* 0.19 (AcOEt/*n*-Hex 33%, v/v);  $\nu_{\max}$  (KBr) cm<sup>-1</sup>, 2935 (C-H), 1726 (C=O), 1635 (C=C), 1549 (aromatic), 1244 (C-O), 1186 (C-N), 1106 (*O*-C=O);  $\delta_{\text{H}}$  (400 MHz, DMSO-*d*<sub>6</sub>) 5.34 (2H, s, OCH<sub>2</sub>), 6.54 (1H, d, *J* 9.4, 3-H), 7.36 (1H, m, 7-H), 7.42 (1H, m, 8-H), 7.51 (1H, d, *J* 2.8, 5-H), 7.54 (1H, m, 4''-H), 7.65 (1H, m, 3''-H), 7.94 (1H, m, 2''-H), 8.06 (1H, d, *J* 9.4, 4-H), 9.01 (1H, s, 5'-H);  $\delta_{\text{c}}$  (100 MHz, DMSO-*d*<sub>6</sub>) 161.0, 155.2, 149.0, 144.9, 144.5, 137.5, 130.8, 129.7, 123.9, 121.1, 120.9, 120.1, 118.4, 117.6, 112.9, 62.6.

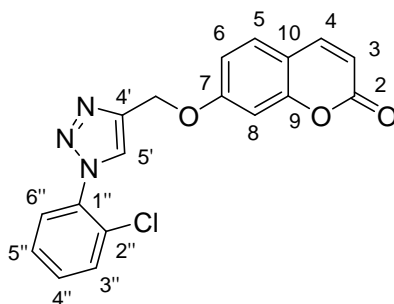
### 7-((1'-phenyl-1''H-1',2',3'-triazol-4'-yl)methoxy)-2H-chromen-2-one (124)



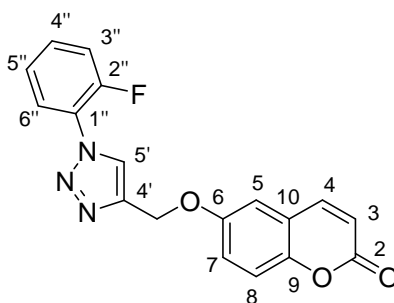
Compound **124** was synthesized by reacting azidobenzene **118** (0.52g, 1.1 eq) with 7-(prop-2-ynyloxy)-2H-chromen-2-one **117** (0.8g, 1.0 eq.), dissolved in *tert*-ButOH/H<sub>2</sub>O (1/1 v/v, 2.0 ml) in presence of tetramethylammonium chloride (0.04g, 1.0 eq) and copper nanosize (5 % mol), following the general procedure mentioned above. The crude was purified by silica gel column chromatography eluting with 33% ethyl acetate in *n*-hexane to afford **124** as a light brown solid in 40% yield. mp 163-165 °C; silica gel TLC *R<sub>f</sub>* 0.11 (AcOEt/*n*-Hex 33%, v/v);  $\nu_{\max}$  (KBr) cm<sup>-1</sup>, 2938 (C-H), 1719 (C=O), 1642 (C=C), 1538 (aromatic), 1243 (C-O), 1191 (C-N), 1111 (*O*-C=O);  $\delta_{\text{H}}$  (400 MHz, DMSO-*d*<sub>6</sub>) 5.41 (2H, s, OCH<sub>2</sub>), 6.35 (1H, d, *J* 9.4, 3-H), 7.10 (1H, dd *J* 8.4, 2.4, 6-H), 7.25 (1H, d *J* 2.4, 8-H), 7.54 (1H, m, 4''-H), 7.65 (1H, m, 3''-H), 7.70 (1H, m, 5-H), 7.95 (1H, m, 2''-H), 8.05 (1H, d, *J* 9.4, 4-H), 9.04 (1H, s, 5'-H);  $\delta_{\text{c}}$  (100 MHz, DMSO-*d*<sub>6</sub>) 161.9, 161.1, 156.2, 145.2, 144.1, 138.9, 130.8, 130.4, 129.7, 124.1, 121.1, 113.8, 113.7, 113.6, 102.6, 62.6.

**6-((1'-(2''-chlorophenyl)-1''H-1',2',3'-triazol-4'-yl)methoxy)-2H-chromen-2-one (125)**

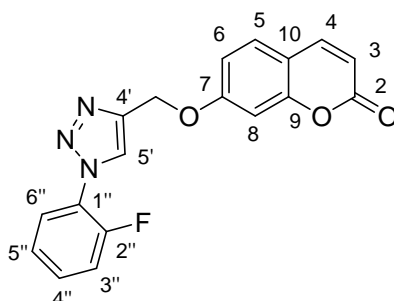
Compound **125** was synthesized by reacting 1-azido-2-chlorobenzene **119** (0.07g, 1.1 eq) with 6-(prop-2-ynyloxy)-2H-chromen-2-one **116** (0.08g, 1.0 eq.), dissolved in *tert*-ButOH/H<sub>2</sub>O (1/1 v/v, 2.0 ml) in presence of tetramethylammonium chloride (0.04g, 1.0 eq) and copper nanosize (5 % mol), following the general procedure mentioned above. The crude was purified by silica gel column chromatography eluting with 33% ethyl acetate in *n*-hexane to afford **125** as a light brown solid in 45% yield. mp 164-166 °C; silica gel TLC *R<sub>f</sub>* 0.11 (AcOEt/*n*-Hex 33%, v/v);  $\nu_{\max}$  (KBr) cm<sup>-1</sup>, 2914 (C-H), 1761 (C=O), 1648 (C=C), 1552 (aromatic), 1266 (C-O), 1210 (C-N), 1137 (O-C=O);  $\delta_{\text{H}}$  (400 MHz, DMSO-*d*<sub>6</sub>) 5.35 (2H, s, OCH<sub>2</sub>), 6.54 (1H, d, *J* 9.6, 3-H), 7.37 (1H, m, 7-H), 7.42 (1H, m, 8-H), 7.51 (1H, d, *J* 2.8, 5-H), 7.64 (1H, m, 5''-H), 7.68 (1H, m, 4''-H), 7.76 (1H, m, 6''-H), 7.82 (1H, m, 3''-H), 8.06 (1H, d, *J* 9.6, 4-H), 8.77 (1H, s, 5'-H);  $\delta_{\text{C}}$  (100 MHz, DMSO-*d*<sub>6</sub>) 161.0 (C-2), 155.2 (C-9), 149.0 (C-6), 144.9 (C-4), 143.4 (C-4'), 135.3 (C-2''), 132.7 (C-4''), 131.5 (C-3''), 129.5 (C-1''), 129.4 (C-5''), 129.3 (C-6''), 127.9 (C-5'), 121.0 (C-7), 120.1 (C-10), 118.4 (C-8), 117.6 (C-3), 113.1 (C-5), 62.4 (OCH<sub>2</sub>).

**7-((1'-(2''-chlorophenyl)-1''H-1',2',3'-triazol-4'-yl)methoxy)-2H-chromen-2-one (126)**

Compound **126** was synthesized by reacting 1-azido-2-chlorobenzene **119** (0.07g, 1.1 eq) with 7-(prop-2-ynyloxy)-2H-chromen-2-one **117** (0.08g, 1.0 eq.), dissolved in *tert*-ButOH/H<sub>2</sub>O (1/1 v/v, 2.0 ml) in presence of tetramethylammonium chloride (0.04g, 1.0 eq) and copper nanosize (5 % mol), following the general procedure mentioned above. The crude was purified by silica gel column chromatography eluting with 33% ethyl acetate in *n*-hexane to afford **126** as a light brown solid in 45% yield. mp 136-138 °C; silica gel TLC *R<sub>f</sub>* 0.11 (AcOEt/*n*-Hex 33%, v/v);  $\nu_{\max}$  (KBr) cm<sup>-1</sup>, 2925 (C-H), 1725 (C=O), 1653 (C=C), 1560 (aromatic), 1280 (C-O), 1208 (C-N), 1154 (O-C=O);  $\delta_{\text{H}}$  (400 MHz, DMSO-*d*<sub>6</sub>) 5.42 (2H, s, OCH<sub>2</sub>), 6.34 (1H, d, *J* 9.6, 3-H), 7.11 (1H, dd *J* 8.4, 2.4, 6-H), 7.24 (1H, d *J* 2.4, 8-H), 7.63 (1H, m, 6''-H), 7.68 (1H, m, 5''-H), 7.70 (1H, m, 5-H), 7.76 (1H, m, 4''-H), 7.82 (1H, m, 3''-H), 8.04 (1H, d, *J* 9.6, 4-H), 8.78 (1H, s, 5'-H);  $\delta_{\text{C}}$  (100 MHz, DMSO-*d*<sub>6</sub>) 162.0 (C-7), 161.1 (C-2), 156.2 (C-9), 145.2 (C-4), 143.0 (C-4'), 135.3 (C-2''), 132.7 (C-5''), 131.5 (C-3''), 130.5 (C-5), 129.5 (C-1''), 129.4 (C-6''), 129.3 (C-4''), 113.8 (C-6), 113.7 (C-3), 113.6 (C-10), 102.6 (C-8), 62.4 (OCH<sub>2</sub>).

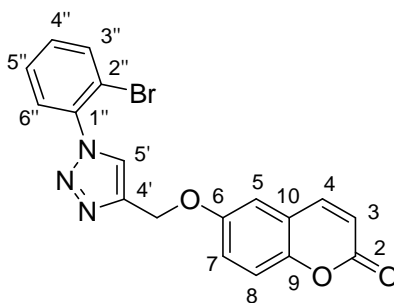
**6-((1'-(2''-fluorophenyl)-1''H-1',2',3'-triazol-4'-yl)methoxy)-2H-chromen-2-one (127)**

Compound **127** was synthesized by reacting 1-azido-2-fluorobenzene **120** (0.08g, 1.1 eq) with 6-(prop-2-ynoxy)-2H-chromen-2-one **116** (0.08g, 1.0 eq.), dissolved in *tert*-ButOH/H<sub>2</sub>O (1/1 v/v, 2.0 ml) in presence of tetramethylammonium chloride (0.04g, 1.0 eq) and copper nanosize (5 % mol), following the general procedure mentioned above. The crude was purified by silica gel column chromatography eluting with 33% ethyl acetate in *n*-hexane to afford **127** as a light brown solid in 40% yield. mp 156-158 °C; silica gel TLC *R<sub>f</sub>* 0.14 (AcOEt/*n*-Hex 33%, v/v);  $\nu_{\max}$  (KBr) cm<sup>-1</sup>, 2918 (C-H), 1721 (C=O), 1647 (C=C), 1563 (aromatic), 1274 (C-O), 1213 (C-N), 1160 (*O*-C=O);  $\delta_{\text{H}}$  (400 MHz, DMSO-*d*<sub>6</sub>) 5.42 (2H, s, OCH<sub>2</sub>), 6.54 (1H, d, *J* 9.6, 3-H), 7.37 (m, 1H), 7.41 (m, 1H), 7.49 (m, 1H), 7.52 (m, 1H), 7.62 (m, 1H), 7.67 (m, 1H), 7.90 (m, 1H), 8.06 (1H, d, *J* 9.6, 4-H), 8.81 (1H, s, 5'-H);  $\delta_{\text{F}}$  (376 MHz, DMSO-*d*<sub>6</sub>) -127.1 (s, 1F);  $\delta_{\text{C}}$  (100 MHz, DMSO-*d*<sub>6</sub>) 161.0, 155.1, 154.6, 149.1, 144.9, 143.9, 132.3, 127.2, 126.8, 126.5, 120.9, 120.1, 118.4, 118.1, 117.9, 117.6, 112.9, 62.4.

**7-((1'-(2''-fluorophenyl)-1''H-1',2',3'-triazol-4'-yl)methoxy)-2H-chromen-2-one (128)**

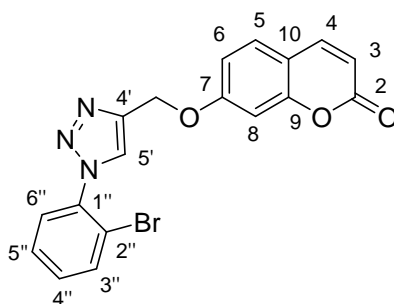
Compound **128** was synthesized by reacting 1-azido-2-fluorobenzene **120** (0.08g, 1.1 eq) with 7-(prop-2-ynoxy)-2H-chromen-2-one **117** (0.08g, 1.0 eq.), dissolved in *tert*-ButOH/H<sub>2</sub>O (1/1 v/v, 2.0 ml) in presence of tetramethylammonium chloride (0.04g, 1.0 eq) and copper nanosize (5 % mol), following the general procedure mentioned above. The crude was purified by silica gel column chromatography eluting with 25% ethyl acetate in *n*-hexane to afford **128** as a light brown solid in 30% yield. mp 161-163 °C; silica gel TLC *R<sub>f</sub>* 0.09 (AcOEt/*n*-Hex 25%, v/v);  $\nu_{\max}$  (KBr) cm<sup>-1</sup>, 2922 (C-H), 1730 (C=O), 1626 (C=C), 1548 (aromatic), 1271 (C-O), 1221 (C-N), 1155 (*O*-C=O);  $\delta_{\text{H}}$  (400 MHz, DMSO-*d*<sub>6</sub>) 5.42 (2H, s, OCH<sub>2</sub>), 6.35 (1H, d, *J* 9.6, 3-H), 7.11 (m, 1H), 7.25 (m, 1H), 7.49 (m, 1H), 7.61 (m, 1H), 7.64 (m, 1H), 7.67 (m, 1H), 7.71 (m, 1H), 7.90 (m, 1H), 8.04 (1H, d, *J* 9.6, 4-H), 8.83 (1H, s, 5'-H);  $\delta_{\text{F}}$  (376 MHz, DMSO-*d*<sub>6</sub>) -121.1 (s, 1F);  $\delta_{\text{C}}$  (100 MHz, DMSO-*d*<sub>6</sub>) 161.9, 161.1, 156.2, 154.0, 153.5, 145.2, 143.5, 132.4, 132.3, 130.4, 127.4, 126.9, 126.5, 118.0, 113.8, 113.6, 102.5, 62.3.

**6-((1'-(2''-bromophenyl)-1''H-1',2',3'-triazol-4'-yl)methoxy)-2H-chromen-2-one (129)**



Compound **129** was synthesized by reacting 1-azido-2-bromobenzene **121** (0.09g, 1.1 eq) with 6-(prop-2-ynyloxy)-2H-chromen-2-one **116** (0.04g, 1.0 eq.), dissolved in *tert*-ButOH/H<sub>2</sub>O (1/1 v/v, 2.0 ml) in presence of tetramethylammonium chloride (0.04g, 1.0 eq) and copper nanosize (5 % mol), following the general procedure mentioned above. The crude was purified by silica gel column chromatography eluting with 50% ethyl acetate in *n*-hexane to afford **129** as a light brown solid in 60% yield. mp 174-176 °C; silica gel TLC *R<sub>f</sub>* 0.20 (AcOEt/*n*-Hex 50%, v/v);  $\nu_{\max}$  (KBr) cm<sup>-1</sup>, 2927 (C-H), 1733 (C=O), 1646 (C=C), 1521 (aromatic), 1266 (C-O), 1211 (C-N), 1157 (O-C=O);  $\delta_{\text{H}}$  (400 MHz, DMSO-*d*<sub>6</sub>) 5.35 (2H, s, OCH<sub>2</sub>), 6.55 (1H, d, *J* 9.4, 3-H), 7.37 (1H, m, 7-H), 7.42 (1H, m, 8-H), 7.51 (1H, d, *J* 2.8, 5-H), 7.60 (1H, m, 4''-H), 7.66 (1H, m, 5''H), 7.71 (1H, m, 6''-H), 7.96 (1H, m, 3''-H), 8.06 (1H, d, *J* 9.4, 4-H), 8.75 (1H, s, 5'-H);  $\delta_{\text{C}}$  (100 MHz, DMSO-*d*<sub>6</sub>) 161.0 (C-2), 155.2 (C-9), 149.0 (C-6), 144.9 (C-4), 143.3 (C-4'), 137.4 (C-2''), 134.5 (C-3''), 132.9 (C-4''), 129.9 (C-5''), 129.6 (C-6''), 127.9 (C-5'), 121.0 (C-7), 120.1 (C-10), 119.8 (C-1''), 118.4 (C-8), 117.6 (C-3), 113.1 (C-5), 62.5 (OCH<sub>2</sub>).

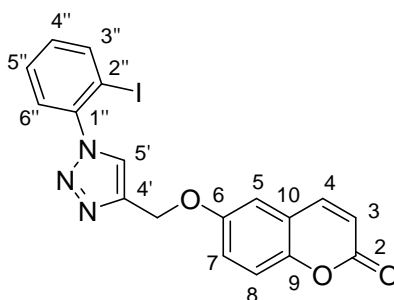
**7-((1'-(2''-bromophenyl)-1''H-1',2',3'-triazol-4'-yl)methoxy)-2H-chromen-2-one (130)**



Compound **130** was synthesized by reacting 1-azido-2-bromobenzene **121** (0.08g, 1.1 eq) with 7-(prop-2-ynyloxy)-2H-chromen-2-one **117** (0.09g, 1.0 eq.), dissolved in *tert*-ButOH/H<sub>2</sub>O (1/1 v/v, 2.0 ml) in presence of tetramethylammonium chloride (0.04g, 1.0 eq) and copper nanosize (5 % mol), following the general procedure mentioned above. The crude was purified by silica gel column chromatography eluting with 33% ethyl acetate in *n*-hexane to afford **130** as a light brown solid in 60% yield. mp 133-135 °C; silica gel TLC *R<sub>f</sub>* 0.16 (AcOEt/*n*-Hex 33%, v/v);  $\nu_{\max}$  (KBr) cm<sup>-1</sup>, 2924 (C-H), 1717 (C=O), 1646 (C=C), 1540 (aromatic), 1295 (C-O), 1207 (C-N), 1126 (O-C=O);  $\delta_{\text{H}}$  (400 MHz, DMSO-*d*<sub>6</sub>) 5.42 (2H, s, OCH<sub>2</sub>), 6.35 (1H, d, *J* 9.6, 3-H), 7.11 (1H, dd *J* 8.4, 2.4, 6-H), 7.26 (1H, d *J* 2.4, 8-H), 7.61 (1H, m, 4''-H), 7.67 (1H, m, 5''-H), 7.71 (1H, m, 6''-H), 7.72 (1H, m, 5-H), 7.96 (1H, m, 3''-H), 8.05 (1H, d, *J* 9.6, 4-H), 8.78 (1H, s, 5'-H);  $\delta_{\text{C}}$  (100 MHz, DMSO-*d*<sub>6</sub>) 162.0 (C-7), 161.1 (C-2), 156.2 (C-9), 145.2 (C-4), 142.9 (C-4'), 136.9 (C-2''), 134.5

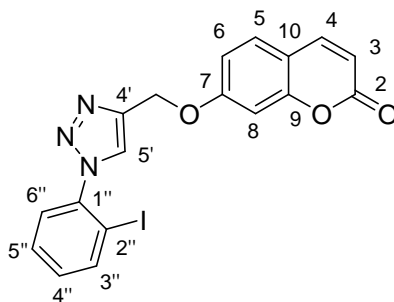
(C-3''), 132.9 (C-4''), 130.5 (C-5), 129.9 (C-6''), 129.7 (C-5''), 128.0 (C-5'), 119.8 (C-1''), 113.9 (C-6), 113.7 (C-3), 113.6 (C-10), 102.6 (C-8), 62.4 (OCH<sub>2</sub>).

**6-((1'-(2''-iodophenyl)-1''H-1',2',3'-triazol-4'-yl)methoxy)-2H-chromen-2-one (131)**



Compound **131** was synthesized by reacting 1-azido-2-iodobenzene **122** (0.11g, 1.1 eq) with 6-(prop-2-ynoxy)-2H-chromen-2-one **116** (0.08g, 1.0 eq.), dissolved in *tert*-ButOH/H<sub>2</sub>O (1/1 v/v, 2.0 ml) in presence of tetramethylammonium chloride (0.04g, 1.0 eq) and copper nanosize (5 % mol), following the general procedure mentioned above. The crude was purified by silica gel column chromatography eluting with 33% ethyl acetate in *n*-hexane to afford **131** as a yellow solid. in 30% yield. mp 162-164 °C; silica gel TLC *R<sub>f</sub>* 0.13 (AcOEt/*n*-Hex 33%, v/v);  $\nu_{\max}$  (KBr) cm<sup>-1</sup>, 2927 (C-H), 1716 (C=O), 1670 (C=C), 1540 (aromatic), 1266 (C-O), 1188 (C-N), 1121 (O-C=O);  $\delta_{\text{H}}$  (400 MHz, DMSO-*d*<sub>6</sub>) 5.35 (2H, s, OCH<sub>2</sub>), 6.54 (1H, d, *J* 9.4, 3-H), 7.37 (1H, m, 7-H), 7.42 (1H, m, 8-H), 7.44 (1H, m, 4''-H), 7.51 (1H, d, *J* 2.8, 5-H), 7.60 (1H, m, 6''-H), 7.66 (1H, m, 5''-H), 8.06 (1H, d, *J* 9.4, 4-H), 8.14 (1H, dd, *J* 9.4, 1.2, 3''-H), 8.69 (1H, s, 5'-H);  $\delta_{\text{C}}$  (100 MHz, DMSO-*d*<sub>6</sub>) 161.0 (C-2), 155.2 (C-9), 149.0 (C-6), 144.9 (C-4), 143.3 (C-4'), 140.7 (C-1''), 140.6 (C-3''), 132.9 (C-4''), 130.4 (C-5''), 128.9 (C-6''), 127.6 (C-5'), 121.0 (C-7), 120.1 (C-10), 118.3 (C-8), 117.6 (C-3), 113.1 (C-5), 96.7 (C-2''), 62.5 (OCH<sub>2</sub>).

**7-((1'-(2''-iodophenyl)-1''H-1',2',3'-triazol-4'-yl)methoxy)-2H-chromen-2-one (132)**



Compound **132** was synthesized by reacting 1-azido-2-iodobenzene **122** (0.11g, 1.1 eq) with 7-(prop-2-ynoxy)-2H-chromen-2-one **117** (0.08g, 1.0 eq.), dissolved in *tert*-ButOH/H<sub>2</sub>O (1/1 v/v, 2.0 ml) in presence of tetramethylammonium chloride (0.04g, 1.0 eq) and copper nanosize (5 % mol), following the general procedure mentioned above. The crude was purified by silica gel column chromatography eluting with 33% ethyl acetate in *n*-hexane to afford **132** as a light brown sticky oil in 30% yield; Silica gel TLC *R<sub>f</sub>* 0.13 (AcOEt/*n*-Hex 33%, v/v);  $\nu_{\max}$  (KBr) cm<sup>-1</sup>, 2928 (C-H), 1722 (C=O), 1632 (C=C), 1539 (aromatic), 1266 (C-O), 1187 (C-N), 1141 (O-C=O);  $\delta_{\text{H}}$  (400 MHz, DMSO-*d*<sub>6</sub>) 5.41 (2H, s, OCH<sub>2</sub>), 6.35 (1H, d, *J* 9.6, 3-H), 7.11 (1H, dd, *J* 8.6, 2.4, 6-H), 7.26 (1H, d, *J* 2.4, 8-H), 7.41 (1H, m, 4''-H), 7.61 (1H, m, 6''-H), 7.65 (1H, m, 5''-H), 7.70 (1H, d, *J* 8.6, 5-H), 8.05 (1H, d, *J* 9.6, 4-H), 8.15 (1H, m, 3''-H), 8.78 (1H, s, 5'-H);  $\delta_{\text{C}}$  (100 MHz, DMSO-*d*<sub>6</sub>) 162.1 (C-

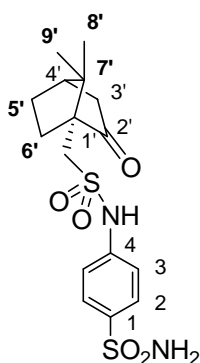
7), 161.2 (C-2), 156.3 (C-9), 145.2 (C-4), 143.0 (C-4'), 140.7 (C-3''), 140.6 (C-2''), 132.9 (C-4''), 130.5 (C-5), 130.3 (C-5''), 129.0 (C-6''), 127.8 (C-5'), 113.9 (C-6), 113.7 (C-3), 113.6 (C-10), 102.6 (C-8), 62.5 (OCH<sub>2</sub>).

### 6.3.5 General procedure for preparation of sulfonamido derivatives 195-204

Reactions of (1*R*)-(-)-10-Camphorsulfonyl chloride **192** and (1*S*)-(+)-10-Camphorsulfonyl chloride **193** (0.3 g, 1.0 eq.) with amino derivatives **137,140, 141, 149, 194** (1.0 eq.) were carried out at 0° to room temperature in Schotten-Baumann conditions under nitrogen atmosphere, in the presence of a stoichiometric amount of dropwisely dry TEA (1.0 eq. for **137, 141, 194** and 2.0 eq. for **140, 149**), in dry DMF as solvent (2 ml).

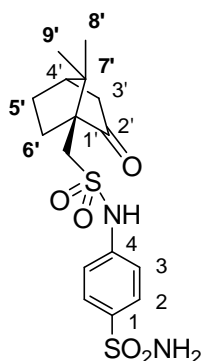
When complete (monitoring by TLC), reactions were quenched with crushed ice, extracted with ethyl acetate (20 ml), washed with 1N HCl (2 x 10 ml) and brine (2 x 10 ml). The collected organic phase was dried on anhydrous Na<sub>2</sub>SO<sub>4</sub>, filtered and evaporated under vacuum. The crude was purified by silica gel column chromatography eluting with *n*-Hexane/ethyl acetate or DCM/methanol to afford compounds **195-204** as white solids in medium yields.

#### 4-(((1*R*)-7',7'-dimethyl-2'-oxobicyclo[2'.2'.1']heptan-1'-yl)methylsulfonamido) benzenesulfonamide (**195**)



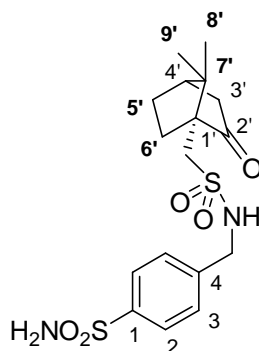
Compound **195** was synthesized by reacting (1*R*)-(-)-10-Camphorsulfonyl chloride **192** (1.19 mmol, 300 mg) with sulfanilamide **137** (1.19 mmol, 204.9 mg) following the general procedure mentioned above. The crude was purified by silica gel column chromatography eluting with 3% MeOH in DCM to afford compounds **195** as white solid in 60% yield. mp 150-152 °C;  $[\alpha]_D^{20}$  -6.3; silica gel TLC *R<sub>f</sub>* 0.27 (MeOH/DCM 3% v/v);  $\nu_{\max}$  (KBr) cm<sup>-1</sup>, 3263 (N-H), 2963 (C-H), 1739 (C=O), 1597 (aromatic), 1333 (SO<sub>2</sub>-NH);  $\delta_H$  (400 MHz, DMSO-*d*<sub>6</sub>) 0.81 (3H, s, 9'-H<sub>3</sub>), 1.04 (3H, s, 8'-H<sub>3</sub>), 1.46 (1H, m, 6'-H), 1.60 (1H, m, 5'-H), 1.96 (1H, m, 3'-H), 1.99 (1H, m, 6'-H), 2.10 (1H, m, 3'-H), 2.37 (1H, m, 5'-H), 2.38 (1H, m, 4'-H), 3.12 (1H, d, *J* 14.8, SO<sub>2</sub>CH), 3.49 (1H, d, *J* 14.8, SO<sub>2</sub>CH), 7.30 (2H, s, SO<sub>2</sub>NH<sub>2</sub>, exchange with D<sub>2</sub>O), 7.40 (2H, m, 2 x 3-H), 7.81 (2H, m, 2 x 2-H), 10.39 (1H, s, SO<sub>2</sub>NH, exchange with D<sub>2</sub>O);  $\delta_C$  (100 MHz, DMSO-*d*<sub>6</sub>) 215.0 (C-2'), 142.5 (ipso), 139.2 (ipso), 128.1 (C-2), 118.6 (C-3), 58.7 (C-1'), 49.1 (SO<sub>2</sub>CH<sub>2</sub>), 48.6 (C-7'), 42.9 (C-4'), 42.8 (C-3'), 27.1 (C-6'), 25.5 (C-5'), 20.2 (C-8'), 20.1 (C-9'); *m/z* (ESI-) 385.1 ([M-H]<sup>-</sup> 100%), 771.2 ([2M-H]<sup>-</sup> 5%); *m/z* (ESI+) 387.2 ([M+H]<sup>+</sup> 85%), 773.3 ([2M+H]<sup>+</sup> 15%).

**4-(((1'S)-7',7'-dimethyl-2'-oxobicyclo[2'.2'.1']heptan-1'-yl)methylsulfonamido)benzene sulfonamide (196)**



Compound **196** was synthesized by reacting (1*S*)-(+)-10-Camphorsulfonyl chloride **193** (1.19 mmol, 300 mg) with sulfanilamide **137** (1.19 mmol, 204.9 mg) following the general procedure mentioned above. The crude was purified by silica gel column chromatography eluting with 3% MeOH in DCM to afford compounds **196** as white solid in 63% yield. mp 151-153 °C;  $[\alpha]_D^{20} +6.1$ ; silica gel TLC  $R_f$  0.27 (MeOH/DCM 3% v/v);  $\nu_{\max}$  (KBr)  $\text{cm}^{-1}$ , 3265 (N-H), 2959 (C-H), 1741 (C=O), 1595 (aromatic), 1336 (SO<sub>2</sub>-NH);  $\delta_{\text{H}}$  (400 MHz, DMSO-*d*<sub>6</sub>) 0.81 (3H, s, 9'-H<sub>3</sub>), 1.05 (3H, s, 8'-H<sub>3</sub>), 1.46 (1H, m, 6'-H), 1.59 (1H, m, 5'-H), 1.96 (1H, m, 3'-H), 1.98 (1H, m, 6'-H), 2.10 (1H, m, 3'-H), 2.36 (1H, m, 5'-H), 2.38 (1H, m, 4'-H), 3.12 (1H, d,  $J$  14.8, SO<sub>2</sub>CH), 3.50 (1H, d,  $J$  14.8, SO<sub>2</sub>CH), 7.31 (2H, s, SO<sub>2</sub>NH<sub>2</sub>, exchange with D<sub>2</sub>O), 7.40 (2H, m, 2 x 3-H), 7.81 (2H, m, 2 x 2-H), 10.4 (1H, s, SO<sub>2</sub>NH, exchange with D<sub>2</sub>O);  $\delta_{\text{C}}$  (100 MHz, DMSO-*d*<sub>6</sub>) 215.0 (C-2'), 142.4 (ipso), 139.2 (ipso), 128.0 (C-2), 118.6 (C-3), 58.7 (C-1'), 49.1 (C-SO<sub>2</sub>CH), 48.5 (C-7'), 42.9 (C-4'), 42.8 (C-3'), 27.2 (C-6'), 25.5 (C-5'), 20.2 (C-8'), 20.1 (C-9');  $m/z$  (ESI-) 385.1 ([M-H]<sup>-</sup> 100%), 771.2 ([2M-H]<sup>-</sup> 5%);  $m/z$  (ESI+) 387.1 ([M+H]<sup>+</sup> 75%), 773.1 ([2M+H]<sup>+</sup> 25%).

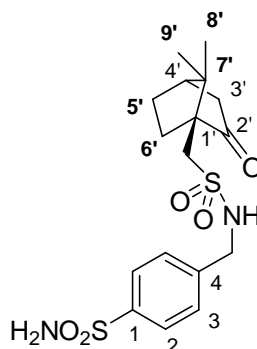
**4-(((1'R)-7',7'-dimethyl-2'-oxobicyclo[2'.2'.1']heptan-1'-yl)methylsulfonamido)methyl benzenesulfonamide (197)**



Compound **197** was synthesized by reacting (1*R*)-(-)-10-Camphorsulfonyl chloride **192** (1.19 mmol, 300 mg) with 4-Aminomethylbenzenesulfonamide hydrochloride **140** (1.19 mmol, 265 mg) following the general procedure mentioned above. The crude was purified by silica gel column chromatography eluting with 5% MeOH in DCM to afford compounds **197** as white solid in 55% yield. mp 160-162 °C;  $[\alpha]_D^{20} -13.2$ ; silica gel TLC  $R_f$  0.28 (MeOH/DCM 5% v/v);  $\nu_{\max}$  (KBr)  $\text{cm}^{-1}$ , 3256 (N-H), 2965 (C-H), 1730 (C=O), 1601 (aromatic), 1324 (SO<sub>2</sub>-NH);  $\delta_{\text{H}}$  (400 MHz, DMSO-*d*<sub>6</sub>) 0.81 (3H, s, 9'-H<sub>3</sub>), 1.04 (3H, s, 8'-H<sub>3</sub>), 1.43 (1H, m, 6'-H), 1.59 (1H, m, 5'-H), 1.95 (1H, m, 3'-H), 1.97 (1H, m, 6'-H), 2.08 (1H, m, 3'-H), 2.36 (1H, m, 5'-H), 2.39 (1H, m, 4'-H), 2.93 (1H, d,  $J$  10.4, SO<sub>2</sub>CH), 3.36

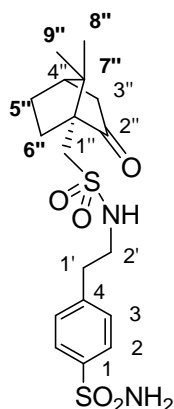
(1H, d,  $J$  10.4,  $\text{SO}_2\text{CH}$ ), 4.33 (2H, d,  $J$  6.4,  $\text{CH}_2\text{NH}$ ), 7.37 (2H, s,  $\text{SO}_2\text{NH}_2$ , exchange with  $\text{D}_2\text{O}$ ), 7.56 (2H, m, 2 x 3-H), 7.83 (2H, m, 2 x 2-H), 9.72 (1H, t,  $J$  6.4,  $\text{SO}_2\text{NH}$ , exchange with  $\text{D}_2\text{O}$ );  $\delta_{\text{C}}$  (100 MHz,  $\text{DMSO}-d_6$ ) 215.6 (C-2'), 143.9 (ipso), 143.5 (ipso), 128.8 (C-3), 126.6 (C-2), 58.7 (C-1'), 49.3 (C-  $\text{SO}_2\text{CH}_2$ ), 48.5 (C-7'), 46.6 ( $\text{CH}_2\text{NH}$ ), 43.0 (C-3'), 42.9 (C-4'), 27.2 (C-6'), 25.4 (C-5'), 20.3 (C-8'), 20.2 (C-9');  $m/z$  (ESI-) 399.1 ([M-H]- 100%), 799.3 ([2M-H]- 5%);  $m/z$  (ESI+) 401.2 ([M+H]+ 100%), 801.3 ([2M+H]+ 18%).

**4-(((1'S)-7',7'-dimethyl-2'-oxobicyclo[2'.2'.1']heptan-1'-yl)methylsulfonamido)methyl benzenesulfonamide (198)**



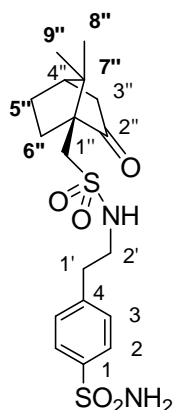
Compound **198** was synthesized by reacting (1S)-(+)-10-Camphorsulfonyl chloride **193** (1.19 mmol, 300 mg) with 4-Aminomethylbenzenesulfonamide hydrochloride **140** (1.19 mmol, 265 mg) following the general procedure mentioned above. The crude was purified by silica gel column chromatography eluting with 5% MeOH in DCM to afford compounds **198** as white solid in 55% yield. mp 162-163 °C;  $[\alpha]_{\text{D}}^{20}$  -12.9; silica gel TLC  $R_f$  0.28 (MeOH/DCM 5% v/v);  $\nu_{\text{max}}$  (KBr)  $\text{cm}^{-1}$ , 3259 (N-H), 2964 (C-H), 1733 (C=O), 1604 (aromatic), 1327 ( $\text{SO}_2\text{-NH}$ );  $\delta_{\text{H}}$  (400 MHz,  $\text{DMSO}-d_6$ ) 0.81 (3H, s, 9'-H<sub>3</sub>), 1.05 (3H, s, 8'-H<sub>3</sub>), 1.43 (1H, m, 6'-H), 1.57 (1H, m, 5'-H), 1.95 (1H, m, 3'-H), 1.97 (1H, m, 6'-H), 2.09 (1H, m, 3'-H), 2.36 (1H, m, 5'-H), 2.40 (1H, m, 4'-H), 2.93 (1H, d,  $J$  10.4,  $\text{SO}_2\text{CH}$ ), 3.35 (1H, d,  $J$  10.4,  $\text{SO}_2\text{CH}$ ), 4.33 (2H, d,  $J$  6.4,  $\text{CH}_2\text{NH}$ ), 7.37 (2H, s,  $\text{SO}_2\text{NH}_2$ , exchange with  $\text{D}_2\text{O}$ ), 7.56 (2H, m, 2 x 3-H), 7.83 (2H, m, 2 x 2-H), 9.72 (1H, t,  $J$  6.4,  $\text{SO}_2\text{NH}$ , exchange with  $\text{D}_2\text{O}$ );  $\delta_{\text{C}}$  (100 MHz,  $\text{DMSO}-d_6$ ) 215.5 (C-2'), 143.8 (ipso), 143.5 (ipso), 128.6 (C-3), 126.6 (C-2), 58.7 (C-1'), 49.3 (C-  $\text{SO}_2\text{CH}_2$ ), 48.6 (C-7'), 46.6 ( $\text{CH}_2\text{NH}$ ), 43.1 (C-3'), 42.9 (C-4'), 27.3 (C-6'), 25.5 (C-5'), 20.3 (C-8'), 20.2 (C-9');  $m/z$  (ESI-) 399.1 ([M-H]- 100%), 799.3 ([2M-H]- 8%);  $m/z$  (ESI+) 401.2 ([M+H]+ 100%), 801.3 ([2M+H]+ 48%).

**4-(2'-(((1''R)-7'',7''-dimethyl-2''-oxobicyclo[2''.2''.1'']heptan-1''-yl)methyl sulfonamido)ethyl) benzenesulfonamide (199)**



Compound **199** was synthesized by reacting (1R)-(-)-10-Camphorsulfonyl chloride **193** (1.19 mmol, 300 mg) with 4-(2-Aminoethyl)benzenesulfonamide **141** (1.19 mmol, 238.3 mg) following the general procedure mentioned above. The crude was purified by silica gel column chromatography eluting with 2.5% MeOH in DCM to afford compounds **199** as white solid in 65% yield. mp 139-141 °C;  $[\alpha]_D^{20}$  -11.1; silica gel TLC  $R_f$  0.27 (MeOH/DCM 2.5% v/v);  $\nu_{\max}$  (KBr)  $\text{cm}^{-1}$ , 3251 (N-H), 2956 (C-H), 1745 (C=O), 1599 (aromatic), 1326 (SO<sub>2</sub>-NH);  $\delta_{\text{H}}$  (400 MHz, DMSO-*d*<sub>6</sub>) 0.82 (3H, s, 9''-H<sub>3</sub>), 1.03 (3H, s, 8''-H<sub>3</sub>), 1.42 (1H, m, 6''-H), 1.53 (1H, m, 5''-H), 1.93 (1H, m, 3''-H), 1.96 (1H, m, 6''-H), 2.07 (1H, m, 3''-H), 2.34 (1H, m, 5''-H), 2.36 (1H, m, 4''-H), 2.90 (3H, m, 1'-H<sub>2</sub>, SO<sub>2</sub>CH), 3.28 (3H, m, 2'-H<sub>2</sub>, SO<sub>2</sub>CH), 7.29 (2H, s, SO<sub>2</sub>NH<sub>2</sub>, exchange with D<sub>2</sub>O), 7.47 (2H, m, 2 x 3-H), 7.79 (2H, m, 2 x 2-H);  $\delta_{\text{C}}$  (100 MHz, DMSO-*d*<sub>6</sub>) 215.5 (C-2''), 144.0 (ipso), 143.1 (ipso), 130.2 (C-3), 126.6 (C-2), 58.7 (C-1''), 48.5 (C-SO<sub>2</sub>CH<sub>2</sub>), 48.4 (C-7''), 44.5 (C-2'), 42.9 (C-3''), 42.8 (C-4''), 36.4 (C-1'), 27.2 (C-6''), 25.3 (C-5''), 20.3 (C-8''), 20.2 (C-9''); m/z (ESI-) 413.2 ([M-H]<sup>-</sup> 100%), 827.3 ([2M-H]<sup>-</sup> 2%); m/z (ESI+) 415.2 ([M+H]<sup>+</sup> 100%), 829.4 ([2M+H]<sup>+</sup> 28%).

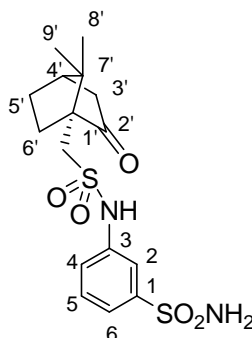
**4-(2'-(((1''S)-7'',7''-dimethyl-2''-oxobicyclo[2''.2''.1'']heptan-1''-yl)methyl sulfonamido)ethyl) benzenesulfonamide (200)**



Compound **200** was synthesized by reacting (1S)-(+)-10-Camphorsulfonyl chloride **193** (1.19 mmol, 300 mg) with 4-(2-Aminoethyl)benzenesulfonamide **141** (1.19 mmol, 238.3 mg) following the general procedure mentioned above. The crude was purified by silica gel column chromatography eluting with 2.5% MeOH in DCM to afford compounds **200** as white solid in 70% yield. mp 140-142 °C;  $[\alpha]_D^{20}$  +11.1; silica gel TLC  $R_f$  0.27

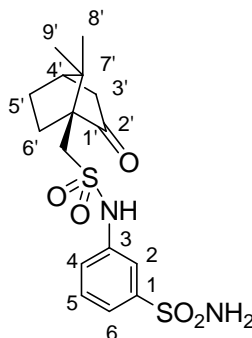
(MeOH/DCM 2.5% v/v);  $\nu_{\max}$  (KBr)  $\text{cm}^{-1}$ , 3250 (N-H), 2954 (C-H), 1741 (C=O), 1599 (aromatic), 1328 (SO<sub>2</sub>-NH);  $\delta_{\text{H}}$  (400 MHz, DMSO-*d*<sub>6</sub>) 0.83 (3H, s, 9''-H<sub>3</sub>), 1.03 (3H, s, 8''-H<sub>3</sub>), 1.42 (1H, m, 6''-H), 1.51 (1H, m, 4''-H), 1.92 (1H, m, 3''-H), 1.97 (1H, m, 6''-H), 2.07 (1H, m, 3''-H), 2.34 (1H, m, 5''-H), 2.35 (1H, m, 4''-H), 2.89 (3H, m, 1'-H<sub>2</sub>, SO<sub>2</sub>CH), 3.29 (3H, m, 2'-H<sub>2</sub>, SO<sub>2</sub>CH), 7.29 (2H, s, SO<sub>2</sub>NH<sub>2</sub>, exchange with D<sub>2</sub>O), 7.48 (2H, m, 2 x 3-H), 7.79 (2H, m, 2 x 2-H);  $\delta_{\text{C}}$  (100 MHz, DMSO-*d*<sub>6</sub>) 215.6 (C-2''), 144.2 (ipso), 143.1 (ipso), 130.3 (C-3), 126.8 (C-2), 58.7 (C-1''), 48.5 (SO<sub>2</sub>CH<sub>2</sub>), 48.4 (C-7''), 44.5 (C-2'), 42.9 (C-3''), 42.8 (C-4''), 36.5 (C-1'), 27.2 (C-6''), 25.3 (C-5''), 20.3 (C-8''), 20.3 (C-9''); *m/z* (ESI-) 413.1 ([M-H]<sup>-</sup> 100%), 827.3 ([2M-H]<sup>-</sup> 18%); *m/z* (ESI+) 415.2 ([M+H]<sup>+</sup> 100%), 829.3 ([2M+H]<sup>+</sup> 50%).

**3-(((1'R)-7',7'-dimethyl-2'-oxobicyclo[2'.2'.1']heptan-1'-yl)methylsulfonamido)benzene sulfonamide (201)**



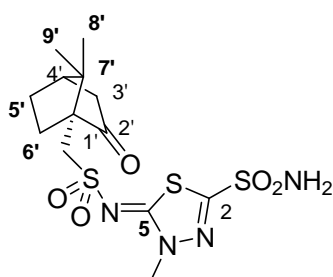
Compound **201** was synthesized by reacting (1*R*)-(-)-10-Camphorsulfonyl chloride **192** (0.08 mmol, 200 mg) with metanilamide **194** (0.08 mmol, 137.4 mg) following the general procedure mentioned above. The crude was purified by silica gel column chromatography eluting with 50% ethyl acetate in *n*-Hexane to afford compounds **201** as white solid in 52% yield. mp 148-150 °C;  $[\alpha]_{\text{D}}^{20}$  -13.3; silica gel TLC *R<sub>f</sub>* 0.3 (ethyl acetate/*n*-Hexane 50% v/v);  $\nu_{\max}$  (KBr)  $\text{cm}^{-1}$ , 3263 (N-H), 2963 (C-H), 1739 (C=O), 1600 (aromatic), 1336 (SO<sub>2</sub>-NH);  $\delta_{\text{H}}$  (400 MHz, DMSO-*d*<sub>6</sub>) 0.80 (3H, s, 9'-H<sub>3</sub>), 1.03 (3H, s, 8'-H<sub>3</sub>), 1.45 (1H, m, 6'-H), 1.58 (1H, m, 5'-H), 1.97 (1H, m, 3'-H), 2.00 (1H, m, 6'-H), 2.09 (1H, m, 3'-H), 2.39 (1H, m, 5'-H), 2.40 (1H, m, 4'-H), 3.09 (1H, d, *J* 15.2, SO<sub>2</sub>CH), 3.45 (1H, d, *J* 15.2, SO<sub>2</sub>CH), 7.45 (2H, s, SO<sub>2</sub>NH<sub>2</sub>, exchange with D<sub>2</sub>O), 7.49 (1H, m, 5-H), 7.58 (2H, m, 6-H, 4H), 7.71 (1H, m, 2-H), 10.2 (1H, s, SO<sub>2</sub>NH, exchange with D<sub>2</sub>O);  $\delta_{\text{C}}$  (100 MHz, DMSO-*d*<sub>6</sub>) 215.0 (C-2'), 146.1 (ipso), 139.9 (ipso), 130.9 (C-6), 122.6 (C-2), 121.4 (C-4), 116.8 (C-5), 58.7 (C-1'), 48.9 (SO<sub>2</sub>CH<sub>2</sub>), 48.5 (C-7'), 42.9 (C-4'), 42.8 (C-3'), 27.1 (C-6'), 25.5 (C-5'), 20.3 (C-8'), 20.1 (C-9'); *m/z* (ESI-) 385.1 ([M-H]<sup>-</sup> 100%), 771.2 ([2M-H]<sup>-</sup> 40%); *m/z* (ESI+) 387.1 ([M+H]<sup>+</sup> 100%), 773.3 ([2M+H]<sup>+</sup> 55%).

**3-(((1'S)-7',7'-dimethyl-2'-oxobicyclo[2'.2'.1']heptan-1'-yl)methylsulfonamido)benzene sulfonamide (202)**



Compound **202** was synthesized by reacting (1*S*)-(+)-10-Camphorsulfonyl chloride **193** (0.08 mmol, 200 mg) with metanilamide **194** (0.08 mmol, 137.4 mg) following the general procedure mentioned above. The crude was purified by silica gel column chromatography eluting with 50% ethyl acetate in *n*-Hexane to afford compounds **202** as white solid in 52% yield. mp 149-151 °C;  $[\alpha]_D^{20} +14.4$ ; silica gel TLC  $R_f$  0.3 (ethyl acetate/*n*-Hexane 50% v/v);  $\nu_{\max}$  (KBr)  $\text{cm}^{-1}$ , 3265 (N-H), 2962 (C-H), 1740 (C=O), 1602 (aromatic), 1332 (SO<sub>2</sub>-NH);  $\delta_{\text{H}}$  (400 MHz, DMSO-*d*<sub>6</sub>) 0.80 (3H, s, 9'-H<sub>3</sub>), 1.04 (3H, s, 8'-H<sub>3</sub>), 1.44 (1H, m, 6'-H), 1.58 (1H, m, 5'-H), 1.96 (1H, m, 3'-H), 1.96 (1H, m, 6'-H), 2.09 (1H, m, 3'-H), 2.38 (1H, m, 5'-H), 2.40 (1H, m, 4'-H), 3.08 (1H, d,  $J$  15.2, SO<sub>2</sub>CH), 3.46 (1H, d,  $J$  15.2, SO<sub>2</sub>CH), 7.43 (2H, s, SO<sub>2</sub>NH<sub>2</sub>, exchange with D<sub>2</sub>O), 7.49 (1H, m, 5-H), 7.57 (2H, m, 6-H, 4-H), 7.71 (1H, m, 2-H), 10.2 (1H, s, SO<sub>2</sub>NH, exchange with D<sub>2</sub>O);  $\delta_{\text{C}}$  (100 MHz, DMSO-*d*<sub>6</sub>) 215.1 (C-2'), 146.2 (ipso), 139.9 (ipso), 130.8 (C-6), 122.6 (C-2), 121.4 (C-4), 117.0 (C-5), 58.7 (C-1'), 48.9 (SO<sub>2</sub>CH<sub>2</sub>), 48.6 (C-7'), 42.9 (C-4'), 42.9 (C-3'), 27.1 (C-6'), 25.4 (C-5'), 20.3 (C-8'), 20.1 (C-9');  $m/z$  (ESI-) 385.0 ([M-H]<sup>-</sup> 100%), 771.1 ([2M-H]<sup>-</sup> 5%);  $m/z$  (ESI+) 387.2 ([M+H]<sup>+</sup> 100%), 773.3 ([2M+H]<sup>+</sup> 45%).

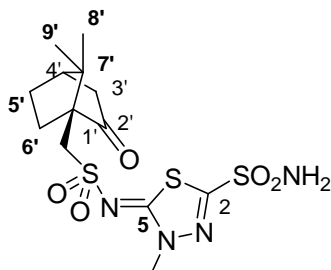
**5-(((1'R)-7',7'-dimethyl-2'-oxobicyclo[2'.2'.1']heptan-1'-yl)methylsulfonylimino)-4-methyl-4,5-dihydro-1,3,4-thiadiazole-2-sulfonamide (203)**



Compound **203** was synthesized by reacting (1*R*)-(-)-10-Camphorsulfonyl chloride **192** (0.08 mmol, 200 mg) with derivative **149**<sup>153</sup> (0.08 mmol, 185. mg) following the general procedure mentioned above. The crude was purified by silica gel column chromatography eluting with 3% MeOH in DCM to afford compounds **203** as white solid in 46% yield. mp 248-250 °C;  $[\alpha]_D^{20} -47.5$ ; silica gel TLC  $R_f$  0.27 (MeOH/DCM 3% v/v);  $\nu_{\max}$  (KBr)  $\text{cm}^{-1}$ , 3265 (N-H), 2962 (C-H), 1736 (C=O), 1654 (C=N), 1372 (SO<sub>2</sub>-NH);  $\delta_{\text{H}}$  (400 MHz, DMSO-*d*<sub>6</sub>) 0.82 (3H, s, 9'-H<sub>3</sub>), 1.06 (3H, s, 8'-H<sub>3</sub>), 1.45 (1H, m, 6'-H), 1.52 (1H, m, 5'-H), 1.96 (1H, m, 3'-H), 1.98 (1H, m, 6'-H), 2.09 (1H, m, 3'-H), 2.38 (1H, m, 5'-H), 2.38 (1H, m, 4'-H), 3.15 (1H, d,  $J$  14.8, SO<sub>2</sub>CH), 3.45 (1H, d,  $J$  14.8, SO<sub>2</sub>CH), 3.74 (3H, s, NCH<sub>3</sub>), 8.60 (2H, s, SO<sub>2</sub>NH<sub>2</sub>, exchange with D<sub>2</sub>O);  $\delta_{\text{C}}$  (100 MHz, DMSO-*d*<sub>6</sub>) 215.4 (C-2'), 165.7 (C-2), 157.0 (C-5), 58.5 (C-1'), 50.5 (SO<sub>2</sub>CH<sub>2</sub>), 48.7 (C-7'), 42.9 (C-3'), 42.8 (C-4'), 38.6

(NCH<sub>3</sub>), 27.2 (C-6'), 25.2 (C-5'), 20.1 (C-8'), 20.1 (C-9'); m/z (ESI-) 407.0 ([M-H]-100%), 815.0 ([2M-H]- 8%); m/z (ESI+) 409.1 ([M+H]+ 100%), 817.2 ([2M+H]+ 5%).

**5-(((1'S)-7',7'-dimethyl-2'-oxobicyclo[2'.2'.1']heptan-1'-yl)methylsulfonylimino)-4-methyl-4,5-dihydro-1,3,4-thiadiazole-2-sulfonamide (204)**



Compound **204** was synthesized by reacting (1*S*)-(+)-10-Camphorsulfonyl chloride **193** (0.08 mmol, 200 mg) with derivative **194**<sup>153</sup> (0.08 mmol, 185 mg) following the general procedure mentioned above. The crude was purified by silica gel column chromatography eluting with 3% MeOH in DCM to afford compounds **204** as white solid in 53% yield. mp 246-248 °C;  $[\alpha]_D^{20}$  -45.6; silica gel TLC  $R_f$  0.27 (MeOH/DCM 3% v/v);  $\nu_{\max}$  (KBr)  $\text{cm}^{-1}$ , 3262 (N-H), 2965 (C-H), 1739 (C=O), 1655 (C=N), 1374 (SO<sub>2</sub>-NH);  $\delta_{\text{H}}$  (400 MHz, DMSO-*d*<sub>6</sub>) 0.81 (3H, s, 9'-H<sub>3</sub>), 1.05 (3H, s, 8'-H<sub>3</sub>), 1.42-1.47 (1H, m, 6'-H), 1.63 (1H, m, 5'-H), 1.96 (1H, m, 3'-H), 1.98 (1H, m, 6'-H), 2.07 (1H, m, 3'-H), 2.39 (1H, m, 5'-H), 2.37 (1H, m, 4'-H), 3.15 (1H, d,  $J$  14.8, SO<sub>2</sub>CH), 3.44 (1H, d,  $J$  14.8, SO<sub>2</sub>CH), 3.73 (1H, s, NCH<sub>3</sub>), 8.59 (2H, s, SO<sub>2</sub>NH<sub>2</sub>, exchange with D<sub>2</sub>O);  $\delta_{\text{C}}$  (100 MHz, DMSO-*d*<sub>6</sub>) 215.5 (C-2'), 165.7 (C-2), 157.2 (C-5), 58.6 (C-1'), 50.5 (SO<sub>2</sub>CH<sub>2</sub>), 48.8 (C-7'), 42.9 (C-3'), 42.8 (C-4'), 38.7 (NCH<sub>3</sub>), 27.2 (C-6'), 25.2 (C-5'), 20.2 (C-8'), 20.1 (C-9'); m/z (ESI-) 407.1 ([M-H]-100%); m/z (ESI+) 409.1 ([M+H]+ 100%), 817.2 ([2M+H]+ 10%).

## References list

- (1) Supuran, C. T. *Nat Rev Drug Discov* **2008**, *7*, 168-181.
- (2) Supuran, C. T.; Scozzafava, A.; Casini, A. *Med. Res. Rev.* **2003**, *23*, 146-189.
- (3) Supuran, C. T. *Curr. Pharm. Des.* **2008**, *14*, 603-614.
- (4) Nishimori, I.; Onishi, S.; Takeuchi, H.; Supuran, C. T. *Curr. Pharm. Des.* **2008**, *14*, 622-630.
- (5) Rowlett, R. S. *BBA* **2010**, *1804*, 362-373.
- (6) Xu, Y.; Feng, L.; Jeffrey, P. D.; Shi, Y.; Morel, F. M. M. *Nature* **2008**, *452*, 56-61.
- (7) Švastová, E.; Hulíková, A.; Rafajová, M.; Zat'ovičová, M.; Gibadulinová, A.; Casini, A.; Cecchi, A.; Scozzafava, A.; Supuran, C. T.; Pastorek, J. *FEBS Letters* **2004**, *577*, 439-445.
- (8) Alterio, V.; Hilvo, M.; Di Fiore, A.; Supuran, C. T.; Pan, P.; Parkkila, S.; Scaloni, A.; Pastorek, J.; Pastorekova, S.; Pedone, C.; Scozzafava, A.; Monti, S. M.; De Simone, G. *Proceedings of the National Academy of Sciences* **2009**, *106*, 16233-16238.
- (9) Ebbesen, P.; Pettersen, E. O.; Gorr, T. A.; Jobst, G.; Williams, K.; Kieninger, J.; Wenger, R. H.; Pastorekova, S.; Dubois, L.; Lambin, P.; Wouters, B. G.; Van Den Beucken, T.; Supuran, C. T.; Poellinger, L.; Ratcliffe, P.; Kanopka, A.; Görlach, A.; Gasmann, M.; Harris, A. L.; Maxwell, P.; Scozzafava, A. *Journal of Enzyme Inhibition and Medicinal Chemistry* **2009**, *24*, 1-39.
- (10) Alterio, V.; Di Fiore, A.; D'Ambrosio, K.; Supuran, C. T.; De Simone, G. In *Drug Design of Zinc-Enzyme Inhibitors: Functional, Structural, and Disease Applications*; Wiley, Hoboken, 2009; pagg. 73-138.
- (11) Moya, A.; Tambutte, S.; Bertucci, A.; Tambutte, E.; Lotto, S.; Vullo, D.; Supuran, C. T.; Allemand, D.; Zoccola, D. *Journal of Biological Chemistry* **2008**, *283*, 25475-25484.
- (12) Supuran, C. T.; Scozzafava, A. *Bioorg. Med. Chem* **2007**, *15*, 4336-4350.
- (13) A. S. Covarrubias *Journal of Biological Chemistry* **2005**, *281*, 4993-4999.
- (14) Temperini, C.; Scozzafava, A.; Vullo, D.; Supuran, C. T. *Journal of Medicinal Chemistry* **2006**, *49*, 3019-3027.
- (15) Temperini, C.; Innocenti, A.; Scozzafava, A.; Supuran, C. T. *Bioorganic & Medicinal Chemistry* **2008**, *16*, 8373-8378.
- (16) Briganti, F.; Mangani, S.; Scozzafava, A.; Vernaglione, G.; Supuran, C. T. *Journal of Biological Inorganic Chemistry* **1999**, *4*, 528-536.
- (17) Guerri, A.; Briganti, F.; Scozzafava, A.; Supuran, C. T.; Mangani, S. *Biochemistry* **2000**, *39*, 12391-12397.
- (18) Supuran, C. T.; Conroy, C. W.; Maren, T. H. *Proteins* **1997**, *27*, 272-278.
- (19) Supuran, C. T.; Scozzafava, A.; Conway, J. *Carbonic anhydrase: its inhibitors and activators*; CRC Press, 2004.
- (20) Supuran, C. T.; Scozzafava, A. *Expert Opin. Ther. Patents* **2000**, *10*, 575-600.
- (21) Smith, K. S.; Ferry, J. G. *FEMS Microbiol. Rev* **2000**, *24*, 335-366.
- (22) Liljas, A.; Kannan, K. K.; Bergstén, P. C.; Waara, I.; Fridborg, K.; Strandberg, B.; Carlbom, U.; Järup, L.; Lövgren, S.; Petef, M. *Nature New Biol* **1972**, *235*, 131-137.
- (23) Liljas, A.; Håkansson, K.; Jonsson, B. H.; Xue, Y. *Eur. J. Biochem* **1994**, *219*, 1-10.
- (24) Supuran, C. T.; Di Fiore, A.; Alterio, V.; Monti, S. M.; De Simone, G. *Curr Pharm Des* **2010**.
- (25) Whittington, D. A.; Waheed, A.; Ulmasov, B.; Shah, G. N.; Grubb, J. H.; Sly, W. S.; Christianson, D. W. *Proc. Natl. Acad. Sci. U.S.A* **2001**, *98*, 9545-9550.
- (26) Whittington, D. A.; Grubb, J. H.; Waheed, A.; Shah, G. N.; Sly, W. S.;

- Christianson, D. W. *J. Biol. Chem* **2004**, *279*, 7223-7228.
- (27) Cronk, J. D.; Endrizzi, J. A.; Cronk, M. R.; O'Neill, J. W.; Zhang, K. Y. *Protein Sci.* **2001**, *10*, 911-922.
- (28) Cox, E. H.; McLendon, G. L.; Morel, F. M. M.; Lane, T. W.; Prince, R. C.; Pickering, I. J.; George, G. N. *Biochemistry* **2000**, *39*, 12128-12130.
- (29) Covarrubias, A. S. *Journal of Biological Chemistry* **2005**, *280*, 18782-18789.
- (30) Kimber, M. S.; Pai, E. F. *EMBO J* **2000**, *19*, 1407-1418.
- (31) Kisker, C.; Schindelin, H.; Alber, B. E.; Ferry, J. G.; Rees, D. C. *EMBO J* **1996**, *15*, 2323-2330.
- (32) Mitsuhashi, S.; Mizushima, T.; Yamashita, E.; Yamamoto, M.; Kumasaka, T.; Moriyama, H.; Ueki, T.; Miyachi, S.; Tsukihara, T. *J. Biol. Chem* **2000**, *275*, 5521-5526.
- (33) Hilvo, M.; Tolvanen, M.; Clark, A.; Shen, B.; Shah, G. N.; Waheed, A.; Halmi, P.; Hänninen, M.; Hämäläinen, J. M.; Vihinen, M.; Sly, W. S.; Parkkila, S. *Biochem. J* **2005**, *392*, 83-92.
- (34) Lane, T. W.; Morel, F. M. *Proc. Natl. Acad. Sci. U.S.A* **2000**, *97*, 4627-4631.
- (35) Briganti, F.; Mangani, S.; Orioli, P.; Scozzafava, A.; Vernaglione, G.; Supuran, C. T. *Biochemistry* **1997**, *36*, 10384-10392.
- (36) Stams, T.; Christianson, D. W. In *The Carbonic Anhydrase-New Horizons*; Chegwiddden W.R.; Edwards Y.; Carter N., 2000; pagg. 159-174.
- (37) Abbate, F.; Casini, A.; Scozzafava, A.; Supuran, C. T. *J Enzyme Inhib Med Chem* **2003**, *18*, 303-308.
- (38) Abbate, F.; Winum, J.; Potter, B. V. L.; Casini, A.; Montero, J.; Scozzafava, A.; Supuran, C. T. *Bioorg. Med. Chem. Lett* **2004**, *14*, 231-234.
- (39) Alterio, V.; Vitale, R. M.; Monti, S. M.; Pedone, C.; Scozzafava, A.; Cecchi, A.; De Simone, G.; Supuran, C. T. *Journal of the American Chemical Society* **2006**, *128*, 8329-8335.
- (40) Casini, A.; Antel, J.; Abbate, F.; Scozzafava, A.; David, S.; Waldeck, H.; Schäfer, S.; Supuran, C. T. *Bioorg. Med. Chem. Lett* **2003**, *13*, 841-845.
- (41) De Simone, G. D.; Fiore, A. D.; Menchise, V.; Pedone, C.; Antel, J.; Casini, A.; Scozzafava, A.; Wurl, M.; Supuran, C. T. *Bioorg. Med. Chem. Lett* **2005**, *15*, 2315-2320.
- (42) Menchise, V.; De Simone, G.; Alterio, V.; Di Fiore, A.; Pedone, C.; Scozzafava, A.; Supuran, C. T. *J. Med. Chem* **2005**, *48*, 5721-5727.
- (43) Winum, J.; Temperini, C.; El Cheikh, K.; Innocenti, A.; Vullo, D.; Ciattini, S.; Montero, J.; Scozzafava, A.; Supuran, C. T. *J. Med. Chem* **2006**, *49*, 7024-7031.
- (44) Innocenti, A.; Vullo, D.; Scozzafava, A.; Supuran, C. T. *Bioorganic & Medicinal Chemistry Letters* **2008**, *18*, 1583-1587.
- (45) Innocenti, A.; Vullo, D.; Scozzafava, A.; Supuran, C. T. *Bioorganic & Medicinal Chemistry* **2008**, *16*, 7424-7428.
- (46) Bayram, E.; Senturk, M.; Irfan Kufrevioglu, O.; Supuran, C. T. *Bioorganic & Medicinal Chemistry* **2008**, *16*, 9101-9105.
- (47) Sentürk, M.; Gülçin, I.; Daştan, A.; Küfrevioğlu, O. I.; Supuran, C. T. *Bioorg. Med. Chem* **2009**, *17*, 3207-3211.
- (48) Innocenti, A.; Beyza Öztürk Sarıkaya, S.; Gülçin, I.; Supuran, C. T. *Bioorganic & Medicinal Chemistry* **2010**, *18*, 2159-2164.
- (49) Davis, R. A.; Innocenti, A.; Poulsen, S.; Supuran, C. T. *Bioorganic & Medicinal Chemistry* **2010**, *18*, 14-18.
- (50) Nair, S. K.; Ludwig, P. A.; Christianson, D. W. *Journal of the American Chemical Society* **1994**, *116*, 3659-3660.
- (51) Maresca, A.; Temperini, C.; Vu, H.; Pham, N. B.; Poulsen, S.; Scozzafava, A.; Quinn, R. J.; Supuran, C. T. *Journal of the American Chemical Society* **2009**, *131*, 3057-3062.

- (52) Strop, P. *J. Biol. Chem* **2000**, *276*, 10299-10305.
- (53) Sawaya, M. R.; Cannon, G. C.; Heinhorst, S.; Tanaka, S.; Williams, E. B.; Yeates, T. O.; Kerfeld, C. A. *J. Biol. Chem* **2006**, *281*, 7546-7555.
- (54) Cronk, J. D.; Rowlett, R. S.; Zhang, K. Y. J.; Tu, C.; Endrizzi, J. A.; Lee, J.; Gareiss, P. C.; Preiss, J. R. *Biochemistry* **2006**, *45*, 4351-4361.
- (55) Smith, K. S.; Ferry, J. G. *J. Bacteriol.* **1999**, *181*, 6247-6253.
- (56) Iverson, T. M.; Alber, B. E.; Kisker, C.; Ferry, J. G.; Rees, D. C. *Biochemistry* **2000**, *39*, 9222-9231.
- (57) Innocenti, A.; Zimmerman, S.; Ferry, J. G.; Scozzafava, A.; Supuran, C. T. *Bioorganic & Medicinal Chemistry Letters* **2004**, *14*, 3327-3331.
- (58) Zimmerman, S.; Innocenti, A.; Casini, A.; Ferry, J. G.; Scozzafava, A.; Supuran, C. T. *Bioorganic & Medicinal Chemistry Letters* **2004**, *14*, 6001-6006.
- (59) Park, Y. I.; Karlsson, J.; Rojdestvenski, I.; Pronina, N.; Klimov, V.; Oquist, G.; Samuelsson, G. *FEBS Lett* **1999**, *444*, 102-105.
- (60) Pastorek, J.; Pastoreková, S.; Callebaut, I.; Mornon, J. P.; Zelník, V.; Opavský, R.; Zatošovicová, M.; Liao, S.; Portetelle, D.; Stanbridge, E. J. *Oncogene* **1994**, *9*, 2877-2888.
- (61) Parkkila, S. In *The Carbonic Anhydrase-New Horizons*; Chegwidde W.R.; Edwards Y.; Carter N., 2000; pagg. 79-93.
- (62) Pastorekova, S.; Parkkila, S.; Pastorek, J.; Supuran, C. T. *J Enzyme Inhib Med Chem* **2004**, *19*, 199-229.
- (63) Thiry, A.; Dogné, J.; Masereel, B.; Supuran, C. T. *Trends in Pharmacological Sciences* **2006**, *27*, 566-573.
- (64) Scozzafava, A.; Mastrolorenzo, A.; Supuran, C. T. *Expert Opin. Ther. Patents* **2006**, *16*, 1627-1664.
- (65) Vullo, D.; Franchi, M.; Gallori, E.; Antel, J.; Scozzafava, A.; Supuran, C. T. *J. Med. Chem* **2004**, *47*, 1272-1279.
- (66) Nishimori, I.; Vullo, D.; Innocenti, A.; Scozzafava, A.; Mastrolorenzo, A.; Supuran, C. T. *J. Med. Chem* **2005**, *48*, 7860-7866.
- (67) Nishimori, I.; Minakuchi, T.; Onishi, S.; Vullo, D.; Scozzafava, A.; Supuran, C. T. *J. Med. Chem* **2007**, *50*, 381-388.
- (68) Vullo, D.; Voipio, J.; Innocenti, A.; Rivera, C.; Ranki, H.; Scozzafava, A.; Kaila, K.; Supuran, C. T. *Bioorg. Med. Chem. Lett* **2005**, *15*, 971-976.
- (69) Vullo, D.; Franchi, M.; Gallori, E.; Pastorek, J.; Scozzafava, A.; Pastorekova, S.; Supuran, C. T. *Bioorg. Med. Chem. Lett* **2003**, *13*, 1005-1009.
- (70) Vullo, D.; Innocenti, A.; Nishimori, I.; Pastorek, J. A. A.; Scozzafava, A.; Pastoreková, S.; Supuran, C. T. *Bioorg. Med. Chem. Lett* **2005**, *15*, 963-969.
- (71) Lehtonen, J. *Journal of Biological Chemistry* **2003**, *279*, 2719-2727.
- (72) Nishimori, I.; Vullo, D.; Innocenti, A.; Scozzafava, A.; Mastrolorenzo, A.; Supuran, C. T. *Bioorg. Med. Chem. Lett* **2005**, *15*, 3828-3833.
- (73) Köhler, K.; Hillebrecht, A.; Schulze Wischeler, J.; Innocenti, A.; Heine, A.; Supuran, C. T.; Klebe, G. *Angew. Chem. Int. Ed. Engl* **2007**, *46*, 7697-7699.
- (74) Supuran, C. T.; Ilies, M. A.; Scozzafava, A. *Eur. J. Med. Chem.* **1998**, *33*, 739-751.
- (75) Supuran, C. T.; Scozzafava, A.; Ilies, M. A.; Briganti, F. *J. Enzym. Inhib* **2000**, *15*, 381-401.
- (76) Scozzafava, A.; Briganti, F.; Ilies, M. A.; Supuran, C. T. *Journal of Medicinal Chemistry* **2000**, *43*, 292-300.
- (77) Saczewski, F.; Slawinski, J.; Kornicka, A.; Brzozowski, Z.; Pomarnacka, E.; Innocenti, A.; Scozzafava, A.; Supuran, C. T. *Bioorganic & Medicinal Chemistry Letters* **2006**, *16*, 4846-4851.
- (78) De Simone, G.; Vitale, R. M.; Di Fiore, A.; Pedone, C.; Scozzafava, A.; Montero, J.; Winum, J.; Supuran, C. T. *Journal of Medicinal Chemistry* **2006**, *49*, 5544-5551.

- (79) Krungkrai, J.; Scozzafava, A.; Reungprapavut, S.; Krungkrai, S. R.; Rattanajak, R.; Kamchonwongpaisan, S.; Supuran, C. T. *Bioorg. Med. Chem* **2005**, *13*, 483-489.
- (80) Nishimori, I.; Minakuchi, T.; Onishi, S.; Vullo, D.; Cecchi, A.; Scozzafava, A.; Supuran, C. T. *Bioorg. Med. Chem* **2007**, *15*, 7229-7236.
- (81) Vu, H.; Pham, N. B.; Quinn, R. J. *Journal of Biomolecular Screening* **2008**, *13*, 265-275.
- (82) Khalifah, R. G. *The Journal of Biological Chemistry* **1971**, *246*, 2561-2573.
- (83) Innocenti, A.; Vullo, D.; Scozzafava, A.; Casey, J. R.; Supuran, C. *Bioorganic & Medicinal Chemistry Letters* **2005**, *15*, 573-578.
- (84) Köhler, K.; Hillebrecht, A.; Schulze Wischeler, J.; Innocenti, A.; Heine, A.; Supuran, C.; Klebe, G. *Angew. Chem. Int. Ed.* **2007**, *46*, 7697-7699.
- (85) Alterio, V.; Vitale, R. M.; Monti, S. M.; Pedone, C.; Scozzafava, A.; Cecchi, A.; De Simone, G.; Supuran, C. T. *Journal of the American Chemical Society* **2006**, *128*, 8329-8335.
- (86) Krishnamurthy, V. M.; Kaufman, G. K.; Urbach, A. R.; Gitlin, I.; Gudiksen, K. L.; Weibel, D. B.; Whitesides, G. M. *Chemical Reviews* **2008**, *108*, 946-1051.
- (87) Innocenti, A.; Scozzafava, A.; Parkkila, S.; Puccetti, L.; De Simone, G.; Supuran, C. T. *Bioorganic & Medicinal Chemistry Letters* **2008**, *18*, 2267-2271.
- (88) Jennings, W. B.; Farrell, B. M.; Malone, J. F. *J. Org. Chem* **2006**, *71*, 2277-2282.
- (89) Guvench, O.; Brooks, C. L. *J. Am. Chem. Soc* **2005**, *127*, 4668-4674.
- (90) Maresca, A.; Temperini, C.; Pochet, L.; Masereel, B.; Scozzafava, A.; Supuran, C. T. *J. Med. Chem* **2010**, *53*, 335-344.
- (91) Pochet, L.; Doucet, C.; Schynts, M.; Thierry, N.; Boggetto, N.; Pirotte, B.; Jiang, K. Y.; Masereel, B.; de Tullio, P.; Delarge, J.; Reboud-Ravaux, M. *Journal of Medicinal Chemistry* **1996**, *39*, 2579-2585.
- (92) Doucet, C.; Pochet, L.; Thierry, N.; Pirotte, B.; Delarge, J.; Reboud-Ravaux, M. *Journal of Medicinal Chemistry* **1999**, *42*, 4161-4171.
- (93) Robert, S.; Bertolla, C.; Masereel, B.; Dogné, J.; Pochet, L. *Journal of Medicinal Chemistry* **2008**, *51*, 3077-3080.
- (94) Jackson, S. A.; Sahni, S.; Lee, L.; Luo, Y.; Nieduzak, T. R.; Liang, G.; Chiang, Y.; Collar, N.; Fink, D.; He, W.; Laoui, A.; Merrill, J.; Boffey, R.; Crackett, P.; Rees, B.; Wong, M.; Guilloteau, J.; Mathieu, M.; Rebello, S. S. *Bioorganic & Medicinal Chemistry* **2005**, *13*, 2723-2739.
- (95) Sethna, S. M.; Shah, N. M. *Chemical Reviews* **1945**, *36*, 1-62.
- (96) Hilvo, M.; Salzano, A. M.; Innocenti, A.; Kulomaa, M. S.; Scozzafava, A.; Scaloni, A.; Parkkila, S.; Supuran, C. T. *Journal of Medicinal Chemistry* **2009**, *52*, 646-654.
- (97) Guler, O. O.; De Simone, G.; Supuran, C. T. *Curr. Med. Chem* **2010**, *17*, 1516-1526.
- (98) Dubois, L.; Lieuwes, N. G.; Maresca, A.; Thiry, A.; Supuran, C. T.; Scozzafava, A.; Wouters, B. G.; Lambin, P. *Radiother Oncol* **2009**, *92*, 423-428.
- (99) SHAH, D. N.; SHAH, N. M. *The Journal of Organic Chemistry* **1954**, *19*, 1681-1685.
- (100) Swamy, K. C. K.; Kumar, N. N. B.; Balaraman, E.; Kumar, K. V. P. P. *Chemical Reviews* **2009**, *109*, 2551-2651.
- (101) Henkel, J. G.; Hane, J. T.; Gianutsos, G. *J. Med. Chem* **1982**, *25*, 51-56.
- (102) Supuran, C. T. *Bioorg. Med. Chem. Lett* **2010**, *20*, 3467-3474.
- (103) Wagner, J.; Avvaru, B. S.; Robbins, A. H.; Scozzafava, A.; Supuran, C. T.; McKenna, R. *Bioorganic & Medicinal Chemistry* **2010**, *18*, 4873-4878.
- (104) Whittaker, M.; Floyd, C. D.; Brown, P.; Gearing, A. J. H. *Chemical Reviews* **1999**, *99*, 2735-2776.
- (105) Sasseti, C. M.; Rubin, E. J. *Proc. Natl. Acad. Sci. U.S.A* **2003**, *100*, 12989-12994.

- (106) Nishimori, I.; Minakuchi, T.; Vullo, D.; Scozzafava, A.; Innocenti, A.; Supuran, C. T. *J. Med. Chem* **2009**, *52*, 3116-3120.
- (107) Gu□zel, O.; Maresca, A.; Scozzafava, A.; Salman, A.; Balaban, A. T.; Supuran, C. T. *J. Med. Chem* **2009**, *52*, 4063-4067.
- (108) Minakuchi, T.; Nishimori, I.; Vullo, D.; Scozzafava, A.; Supuran, C. T. *J. Med. Chem* **2009**, *52*, 2226-2232.
- (109) Innocenti, A.; Mühlshlegel, F. A.; Hall, R. A.; Steegborn, C.; Scozzafava, A.; Supuran, C. T. *Bioorg. Med. Chem. Lett* **2008**, *18*, 5066-5070.
- (110) Innocenti, A.; Hall, R. A.; Schlicker, C.; Mühlshlegel, F. A.; Supuran, C. T. *Bioorg. Med. Chem* **2009**, *17*, 2654-2657.
- (111) Innocenti, A.; Hall, R. A.; Schlicker, C.; Scozzafava, A.; Steegborn, C.; Mühlshlegel, F. A.; Supuran, C. T. *Bioorg. Med. Chem* **2009**, *17*, 4503-4509.
- (112) Innocenti, A.; Leewattanapasuk, W.; Mühlshlegel, F. A.; Mastrolorenzo, A.; Supuran, C. T. *Bioorg. Med. Chem. Lett* **2009**, *19*, 4802-4805.
- (113) Schlicker, C.; Hall, R. A.; Vullo, D.; Middelhaufe, S.; Gertz, M.; Supuran, C. T.; Mühlshlegel, F. A.; Steegborn, C. *J. Mol. Biol.* **2009**, *385*, 1207-1220.
- (114) Innocenti, A.; Winum, J.; Hall, R. A.; Mühlshlegel, F. A.; Scozzafava, A.; Supuran, C. T. *Bioorg. Med. Chem. Lett* **2009**, *19*, 2642-2645.
- (115) Nishimori, I.; Minakuchi, T.; Kohsaki, T.; Onishi, S.; Takeuchi, H.; Vullo, D.; Scozzafava, A.; Supuran, C. T. *Bioorg. Med. Chem. Lett* **2007**, *17*, 3585-3594.
- (116) Nishimori, I.; Minakuchi, T.; Morimoto, K.; Sano, S.; Onishi, S.; Takeuchi, H.; Vullo, D.; Scozzafava, A.; Supuran, C. T. *J. Med. Chem* **2006**, *49*, 2117-2126.
- (117) Smith, K. S.; Jakubzick, C.; Whittam, T. S.; Ferry, J. G. *Proc. Natl. Acad. Sci. U.S.A* **1999**, *96*, 15184-15189.
- (118) Bennett, J. E.; Izumikawa, K.; Marr, K. A. *Antimicrob. Agents Chemother* **2004**, *48*, 1773-1777.
- (119) Fidel, P. L.; Vazquez, J. A.; Sobel, J. D. *Clin. Microbiol. Rev* **1999**, *12*, 80-96.
- (120) Tsai, H.; Krol, A. A.; Sarti, K. E.; Bennett, J. E. *Antimicrob. Agents Chemother* **2006**, *50*, 1384-1392.
- (121) Hanage, W. P.; Fraser, C.; Tang, J.; Connor, T. R.; Corander, J. *Science* **2009**, *324*, 1454-1457.
- (122) Pai, M. P.; Turpin, R. S.; Garey, K. W. *Antimicrob. Agents Chemother* **2007**, *51*, 35-39.
- (123) Dye, C. *Nat. Rev. Microbiol* **2009**, *7*, 81-87.
- (124) Ginsberg, A. M. *Semin Respir Crit Care Med* **2008**, *29*, 552-559.
- (125) Showalter, H. D. H.; Denny, W. A. *Tuberculosis (Edinb)* **2008**, *88 Suppl 1*, S3-17.
- (126) Branden, C. I.; Tooze, J. *Introduction to Protein Structure*; Garland Science.; Garland Publishing, New York, 1999.
- (127) Supuran, C. T. *Curr. Pharm. Des* **2008**, *14*, 641-648.
- (128) Stiti, M.; Cecchi, A.; Rami, M.; Abdaoui, M.; Barragan-Montero, V.; Scozzafava, A.; Guari, Y.; Winum, J.; Supuran, C. T. *J. Am. Chem. Soc.* **2008**, *130*, 16130-16131.
- (129) Camus, J.; Pryor, M. J.; Médigue, C.; Cole, S. T. *Microbiology (Reading, Engl.)* **2002**, *148*, 2967-2973.
- (130) Hilvo, M.; Baranauskiene, L.; Salzano, A. M.; Scaloni, A.; Matulis, D.; Innocenti, A.; Scozzafava, A.; Monti, S. M.; Di Fiore, A.; De Simone, G.; Lindfors, M.; Janis, J.; Valjakka, J.; Pastorekova, S.; Pastorek, J.; Kulomaa, M. S.; Nordlund, H. R.; Supuran, C. T.; Parkkila, S. *J. Biol. Chem* **2008**, *283*, 27799-27809.
- (131) Isik, S.; Kockar, F.; Aydin, M.; Arslan, O.; Guler, O. O.; Innocenti, A.; Scozzafava, A.; Supuran, C. T. *Bioorg. Med. Chem* **2009**, *17*, 1158-1163.
- (132) Alterio, V.; Vitale, R. M.; Monti, S. M.; Pedone, C.; Scozzafava, A.; Cecchi, A.; De Simone, G.; Supuran, C. T. *J. Am. Chem. Soc* **2006**, *128*, 8329-8335.

- (133) Supuran, C. T.; Clare, B. W. *Eur. J. Med. Chem.* **1999**, *34*, 41-50.
- (134) Maresca, A.; Carta, F.; Vullo, D.; Scozzafava, A.; Supuran, C. T. *Bioorg. Med. Chem. Lett* **2009**, *19*, 4929-4932.
- (135) Carta, F.; Pothen, B.; Maresca, A.; Tiwari, M.; Singh, V.; Supuran, C. T. *Chem Biol Drug Des* **2009**, *74*, 196-202.
- (136) Carta, F.; Maresca, A.; Scozzafava, A.; Vullo, D.; Supuran, C. T. *Bioorg. Med. Chem* **2009**, *17*, 7093-7099.
- (137) Sasseti, C. M.; Boyd, D. H.; Rubin, E. J. *Mol. Microbiol* **2003**, *48*, 77-84.
- (138) Betts, J. C.; Lukey, P. T.; Robb, L. C.; McAdam, R. A.; Duncan, K. *Mol. Microbiol* **2002**, *43*, 717-731.
- (139) Güzel, O.; Innocenti, A.; Scozzafava, A.; Salman, A.; Parkkila, S.; Hilvo, M.; Supuran, C. T. *Bioorg. Med. Chem* **2008**, *16*, 9113-9120.
- (140) Güzel, O.; Temperini, C.; Innocenti, A.; Scozzafava, A.; Salman, A.; Supuran, C. T. *Bioorg. Med. Chem. Lett* **2008**, *18*, 152-158.
- (141) Carta, F.; Maresca, A.; Covarrubias, A. S.; Mowbray, S. L.; Jones, T. A.; Supuran, C. T. *Bioorg. Med. Chem. Lett* **2009**, *19*, 6649-6654.
- (142) Mogensen, E. G.; Janbon, G.; Chaloupka, J.; Steegborn, C.; Fu, M. S.; Moyrand, F.; Klengel, T.; Pearson, D. S.; Geeves, M. A.; Buck, J.; Levin, L. R.; Mühlischlegel, F. A. *Eukaryotic Cell* **2006**, *5*, 103-111.
- (143) Bahn, Y.; Mühlischlegel, F. A. *Curr. Opin. Microbiol* **2006**, *9*, 572-578.
- (144) Dodgson, S. J. *J. Appl. Physiol* **1987**, *63*, 2134-2141.
- (145) Dodgson, S. J.; Cherian, K. *Am. J. Physiol* **1989**, *257*, E791-796.
- (146) Chegwiddden, W.; Spencer, I. M. *Comp. Biochem. Physiol.* **1996**, *115*, 247-254.
- (147) Chegwiddden, W. R.; Dodgson, S. J.; Spencer, I. M. In *The Carbonic Anhydrase-New Horizons*; Chegwiddden W.R.; Edwards Y.; Carter N., 2000; pagg. 343-363.
- (148) Lynch, C. J.; Fox, H.; Hazen, S. A.; Stanley, B. A.; Dodgson, S.; Lanoue, K. F. *Biochem. J* **1995**, *310* ( Pt 1), 197-202.
- (149) Hazen, S. A.; Waheed, A.; Sly, W. S.; LaNoue, K. F.; Lynch, C. J. *FASEB J* **1996**, *10*, 481-490.
- (150) Supuran, C. T. *Expert Opin. Ther. Patents* **2003**, *13*, 1545-1550.
- (151) Picard, F.; Deshaies, Y.; Lalonde, J.; Samson, P.; Richard, D. *Obes. Res* **2000**, *8*, 656-663.
- (152) Gadde, K. M.; Franciscy, D. M.; Wagner, H. R.; Krishnan, K. R. R. *JAMA* **2003**, *289*, 1820-1825.
- (153) Young, R. W.; Wood, K. H.; Eichler, J. A.; Vaughan, J. R.; Anderson, G. W. *J. Am. Chem. Soc.* **1956**, *78*, 4649-4654.
- (154) Cecchi, A.; Hulikova, A.; Pastorek, J.; Pastoreková, S.; Scozzafava, A.; Winum, J.; Montero, J.; Supuran, C. T. *J. Med. Chem* **2005**, *48*, 4834-4841.
- (155) Vitale, R. M.; Pedone, C.; Amodeo, P.; Antel, J.; Wurl, M.; Scozzafava, A.; Supuran, C. T.; De Simone, G. *Bioorg. Med. Chem* **2007**, *15*, 4152-4158.
- (156) Alterio, V.; Monti, S. M.; Truppo, E.; Pedone, C.; Supuran, C. T.; De Simone, G. *Org. Biomol. Chem.* **2010**, *8*, 3528.
- (157) Scozzafava, A.; Menabuoni, L.; Mincione, F.; Briganti, F.; Mincione, G.; Supuran, C. T. *J. Med. Chem* **2000**, *43*, 4542-4551.
- (158) Ilies, M.; Supuran, C. T.; Scozzafava, A.; Casini, A.; Mincione, F.; Menabuoni, L.; Caproiu, M. T.; Maganu, M.; Banciu, M. D. *Bioorg. Med. Chem* **2000**, *8*, 2145-2155.
- (159) Pacchiano, F.; Aggarwal, M.; Avvaru, B. S.; Robbins, A. H.; Scozzafava, A.; McKenna, R.; Supuran, C. T. *Chem. Commun. (Camb.)* **2010**, *46*, 8371-8373.
- (160) D'Ambrosio, K.; Masereel, B.; Thiry, A.; Scozzafava, A.; Supuran, C. T.; De Simone, G. *ChemMedChem* **2008**, *3*, 473-477.
- (161) Cravotto, G.; Balliano, G.; Tagliapietra, S.; Palmisano, G.; Penoni, A. *European*

*Journal of Medicinal Chemistry* **2004**, 39, 917-924.

(162) Stokes, B. J.; Jovanović, B.; Dong, H.; Richert, K. J.; Riell, R. D.; Driver, T. G. *The Journal of Organic Chemistry* **2009**, 74, 3225-3228.

## Publications

7,8-Disubstituted- but not 6,7-disubstituted coumarins selectively inhibit the transmembrane, tumor-associated carbonic anhydrase isoforms IX and XII over the cytosolic ones I and II in the low nanomolar/subnanomolar range.

Maresca A, Scozzafava A, Supuran CT.

Bioorg Med Chem Lett. 2010 Dec 15;20(24):7255-8. Epub 2010 Oct 25.

The beta-Carbonic Anhydrases from Mycobacterium tuberculosis as Drug Targets.

Nishimori I, Minakuchi T, Maresca A, Carta F, Scozzafava A, Supuran CT.

Curr Pharm Des. 2010 Sep 7. [Epub ahead of print]

Mutation of Phe91 to Asn in human carbonic anhydrase I unexpectedly enhanced both catalytic activity and affinity for sulfonamide inhibitors.

Kockar F, Maresca A, Aydin M, Işık S, Turkoglu S, Sinan S, Arslan O, Güler OO, Turan Y, Supuran CT.

Bioorg Med Chem. 2010 Aug 1;18(15):5498-503. Epub 2010 Jun 22.

Carbonic anhydrase inhibitors. The X-ray crystal structure of human isoform II in adduct with an adamantyl analogue of acetazolamide resides in a less utilized binding pocket than most hydrophobic inhibitors.

Avvaru BS, Wagner JM, Maresca A, Scozzafava A, Robbins AH, Supuran CT, McKenna R.

Bioorg Med Chem Lett. 2010 Aug 1;20(15):4376-81. Epub 2010 Jun 17.

Coumarins incorporating hydroxy- and chloro-moieties selectively inhibit the transmembrane, tumor-associated carbonic anhydrase isoforms IX and XII over the cytosolic ones I and II.

Maresca A, Supuran CT.

Bioorg Med Chem Lett. 2010 Aug 1;20(15):4511-4. Epub 2010 Jun 10.

Carbonic anhydrase inhibitors. The beta-carbonic anhydrases from the fungal pathogens Cryptococcus neoformans and Candida albicans are strongly inhibited by substituted-phenyl-1H-indole-5-sulfonamides.

Güzel O, Maresca A, Hall RA, Scozzafava A, Mastrolorenzo A, Mühlshlegel FA, Supuran CT.

Bioorg Med Chem Lett. 2010 Apr 15;20(8):2508-11.

Deciphering the mechanism of carbonic anhydrase inhibition with coumarins and thiocoumarins.

Maresca A, Temperini C, Pochet L, Masereel B, Scozzafava A, Supuran CT.

J Med Chem. 2010 Jan 14;53(1):335-44.

Carbonic anhydrase inhibitors. Characterization and inhibition studies of the most active beta-carbonic anhydrase from Mycobacterium tuberculosis, Rv3588c.

Carta F, Maresca A, Covarrubias AS, Mowbray SL, Jones TA, Supuran CT.

Bioorg Med Chem Lett. 2009 Dec 1;19(23):6649-54.

Carbonic anhydrase inhibitors. Diazenylbenzenesulfonamides are potent and selective inhibitors of the tumor-associated isozymes IX and XII over the cytosolic isoforms I and II.

Carta F, Maresca A, Scozzafava A, Vullo D, Supuran CT.  
Bioorg Med Chem. 2009 Oct 15;17(20):7093-9.

Carbonic anhydrase inhibitors. Inhibition of the Rv1284 and Rv3273 beta-carbonic anhydrases from Mycobacterium tuberculosis with diazenylbenzenesulfonamides.

Maresca A, Carta F, Vullo D, Scozzafava A, Supuran CT.  
Bioorg Med Chem Lett. 2009 Sep 1;19(17):4929-32.

Imaging of CA IX with fluorescent labelled sulfonamides distinguishes hypoxic and (re)-oxygenated cells in a xenograft tumour model.

Dubois L, Lieuwes NG, Maresca A, Thiry A, Supuran CT, Scozzafava A, Wouters BG, Lambin P.  
Radiother Oncol. 2009 Sep;92(3):423-8.

Carbonic anhydrase inhibitors: inhibition of cytosolic carbonic anhydrase isozymes II and VII with simple aromatic sulfonamides and some azo dyes.

Carta F, Pothen B, Maresca A, Tiwari M, Singh V, Supuran CT.  
Chem Biol Drug Des. 2009 Aug;74(2):196-202.

Discovery of low nanomolar and subnanomolar inhibitors of the mycobacterial beta-carbonic anhydrases Rv1284 and Rv3273.

Güzel O, Maresca A, Scozzafava A, Salman A, Balaban AT, Supuran CT.  
J Med Chem. 2009 Jul 9;52(13):4063-7.

Carbonic anhydrase inhibitors. Synthesis of 2,4,6-trimethylpyridinium derivatives of 2-(hydrazinocarbonyl)-3-aryl-1H-indole-5-sulfonamides acting as potent inhibitors of the tumor-associated isoform IX and XII.

Güzel O, Maresca A, Scozzafava A, Salman A, Balaban AT, Supuran CT.  
Bioorg Med Chem Lett. 2009 Jun 1;19(11):2931-4.

A thiabendazole sulfonamide shows potent inhibitory activity against mammalian and nematode alpha-carbonic anhydrases.

Crocetti L, Maresca A, Temperini C, Hall RA, Scozzafava A, Mühlischlegel FA, Supuran CT.  
Bioorg Med Chem Lett. 2009 Mar 1;19(5):1371-5.

Non-Zinc mediated inhibition of Carbonic Anhydrases: Coumarin are a new class of suicide inhibitors.

Maresca A, Temperini C, Vu H, Pham NB, Poulsen SA, Scozzafava A, Quinn RJ, Supuran CT.  
J. Am. Chem. Soc. 2009, 131 (8), 3057-3062

Carbonic Anhydrase inhibitors: thioxolone versus sulfonamides for obtaining isozyme-selective inhibitors?

Innocenti A, Maresca A, Scozzafava A, Supuran CT.  
Bioorg Med Chem Lett. 2008 Jul 15;18(14):3938-41.

Muscarinic acetylcholine receptors as therapeutic targets for obesity.

A. Maresca, C.T. Supuran  
Expert Opin Ther Targets. 2008 Sep;12(9):1167-75. Review.